UNIVERSITY OF SOUTHAMPTON
FACULTY OF ENGINEERING, SCIENCE AND MATHEMATICS
School of Ocean and Earth Science

# Investigating and modelling the body size structure of benthic communities

**Janne Ilkka Kaariainen**

Thesis submitted for the degree of Doctor of Philosophy

February 2006

UNIVERSITY OF SOUTHAMPTON

ABSTRACT

FACULTY OF ENGINEERING, SCIENCE AND MATHEMATICS

SCHOOL OF OCEAN AND EARTH SCIENCE

Doctor of Philosophy

# INVESTIGATING AND MODELLING THE BODY SIZE STRUCTURE OF BENTHIC COMMUNITIES

by Janne Ilkka Kaariainen

Benthic communities were investigated in terms of their body size distributions at three environmentally contrasting study sites: (i) a shallow-water location on the Fladen Ground, North Sea, (ii) a deep-water location in the Faroe-Shetland Channel and (iii) and a mid-slope oxygen minimum zone location on the Oman Margin, Arabian Sea. The construction of body size spectra formed a central component of this analysis and it served as a foundation for further investigations into the functioning and dynamics of these communities. The shape of the biomass size spectra at all three locations could best be described by biomass increasing as a function of body size. In contrast to earlier studies, the biomass distribution patterns did not display distinct evidence of bimodality, implying that biomass size spectra do not distinguish meio- and macro-fauna as two functionally distinct groups of benthic organisms.

The body size spectra were found to vary in different environmental conditions. Comparisons of the two NE Atlantic locations revealed that the deeper Faroe-Shetland Channel site (1600 m) was dominated by smaller individuals than the shallower Fladen Ground site (150 m) hence conforming to the deep-sea size miniaturisation hypothesis as suggested by Thiel (1975). The size distribution patterns at the Arabian Sea site also differed significantly from the other two locations. Two taxonomic units (nematodes and polychaetes) overwhelmingly dominated the fauna in the low oxygen environment and this was reflected in the shape of the size spectra.

The empirical results formed a basis for a benthic simulation model that attempted to reproduce the trends observed in the field data. The size-based approach was observed to be successful in modelling the benthic biomass distributions. The results suggested that defecation and mortality imposed a strong influence on community size structure. Production and energy flow were also estimated at community level by utilising the empirical size distribution data and the previously established allometric relations

**DECLARATION OF AUTHORSHIP**

I, Janne Ilkka Kaariainen, declare that the thesis entitled "Investigating and modelling the body size structure of benthic communities" and the work presented in it are my own. I confirm that:

- this work was done wholly or mainly while in candidature for a research degree at this University;
- where any part of this thesis has previously been submitted for a degree or any other qualification at this University or any other institution, this has been clearly stated;
- where I have consulted the published work of others, this is always clearly attributed;
- where I have quoted from the work of others, the source is always given. With the exception of such quotations, this thesis is entirely my own work;
- I have acknowledged all main sources of help;
- where the thesis is based on work done by myself jointly with others, I have made clear exactly what was done by others and what I have contributed myself;
- none of this work has been published before submission;

Signed:

Date:

**GRADUATE SCHOOL OF THE**
**NATIONAL OCEANOGRAPHY CENTRE, SOUTHAMPTON**

This PhD dissertation by

*Janne Ilkka Kaariainen*

has been produced under the supervision of the following persons

Supervisor/s

Dr. Brian J. Bett
Dr. John D. Gage
Prof. Paul A. Tyler

Chair of Advisory Panel

Dr. Martin Sheader

Member/s of Advisory Panel

Dr. Brian J. Bett
Prof. Paul A. Tyler

## ACKNOWLEDGEMENTS

I would like to acknowledge my supervisors John Gage, Paul Tyler and in particular Brian Bett whose advice throughout this project has been invaluable. I am also grateful to all the colleagues (staff and students) at the George Deacon Division that have provided help and assistance not only during research cruises but also in the office and laboratory. Specifically, I would like to mention the guidance and advice of Boris Kelly-Gerreyn and Tom Anderson in the process of developing the simulation model.

My wife, Jemma, has undoubtedly experienced the pros and cons of marrying a marine scientist and a PhD-student and without her love, support and understanding this project would not have been possible.

Finally, my family has supported me over the years in so many ways that I dedicate this work to them.

This PhD was funded by the National Oceanography Centre, Southampton and the University of Southampton.

# TABLE OF CONTENTS

# LIST OF FIGURES

# LIST OF TABLES

# 1. INTRODUCTION

## 1.1 General introduction

One of the primary goals of ecology is to gain an understanding of the functioning and dynamics of the faunal assemblages on a system-wide scale. The first step in achieving this goal involves characterising the communities in terms of their constituent components. For example, benthic communities have been traditionally described by using a taxonomic approach. This is a process that involves identifying the individual organisms to species level and providing an estimate of their abundance. Such analysis is typically carried out for a limited size range (e.g. organisms retained on a 500 μm mesh) as counting and identifying all the different species at community or ecosystem level is both time-consuming and requires a considerable level of expertise (Saiz-Salinas & Ramos, 1999; Robson et al., 2005).

An alternative method of studying marine benthic communities is the investigation of their size structure. The way biomass is distributed among the component individuals is an important attribute of any community as it is often closely linked to its functioning (Strayer, 1986). As such, description of size distribution contains latent information about the system dynamics that cannot be obtained by a conventional taxonomic approach alone (Platt, 1985). The size-based approach hence offers a tool for community analysis at a general level and can provide an alternative or complimentary perspective to taxonomic techniques (Rasmussen, 1993).

This thesis examines the body size structure of benthic infaunal communities by constructing biomass and abundance size spectra for three environmentally contrasting locations. The size distributions are used to characterise the benthic communities and to assess some of the existing hypotheses that have been central to benthic ecology as well as to make further predictions about the functioning and controls of benthic systems. The thesis begins by introducing the basic concepts of size-based community analysis. The subsequent chapters describe the environmental settings of the study sites (chapter 2), the methods used (chapter 3) and a general biological description of the benthic communities (chapter 4). Chapter 5 forms the backbone of the thesis as it presents the results of the size spectral analysis from the three sampling locations. The following three chapters draw on these data to investigate body size miniaturisation in the deep-sea (chapter 6), to estimate production and energy flow (chapter 7) and to examine some of the processes that control the observed biomass size distributions of benthic communities by using simulation modelling (chapter 8). The results are brought together in chapter 9, which considers the wider implications and places the conclusions into context with our current understanding of benthic ecology.

## 1.2 Ecological implications of body size

Individual body size is probably the single most important factor in determining and controlling the course of life for aquatic animals. Body size can largely determine what an organism requires in order to survive and how much of its time and resources it spends in meeting those demands (Han & Straskraba, 1998). Entire life cycles are often governed by the restrictions or opportunities that the animal encounters as a

result of its body dimensions. Numerous biological process have been shown to correlate strongly with individual body size (e.g. metabolism, abundance, biomass production, nutrient recycling, home range size etc; Peters, 1983; Schmidt-Nielsen, 1984; Brown et al., 2004). These relationships typically take the form of a power function

$$Y = aM^b \quad (1.1)$$

where Y is the predicted biological characteristic (dependent variable), M is the animal body mass (independent variable) and the two coefficients a and b refer to an empirically defined normalisation constant and a scaling exponent, respectively. Depending on the value of the exponent these relationships are classified as either allometric ($a \neq 1$) or isometric ($a = 1$; Marquet et al., 2005). Most biological processes are allometric functions of body size and they plot as a curve on a linear axis (Peters, 1983). As these data often span a wide range of body sizes, it can be visually more informative to express them on logarithmic scales. Logarithmic transformation of the allometric power function takes the form of the equation for a straight line

$$\log Y = \log a + b \log M \quad (1.2)$$

where the value of the constant log a corresponds to the Y-intercept and the value of b to the slope of this line. An interesting property of these scaling relations is that with many biological processes, such as respiration or intrinsic growth rates, the value of b has been shown to approximate 3/4 for whole-organism rates and –1/4 ($M^{3/4}/M =$

$M^{(3/4-4/4)} = M^{-1/4}$) for mass-specific rates (Peters, 1983; Schmidt-Nielsen, 1984; Brown et al., 2004).

As a consequence of biological processes scaling closely with individual body size, it is reasonable to expect that body size will also have direct implications on population, community and ecosystem structures. Consequently, the allometric relations can provide a useful conceptual framework for relating individual organisms to the structure and dynamics at higher ecological levels.

## 1.3 Body size spectra

### 1.3.1 Variety in format

A primary tool for the investigation of community size structure is the construction of body size spectra. This involves expressing body size as a series of classes on the x-axis and plotting a measurement of organism abundance on the y-axis. In other words, each individual is assigned to a size class and the measure of abundance in each class represents the summed total of its constituents.

These size classes are often expressed on a logarithmic scale (such as the geometric scale) where each size class is twice the size of its smaller neighbour. The size classes may be based on a direct measurement of a particular body dimension (e.g. maximum body length), volume, body mass (dry mass, wet mass, organic carbon) or equivalent spherical diameter (ESD), which refers to the diameter of a sphere that has the same volume as the measured organism.

Abundance on the y-axis can be expressed as total biomass, number of individuals or number of species resulting in *biomass*-, *abundance*- or *species*- size spectrum, respectively. The data on the y-axis (measure of abundance) can be presented in a number of different ways. *Regular body sizes spectrum* plots the actual measured values in each size class. *Relative size spectrum* involves converting the actual measurements into percentages allowing a direct comparison of the shapes of two or more different spectra. *Cumulative size spectrum* sums the running total in each size class and all the classes below it and can be particularly useful in gauging the relative contributions of different size classes to the size distribution as a whole. As with the size classes on the x-axis, biomass and abundance measurements are regularly expressed on a $\log_{10}$- scale effectively resulting in $\log_{10} - \log_2$ plots.

Platt and Denmann (1978) outlined the problem of cross-comparing the biomass size distributions as the width of the size classes varies considerably (i.e. smaller size classes contain organisms of similar size whilst variation of individual body sizes is greater in the larger size classes). They proposed that the construction of *normalised size spectrum* may help to correct for this by diving the summed total in each size class by its width.

Vidondo et al. (1997) proposed the use power law probability or *Pareto type distributions* to describe body size spectra. This approach is based on an idea of plotting the probability that size $s$ of a particle at random will be greater than size $S$ (prob[$s>S$] as a function of $S$ on a double-logarithmic scale (for details see Vidondo et al., 1997). In the case of non-taxonomic size distributions this means that the term

prob($s$>$S$) is calculated for each measured organism as the fraction of all organisms larger than or equal to itself. If the community biomass distribution follows a Pareto type distribution then the plotted data will take the form of a straight line. Fitting a regression line through these data points will then produce the necessary statistics to evaluate the relevant parameters of the underlying Pareto distribution. The advantage of this approach is that each measurement contributes one data point to the resulting plot hence incorporating all the information from the observations. However, systems that are not in equilibrium cannot be appropriately described by the Pareto type distribution (Vanaverbeke et al., 2003; Marquet et al., 2005) and it is not recommended from the statistical standpoint (Vidondo et al., 1997).

The criteria for inclusion and measurement of individuals also varies depending on the nature of the study. Some size spectra have included only certain size fractions of the benthic community (e.g. macrofauna; Parry et al., 1999) or specific taxa (e.g. nematodes; Vanaverbeke et al., 2003). Other studies have excluded juveniles (Warwick, 1984) or have assigned each species uniquely to one size class (by average or maximum body size; Kendall et al., 1997). The last type of size spectrum can be constructed with a species list and single measurement of body size for each species and therefore represent an abstraction of the system as a whole.

### 1.3.2 Approach in the current study

Several methods exist to construct a body size spectrum reflecting the underlying community size structure. The current study has adopted a non-taxonomic approach by constructing biomass- and abundance- size spectra for the benthic communities.

The size classes are based on body mass (wet weight) and they are expressed on a geometric ($log_2$) size scale. No distinction has been made between juveniles and adults as any individual present in a size class contributes to the functioning and dynamics of that group.

Due to sampling and sample processing, some of the organisms could not obtained intact, resulting in the presence of fragmented body parts. This was mainly an issue with larger polychaete worms and it was decided that only the fractions with heads contributed towards the total abundance estimates. However, all fractions were measured for biomass and the fragmented body parts were allocated into their respective size classes based on these measurements. Although this may have resulted in some of the biomass being assigned into wrong size class, in reality the fragments were probably only shifted by one size category (e.g. fragments allocated to size class 16 belonged to either that size class or class 17 due to logarithmic scaling). Due to relatively low number of fragments present in the samples, this was unlikely to have a significant influence on the shape of the biomass size spectra.

### 1.3.3 History of size spectral analysis

Schwinghamer (1981) was the first to apply the size spectral analysis to marine benthic communities. He investigated body sizes ranging from bacteria to macrofauna by plotting total biomass against equivalent spherical diameter (ESD) on a logarithmic scale (base 2). The results for six intertidal stations showed a trimodal distribution with three biomass peaks at 0.5-1 μm, 64-125 μm and >2mm corresponding to micro-, meio- and macro-fauna, respectively. The peaks were

separated by biomass troughs reflecting the transitions between these three groups of organisms.

Subsequently, Schwinghamer extended these investigations to coastal sublittoral (1983) and to continental shelf and abyssal communities (1985) in order to examine the environmental variation in biomass spectra. At all locations the size spectra followed the previously established trimodal distribution. Similar observations resulted from a temporal study where the size distributions were investigated at an intertidal station sampled over an annual cycle (Schwinghamer, 1983). This led Schwinghamer to conclude that size structure is a conservative and predictable feature of benthic communities. Schwinghamer explained these results by the variable sediment perception hypothesis with the three groups occupying different aspects of the sediment environment. Microfauna colonise the surfaces of individual particles whilst macrofauna regard the sediment as effectively non-particulate either living on its surface or burrowing through it. Meiofauna are restricted to a life in the pore spaces between the particles. Changes in sediment characteristics, such as water content or grain size distribution, were thought to have a modifying effect on the size spectra resulting in possible shifts along one or both of the axes (Schwinghamer, 1985). Subsequent studies have investigated the effect of habitat architecture on the biomass and abundance size spectra but have regularly failed to find any shifts in the size distribution in response to changes in granulometry (Strayer, 1986; Duplisea & Drgas, 1999; Leaper et al., 2001).

Warwick adopted a different approach (1984) to the construction of size spectra as he studied the number of species present in each size category. For taxonomic reasons

the analysis was restricted to metazoans ranging in size from meio- to macro-fauna. The resulting size spectra were remarkably similar to those obtained by Schwinghamer (1981, 1983, 1985). The meiofaunal mode occurred at dry body weight of 0.64 μg (200 μm ESD) and the macrofaunal mode at 3.2 mg (1.5 mm ESD) with the trough in between at 45 μg (850 μm ESD). Warwick also reported the bimodality of meio- and macro-fauna to be invariant with respect to sediment particle size. Instead Warwick offered evolutionary explanations (development-, reproduction- and feeding-modes, generation time etc) for the observed dichotomy, suggesting that meio- and macro-fauna both had an internally coherent set of biological characteristics. According to his hypothesis there are two modal size classes (corresponding to meio- and macro-fauna) where these two sets of traits are optimised. Organisms that fall into size classes on either side of these optima are at a disadvantage.

The pioneering studies of Schwinghamer (1981) and Warwick (1984) have been widely quoted as evidence that meio- and macro-faunal groups represent two functionally distinct assemblages (Parsons et al., 1984; Giere, 1993). However, subsequent studies have frequently produced contrasting patterns, yet few have challenged the theory directly. The construction of reliable body size spectra can help to elucidate whether biomass and abundance distributions are adequate in reliably differentiating between the two faunal groups.

### 1.4 Modelling benthic communities

The construction and analysis of biomass and abundance size spectra are important in characterising the benthic community structure. These size spectra have generated several hypotheses concerning the factors controlling the size distributions. One way of testing these hypotheses is to carry out further experimental work but due to the complexity of biological systems and the large number of potential factors involved, such studies can be extremely time-consuming. Numerical simulation modelling offers a useful tool in focusing these experimental research efforts.

An appropriate simulation model is dependent on two important attributes. First, the structure of the constructed model must reflect the structure of the biological system it attempts to simulate. Second, the processes that govern the interactions between the different parts (variables) of the model must be accurately parameterised. Modelling of benthic systems has been hindered by the lack of information on many of these processes. However, all organisms, regardless of their taxonomic identity or environmental setting, must follow the basic laws of physics, chemical stoichiometry and thermodynamics. As most of the biological processes scale with body size in a predictable manner (Peters, 1983; Brown et al., 2004), a body size-based approach may prove as a good starting point for modelling benthic communities. Such a modelling approach can provide additional insights into benthic community dynamics and generate testable hypothesis that could help to guide the future experimental studies.

## 1.5 Aims

The main objective of this thesis is to investigate marine benthic communities in terms of their size structure. As body size scales closely with a number of biological processes, the resulting data can be used to further examine the factors that influence marine benthos. The specific aims of the project included:

1. Construction of reliable biomass and abundance size spectra for a number of environmentally contrasting benthic communities. This enables a close scrutiny of the shape of the spectra under different environmental conditions as well as examining the existence of a true functional distinction between meio- and macro-fauna.

2. Investigation of the suggested body size miniaturisation of the deep-sea benthos.

3. Estimation of community production and energy flow by utilising the empirical size distribution data and the previously established allometric relations.

4. Development of a simple size-dependent benthic ecosystem model to assess the suitability of a size-based modelling approach in providing reasonable approximations of the field data. This also helps to identify the biological processes that are important in maintaining and controlling the observed community size structure.

# 2. STUDY SITES

## 2.1 Introduction

Samples for this project were collected from three different sites: (i) a shallow-water location on the Fladen Ground, North Sea, (ii) a deep-water location in the Faroe-Shetland Channel and (iii) and a mid-slope oxygen minimum zone location on the Oman Margin, Arabian Sea. The samples from the NE Atlantic were collected prior to the commencement of this PhD whilst the sampling in the Arabian Sea provided an opportunity to conduct field work (and collect a further sample set) within the project itself.

The Fladen Ground site (FG) is located in the northern North Sea, approximately 100 miles east of Aberdeen, Scotland (figure 2.1). It forms a part of a flat muddy ground characterised by an irregular pattern of glacial depressions between 100 and 150 m depth (Bashford & Eleftheriou, 1988). This area is further characterised by extensive oil industry activity and may be subjected to considerable fishing pressure (Jennings et al., 1999).

The Faroe-Shetland Channel site (FSC) is a deep-water location (1,600 m) separating Faroe Plateau from the Scottish Continental Shelf (figure 2.2). The channel itself is important in the exchange of water between the Atlantic and Norwegian basins. Although the area has been a target for some oil exploration over the past 30 years (Ferguson, 1997), it is still essentially a pristine deep-water habitat.

The Arabian Sea sampling site is located on the Oman Margin (OM; figure 2.3) and is characterised by a well-developed oxygen minimum zone (OMZ) that extends from about 100 to 1000 m water depth. The samples were collected from the core of the OMZ (500 m) where the benthic communities are subjected to an existence in hypoxic conditions. Geographically this location is part of the continental margin characterised by steep descending rocky outcrops and underwater canyon systems best described as a direct continuation of the coastal mountain range (figure 2.4).

These locations were chosen on the merit of their contrasting environmental settings and as the emphasis of the study was to compare the influence of these environmental gradients on biomass distribution, the actual geographical locations of the sampling sites were not as important. The details of the sampling locations are summarised in tables 2.1 and 2.2.

**2.2 Hydrography**

The Fladen Ground sampling site lies in the deeper part of the North Sea. It forms a centre of a gyre with limited current movements and is surrounded by major water inflows from the Atlantic into the North Sea ('Fair Isle Current' and 'East Shetland Atlantic inflow'; Turrell, 1992). Whilst the surface waters are characterised by weak tidal and residual currents (although the prevailing winds may influence the surface current patterns), the bottom water currents are thought to be slight (< 0.25 m $s^{-1}$; De Wilde et al., 1986). Fladen Ground is thermally stratified during the summer months when the thermocline can be found between 30 and 70 m (figure 2.5). The annual

variation in the bottom water temperature is small with the range varying from 6 to 8 C° (McIntyre, 1961; Lee, 1980; Faubel et al., 1983).

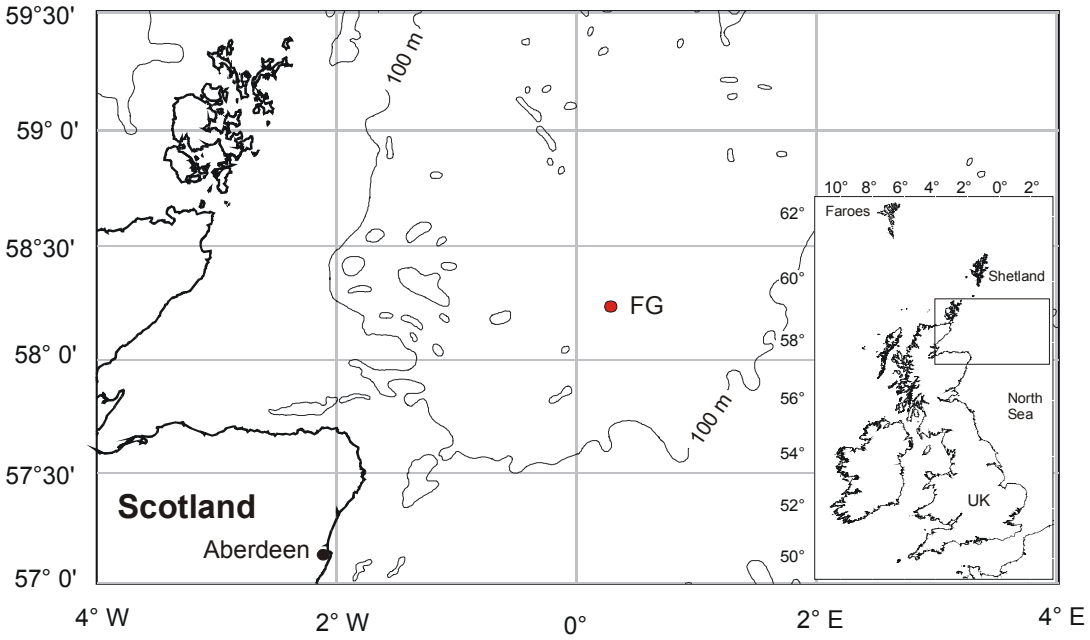


Figure 2.1. Fladen Ground sampling location

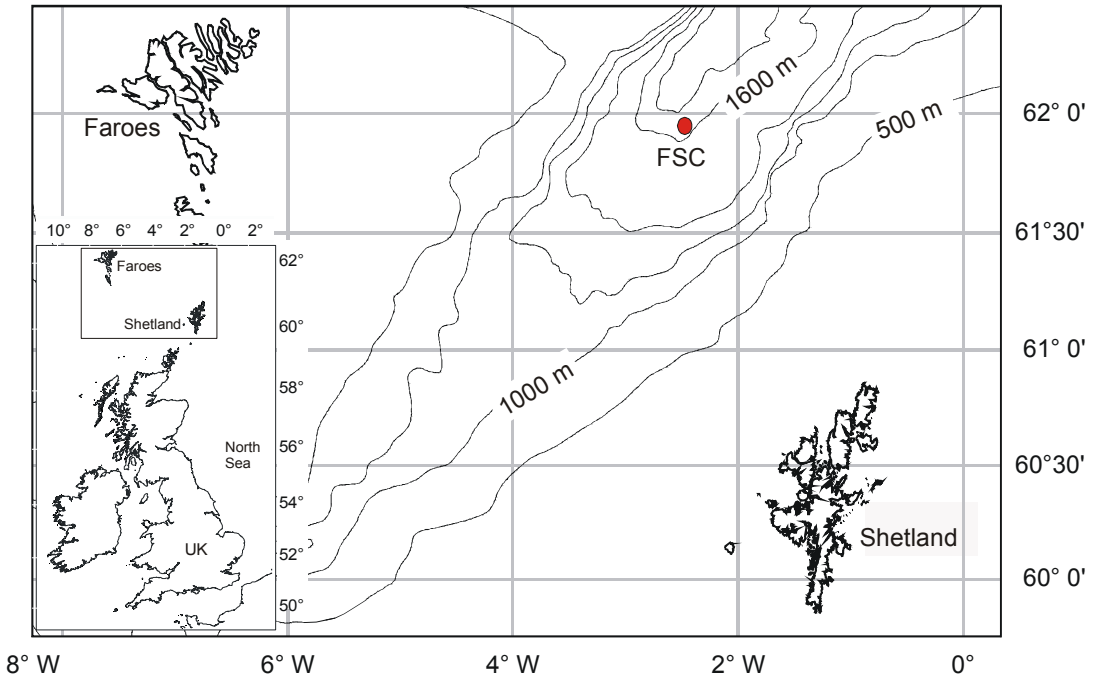


Figure 2.2. Faroe-Shetland Channel sampling location

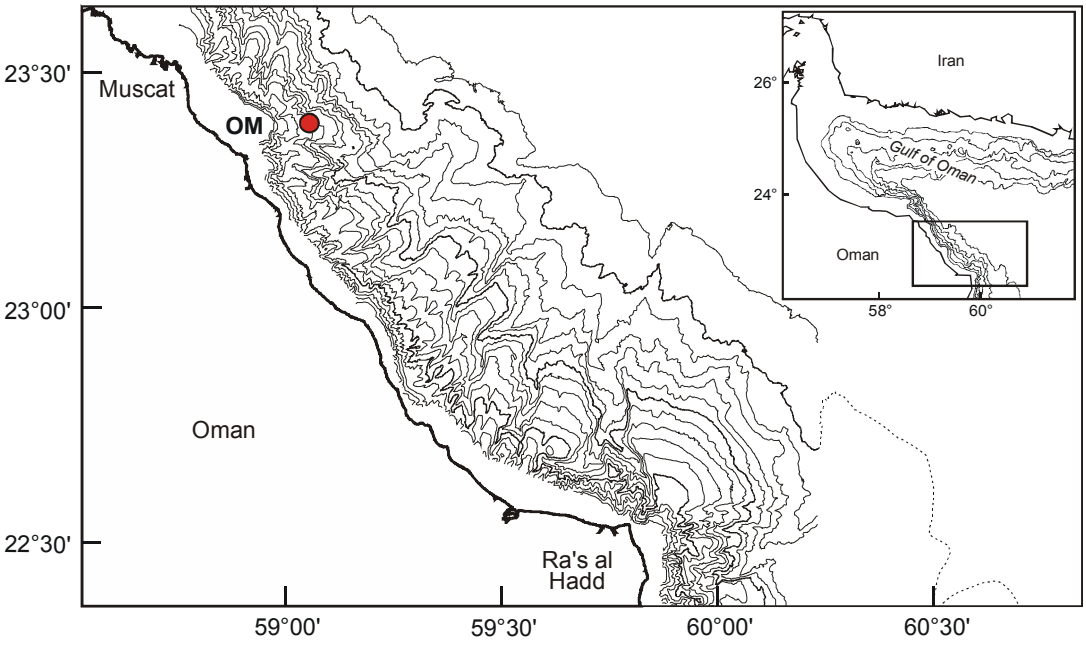


Figure 2.3. Oman Margin sampling location.

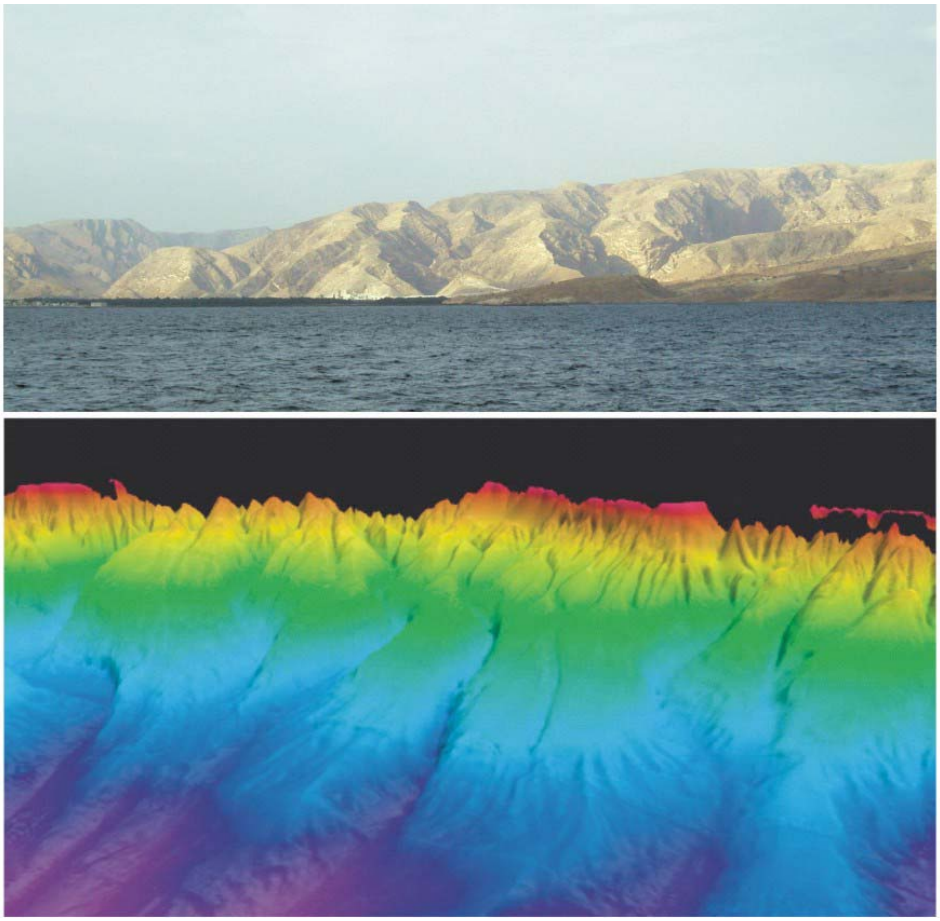

Figure 2.4. The coast of Oman above and below the surface. The 3D view of the coastal bathymetry bears close resemblance to the geography on land.

Table 2.1. Summary of the sampling locations.

| Site | Date | Station number | Depth (m) | Latitude | Longitude |
|---|---|---|---|---|---|
| Fladen Ground | | | | | |
| | 11/09/00 | 55526#1 | 154 | 58˚15'33 N | 00˚44'87 E |
| | 11/09/00 | 55526#2 | 153 | 58˚15'35 N | 00˚44'94 E |
| | 11/09/00 | 55527#2 | 153 | 58˚11'65 N | 00˚56'59 E |
| | 11/09/00 | 55528#1 | 154 | 58˚18.77 N | 00˚58'35 E |
| | 11/09/00 | 55528#2 | 150 | 58˚18.84 N | 00˚58'43 E |
| Faroe-Shetland Channel | | | | | |
| | 02/09/00 | 55447#6 | 1622 | 61˚55'03 N | 02˚48'30 W |
| | 02/09/00 | 55447#8 | 1623 | 61˚54'87 N | 02˚48'18 W |
| | 02/09/00 | 55447#9 | 1624 | 61˚55'05 N | 02˚48'12 W |
| | 02/09/00 | 55447#10 | 1623 | 61˚54'89 N | 02˚47'94 W |
| | 02/09/00 | 55447#11 | 1624 | 61˚54'95 N | 02˚48'06 W |
| Oman Margin | | | | | |
| | 09/12/02 | 55754#1 | 504 | 23˚22'98 N | 59˚00'00 W |
| | 09/12/02 | 55754#2 | 505 | 23˚23'02 N | 58˚59'99 W |
| | 09/12/02 | 55754#3 | 511 | 23˚23'01 N | 58˚59'93 W |
| | 09/12/02 | 55754#4 | 492 | 23˚23'08 N | 58˚59'91 W |
| | 09/12/02 | 55754#5 | 528 | 23˚23'09 N | 59˚00'09 W |
| | 11/12/02 | 55764#1 | 502 | 23˚22'94 N | 58˚59'98 W |

Table 2.2. Summary of the environmental conditions at the sampling locations.

| | FG | FSC | OM |
|---|---|---|---|
| Date | Sept 2000 | Sept 2000 | Dec 2002 |
| **Oceanographic information** | | | |
| Depth (m) | 150 | 1600 | 500 |
| Temperature (ºC) | 6-8 | -0.5 | 13.1 |
| Bottom water oxygen concentration (ml/l) | 6-7 | 6-7 | 0.11 |
| **Sediment information** | | | |
| Median grain size (phi) | 5.2 | 5.8 | 5.2 |
| Percentage of fines | >80 | >82 | >74 |
| Sediment classification | Coarse silt | Medium silt | Medium silt |
| Organic content | 1-5 % | 1.08 µg/g | 4-6 % |
| **Production information** | | | |
| Estimated annual surface primary production ($g\ C\ m^{-2}\ y^{-1}$) | 200-300 | 200-300 | 450 |
| Estimated flux to the seabed ($g\ C\ m^{-2}\ y^{-1}$) | 53-80 | 5.2-7.8 | 37 |

The FSC as a whole is a highly dynamic physical environment with a complex hydrographic setting. The hydrodynamics within the channel can be described as a system of five separate water masses that are identified by their temperature and salinity characteristics (Turrell et al., 1999). The intermediate water masses separate the uppermost warm layer of North Atlantic Water from the sub-zero temperature water of the channel floor (Faeroe-Shetland Channel Bottom Water; figure 2.6) originating from the deep Norwegian Sea (800 m). Although extremely large variations in water temperature have been recorded at intermediate depths within the channel, the bottom water temperatures are more constant with typical values less than -0.5°C (-0.5 to -1.0 °C; Turrell et al., 1999; figure 2.6). Overall the hydrography of the channel plays a very important role both in water exchange between the Atlantic and Arctic basins and in global thermohaline circulation (Hansen & Osterhus, 2000).

The hydrographic setting of the Gulf of Oman is largely driven by the monsoon dynamics. The strong seasonal winds lead to upwelling of nutrient-rich waters during the SW (June – September) and NE monsoons (December - March). The hydrodynamics of the Gulf of Oman are further characterised by intrusion of Arabian Gulf Water flowing in through the Strait of Hormuz at depth of about 200-300 m. This water mass can be identified by its increased oxygen (and temperature) values (figure 2.7). The bottom water temperatures near the study site were measured at 20.1 ˚C at 100 m, 13.1 ˚C at 500 m and then decreasing steadily with water depth to 1.9 ˚C at 3000 m.

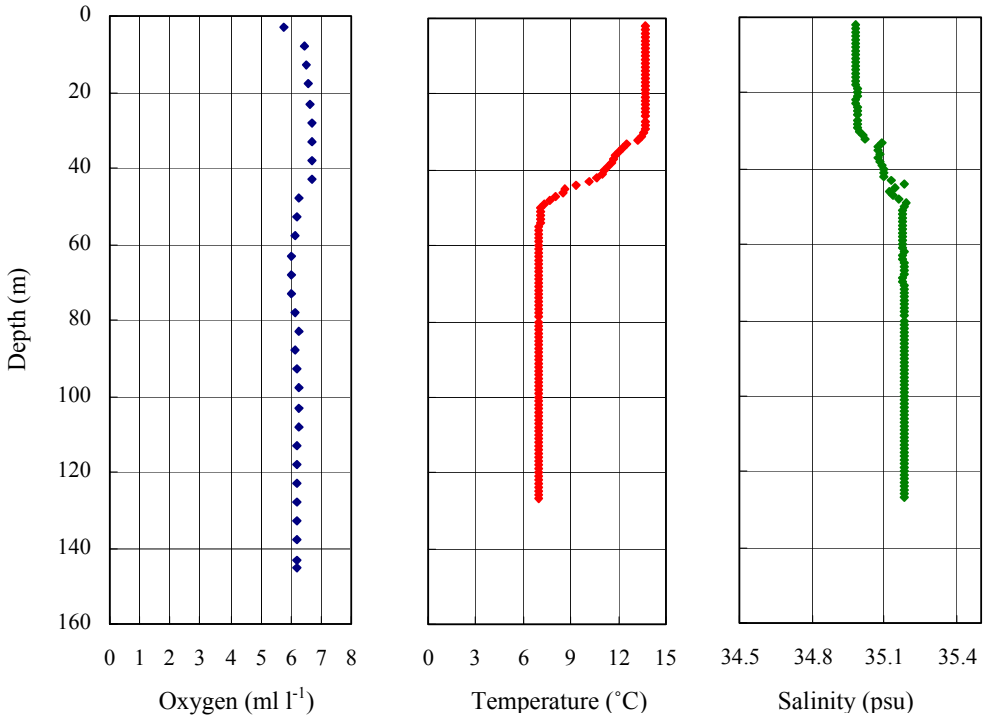


Figure 2.5. Oxygen, temperature and salinity profiles from the FG study area.

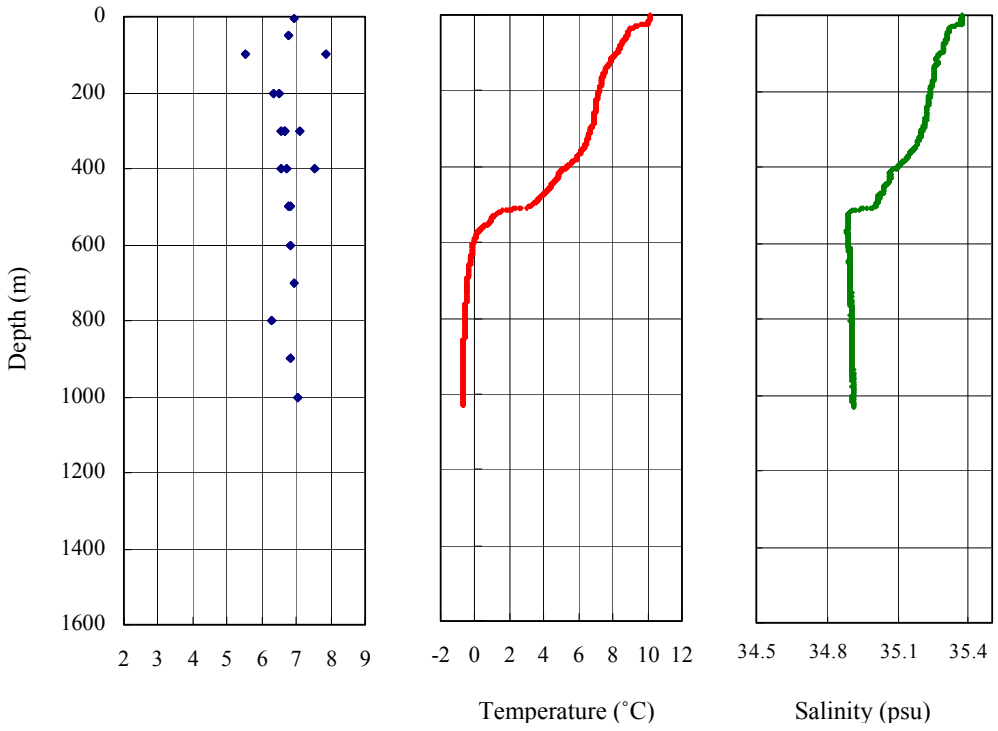


Figure 2.6. Oxygen, temperature and salinity profiles in the FSC study area.

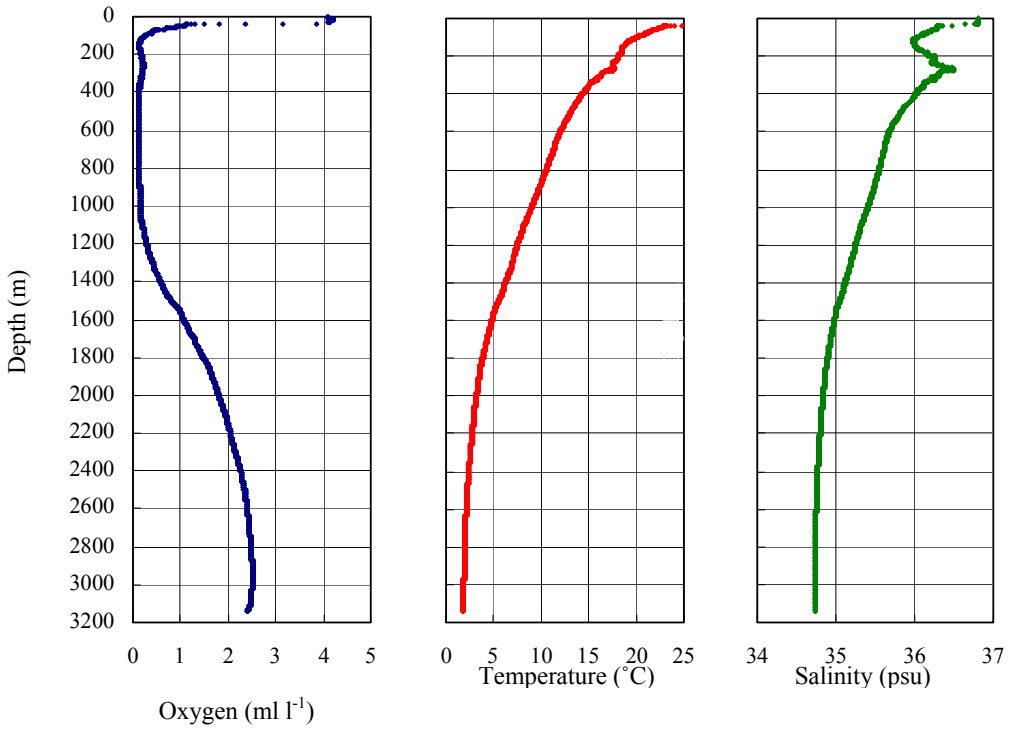


Figure 2.7. Oxygen, temperature and salinity profiles in the OM study area.

## 2.3 Sediments

The sediment environment at Fladen Ground consists essentially of coarse silt with a relatively high percentage of fines (> 80%; table 2.2). The median grain size was recorded as 26.7 μm (5.2 PHI). The percentage of organic matter in the surface sediments is reported to vary from 1 to 5 % (dry weight; Faubel et al., 1983).

The sediment environment in the Faroe-Shetland Channel is highly variable with a number of sediment types and features observed across the continental shelf (Masson, 2001). The study site was characterised by fine-grained sediments (medium silt) with a mean particle size of 18.4 μm (5.8 PHI) and relatively high percentage of fines (> 82%; table 2.2). The total organic carbon content was measured at 1.08 μg $g^{-1}$ sediment.

The sediment environment at the OM site was very similar to the FG location. The sediment was best described as medium silt with a mean particle size of 26.9 μm (5.2 PHI) and high percentage of fines (> 74 %; table 2.2). Total organic carbon content of the sediments at the core of the OMZ off the coast of Oman has been reported to range from approximately 4-6 % (Alagarsamy, 2003).

## 2.4 Oxygen concentrations

The pronounced monsoon regime of the Arabian Sea and the associated upwelling of nutrient-rich waters sustain an increased surface production and a high export flux of the organic matter from the surface waters (Gage et al., 2000). This increased flux of

organic matter coupled with limited mixing results in low mid-water oxygen concentrations. These oxygen minimum zones (OMZ) are defined as areas where $O_2$ < 0.5 ml $l^{-1}$. In areas where the OMZ impinges on the continental margin, the associated benthic communities experience extremely low bottom water oxygen concentrations. These are the conditions that also prevail at the current study location in the Arabian Sea. The measured oxygen concentrations for the Oman Margin area are shown in figure 2.7.

The OMZ was observed to extend from 100 to 1000 m water depth, with the intrusion of the Arabian Gulf water mass detected in the oxygen profiles as a peak of locally increased values around 200 m water depth. The bottom water oxygen values first decreased to 0.11 ml/l at 145 m and then increased to 0.23 ml/l at depth of about 270 m (Gulf of Arabia Water). The oxygen values then decreased again towards the core of the OMZ being 0.11 ml/l at 500 m and then slowly increasing to 0.15 ml/l at 1000 m, 0.28 ml/l at 1200 m, 1.80 ml/l at 2000 m and 2.52 ml/l at 3000 m (figure 2.7). The FG and FSC areas have been reported to have well oxygenated bottom waters (6-7 ml/l; data supplied by ICES Oceanographic Database and Services).

**2.5 Overlying production**

Direct measurements of primary production and the flux of organic matter to the sea floor are not available for the current study sites at the time of sampling. Instead, indirect estimates of primary production have been derived from published ship-based measurements as well as estimates based on the satellite data for the relevant areas. The ship based production estimates are often representative of a specific time period

(e.g. spring phytoplankton bloom) and may vary significantly from the values typical for the rest of the year.

Similarly the estimation of the transport rates of organic material from the euphotic zone to the sea floor is difficult. In general three processes control the content of organic material that reaches the seabed: the amount of surface primary production, the local hydrographic conditions and the biogeochemical processes that take place in the water column. Measuring this flux accurately is difficult and the data generated is often highly dependent on the methods used (Lampitt et al., 2001). Nevertheless, empirical formulas attempting to quantify the organic flux to the seabed have been developed (Suess, 1980; Berger et al., 1988). The problem with these equations is that they generally apply to a continuous rate of transport whereas the current study locations experience a high degree of seasonality in some (if not all) of the three controlling processes. Despite these limitations the empirical equations can be useful in providing estimates of the amount of surface production that may reach the underlying sea floor. Suess (1980) introduced a formula that linked the annual surface primary production (PP in g C $m^{-2}$ $y^{-1}$) and water depth (z in m) to the estimated flux (F in g C $m^{-2}$ $y^{-1}$):

$$F = PP / (0.0238z + 0.212) \quad (2.1)$$

Although other formulas have been developed (Berger et al., 1988; Herguera, 1992), the use of Suess formula was adopted for the current study. Ship-based primary production estimates for the Fladen Ground site have been recorded to range from 0.5 to 3.2 g C $m^{-2}$ $d^{-1}$ (Cadée, 1986). These estimates refer to measurements made during

the spring phytoplankton bloom (April- May) and are therefore likely to be higher than the primary production values during the rest of the year. Overall annual production estimates at this location are thought to vary from 50 - 100 g C $m^{-2}$ $y^{-1}$ (Steele, 1956; Fransz & Gieskes, 1984) with the more recent satellite data suggesting an annual production of 200 – 300 g C $m^{-2}$ $y^{-1}$ (the annual global production maps with SeaWiFS; http://marine.Rutgers.edu/opp/swf/ Production/results/all2_swf.html). The sediment trap data generally suggested that approximately 1% of the surface production reached 70 m water depth (although one sediment trap replicate suggested 9 %; Cadée, 1986). Applying the most recently estimated annual primary production values of 200-300 g C $m^{-2}$ $y^{-1}$ at the Fladen Ground site (150 m) to the Suess formula results in an estimated flux of 52.9-79.3 g C $m^{-2}$ $y^{-1}$ to reach the sea floor. This estimation seems relatively high in comparison to the estimate of 1 % (~2-3 g C $m^{-2}$ $y^{-1}$; or even 9 %) suggested by sediment trap data (Cadée, 1986).

Ship-based daily spring bloom production estimates for the FSC site vary from 1.2 - 1.8 g C $m^{-2}$ $d^{-1}$ (Riegman & Kraay, 2001). Mean daily spring bloom production values for other NE Atlantic sites have been quoted as 1.2 g C $m^{-2}$ $d^{-1}$ (Chipman et al., 1993) whilst the satellite data for the FSC area suggest the annual production levels to be very similar to those estimated for the FG site (200 – 300 g C $m^{-2}$ $y^{-1}$). Applying the Suess formula (1980) to an annual production estimate of 200-300 g C $m^{-2}$ $y^{-1}$ indicates an organic flux of 5.2-7.8 g C $m^{-2}$ $y^{-1}$ to reach the sea floor.

The empirical daily primary production estimates at the OM site vary from 0.4 – 2.67 g C $m^{-2}$ $d^{-1}$ depending on the monsoon season (Jochem et al., 1993; Owens et al., 1993; Barber et al., 2001). The annual mean production was estimated to amount to approximately 480 g C $m^{-2}$ $y^{-1}$ (Barber et al., 2001), which agrees well with the

satellite data estimates of 450 g C $m^{-2}$ $y^{-1}$. Lee et al. (1998) measured the annual surface primary production for their coastal site at 505 g C $m^{-2}$ and stated that approximately 1.6 % of this (8.3 g C $m^{-2}$) was captured in a sediment trap at a depth of 500 m. Applying the Suess formula to a production estimate of 450 g C $m^{-2}$ $y^{-1}$ at the OM site (depth 500 m) results in an estimated flux of 37 g C $m^{-2}$ $y^{-1}$.

It should be stated that at the time of sampling large phytoplankton and jellyfish blooms were observed in the coastal surface waters of Oman, sometimes resulting in thick, soup like appearance (figure 2.8). Although this production was not measured directly, estimates of carbon standing stock on the seabed (at the continental margin) were made based on the congregations of decaying jellyfish carcasses that formed distinct jelly-detritus patches on the seafloor. These estimates ranged from 1.5 to 75 g C $m^{-2}$ exceeding the estimated annual flux from sediment trap studies by approximately an order of magnitude (Billett et al., submitted).

Figure 2.8. The phytoplankton and jellyfish blooms observed in the surface waters during the sampling at the Oman Margin in December 2002.

# 3. METHODS

## 3.1 Sample collection

Sampling at the Fladen Ground and Faroe-Shetland Channel sites took place in the Autumn of 2000 during RRS *Charles Darwin* cruise 123 C4. The Oman margin samples were collected in December 2002 as part of RRS *Charles Darwin* cruise 143. All samples were collected using a Bowers & Connely "Megacorer", capable of taking up to 12 cores of 10 cm internal diameter (figure 3.1). The megacorer has a hydraulically damped action, which helps to reduce core compaction and any potential loss of the flocculent sediment surface layer (Gage & Bett, 2005). The megacorer was deployed repeatedly until five successful sample replicates were collected for large and small macrobenthos, meiobenthos and an intermediate-sized "mesobenthos" from each location (table 2.1; at the OM site only meiofaunal samples were collected from the station 55754#1 and in the subsequent analysis these have been combined with samples from the station 55764#1). Additional samples were collected for sediment particle size analysis.

On recovery of the corer, the function of each coring unit was checked and recorded. Core lengths were measured and recorded and any surface and profile features noted. Sample acceptance was based on the following criteria: cores > 20cm in length, core surfaces essentially level; and, the sediment-water interface intact. Acceptable cores were removed from the corer and transferred to the ship's laboratories for subsequent processing. In all cases processing began with the careful removal of the supernatant water using a gentle overflow, pump siphon, and/or syringe.

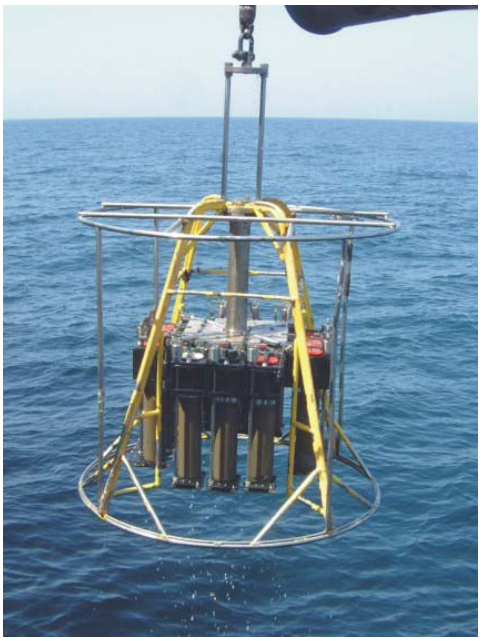

Figure 3.1. All samples were collected using a Bowers & Connely “Megacorer”.

For the macrobenthos samples, cores were extruded and sectioned to a 10 cm horizon (figure 3.2) with the successive cores being pooled (in two fractions) to ideally produce a nominal sample size of 7-8 cores (550-628 $cm^2$) for each replicate. Up to four of the macrofauna cores were elutriated through 500 and 250 μm sieve meshes and the remaining cores through 500 μm only, to separate between the large and small macrofauna samples (figure 3.3). For the mesobenthos sample one core (79 $cm^2$) was sectioned at 10 cm horizon and this was retained unsieved. For the meiobenthos samples three 20ml syringes were used to subsample a single core with a 0-5 cm section retained from each replicate to produce a pooled sample of $10cm^2$. All the material was preserved and fixed in 4%, borax buffered, formaldehyde.

## 3.2 Sample extraction

### 3.2.1 Macrobenthos

In the laboratory all the samples were wet sieved through a nest of sieves. Large and small macrobenthos samples were separated into 500, 355 and 250 μm fractions. The resulting fractions were stained with Rose Bengal, enumerated and sorted to major taxa under a stereomicroscope and preserved in ethanol. All metazoan taxa retained on the sieves were considered.

Figure 3.2. The sample cores were extruded and sectioned to a 10 cm horizon.

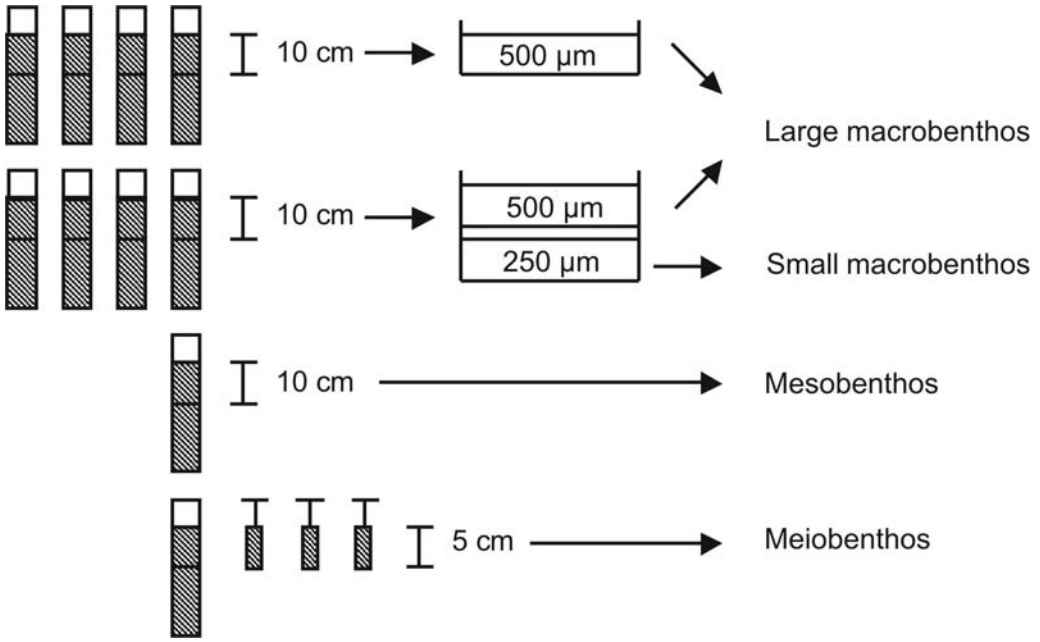


Figure 3.3. Schematic representation of the initial core sample processing procedure at sea. Further sample processing was carried out in the laboratory.

### 3.2.2 Mesobenthos

The mesobenthos samples were divided into 500, 355, 250 and 180μm fractions. Upon initial inspection the 180 μm fraction abundance levels were found to be very high and consequently these fractions were further sub-sampled by using the "Jensen sample splitter" (figure 3.4). This is a "Perspex" cylinder divided radially into eight sections. Prior to sub-sampling the total volume of the fraction was determined. The sample was then washed into the cylinder and allowed to settle into the sub-sections, one of which was randomly chosen for further analysis. To avoid any gradients that may have been inadvertently set up during the procedure, the diametrically opposite section was also included in the final sub-sample. The volume of the total sub-sample was measured and used to determine what percentage of the original sample was analysed. The organisms from the sub-sample were enumerated and sorted to major taxa under a stereomicroscope and preserved in ethanol.

### 3.2.3 Meiobenthos

The meiofauna samples were wet sieved on a 45 μm sieve. The material was collected to one side of the sieve and washed with Ludox (colloidal silica with a specific gravity of 1.15) into a plastic centrifuge tube ensuring that at least four times the sample volume of Ludox was added. The samples were centrifuged at 3000 RPM for 6 minutes to allow the density separation to occur, i.e. less dense, mainly organic particles rose to the Ludox surface while the denser, largely inorganic, particles sank to the bottom of the tube. After this separation the upper layer of Ludox containing the meiofauna and organic debris was decanted through a 45 μm mesh sieve and the

collected material was washed onto a Bogorov-type counting tray. The organisms were enumerated, sorted to major taxa and preserved in ethanol. The process was then repeated four more times and the extracted organisms were pooled with earlier specimens.

To assess the efficiency of the centrifuge extraction technique the number of meiofaunal organisms present in the residue material was compared with the total number of specimens collected in the extraction. As this proved to be particularly time consuming the process was carried out for only two of the five samples. For all the samples the extraction efficiency was found to be greater than 96 %.

All the nematodes found in the samples (macro-, meso- and meiobenthos) were mounted. Initially all nematodes were placed in a solid watch glass filled with a 1:1:18 mixture of glycerol, ethanol and water (Platt & Warwick, 1983). The watch glass was then placed in a dessicator and the water and ethanol were allowed to evaporate off slowly over two to three days. The specimens were then mounted in anhydrous glycerol on glass microscope slides, c. 25 per slide. Cover slips were supported by waxed paper of a thickness appropriate to prevent flattening of the specimens and sealed in place with nail varnish.

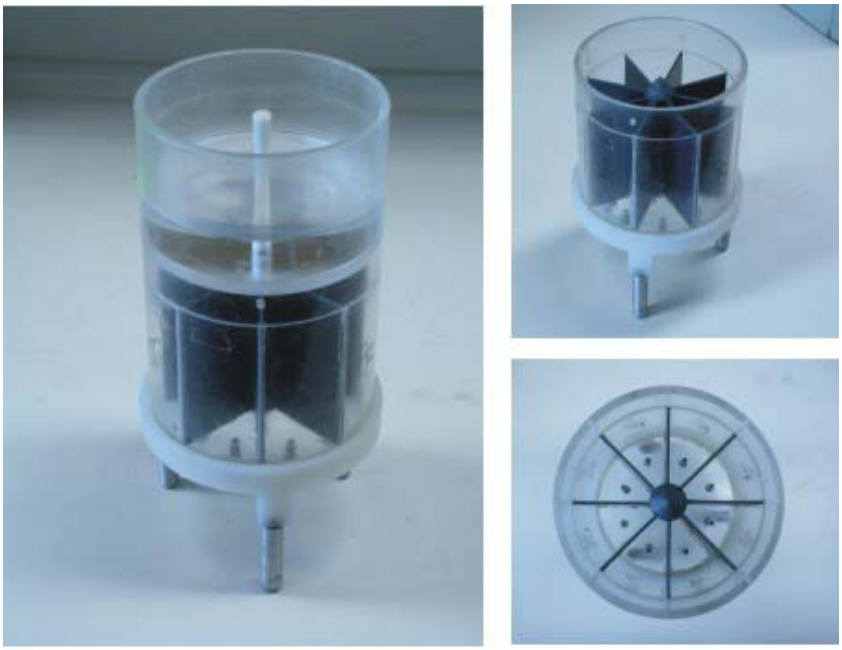

Figure 3.4. The Jensen sample splitter.

### 3.3 Biomass estimation and size spectra

Organism wet weights were estimated as the product of volume and specific gravity (Andrassy, 1956). A specific gravity of 1.13 was assumed for all the organisms used in the biomass estimation. Organism volumes were estimated by resolving the specimen bodies into a number of geometric figures ranging from cylinders and spheres to truncated cones. For Echinodea 50 % of the total volume was assumed to be soft tissue. For other hard bodied taxa (Bivalvia, Ostracoda) the volume of soft tissue could be determined directly.

The specimens were examined using a stereomicroscope (compound micrsocope in the case of mounted nematodes) fitted with a drawing tube that permitted a virtual image of the individual either being drawn or directly measured over the digitising tablet of an image analyser (Sigma Scan Image Analysis – version 2.0). The measurements were made at the highest magnification that provided sufficient field width to encompass the entire specimen to be measured.

In cases where more than 150 specimens of the same taxon were found, 100 individuals were chosen randomly for the biomass estimation and a density sub-sampling factor applied to that taxon accordingly. The sub-sampling was achieved by thoroughly dispersing all the organisms on a gridded petri dish and measuring all the individuals within randomly selected squares, until at least 100 specimens had been measured. In total 8,525 specimens were measured from the Fladen Ground site, 3,164 specimens from the FSC site and 1,975 specimens from the Oman Margin site.

The range of body sizes covered by the nest of mesh sizes used at each study location is shown in figure 3.5. These graphs show that at all locations the size range of organisms included was adequately covered by the set of sieves used.

The spectra were constructed by using the X2 geometric size classes of Warwick (1984) where each class is twice the biomass of the class below. The choice of a logarithmic scale is useful in visualising a large range of body sizes and has been widely used previously. All the specimens were assigned a body size class and the total biomass and abundance in each size class was then used to produce biomass and abundance size spectra, respectively.

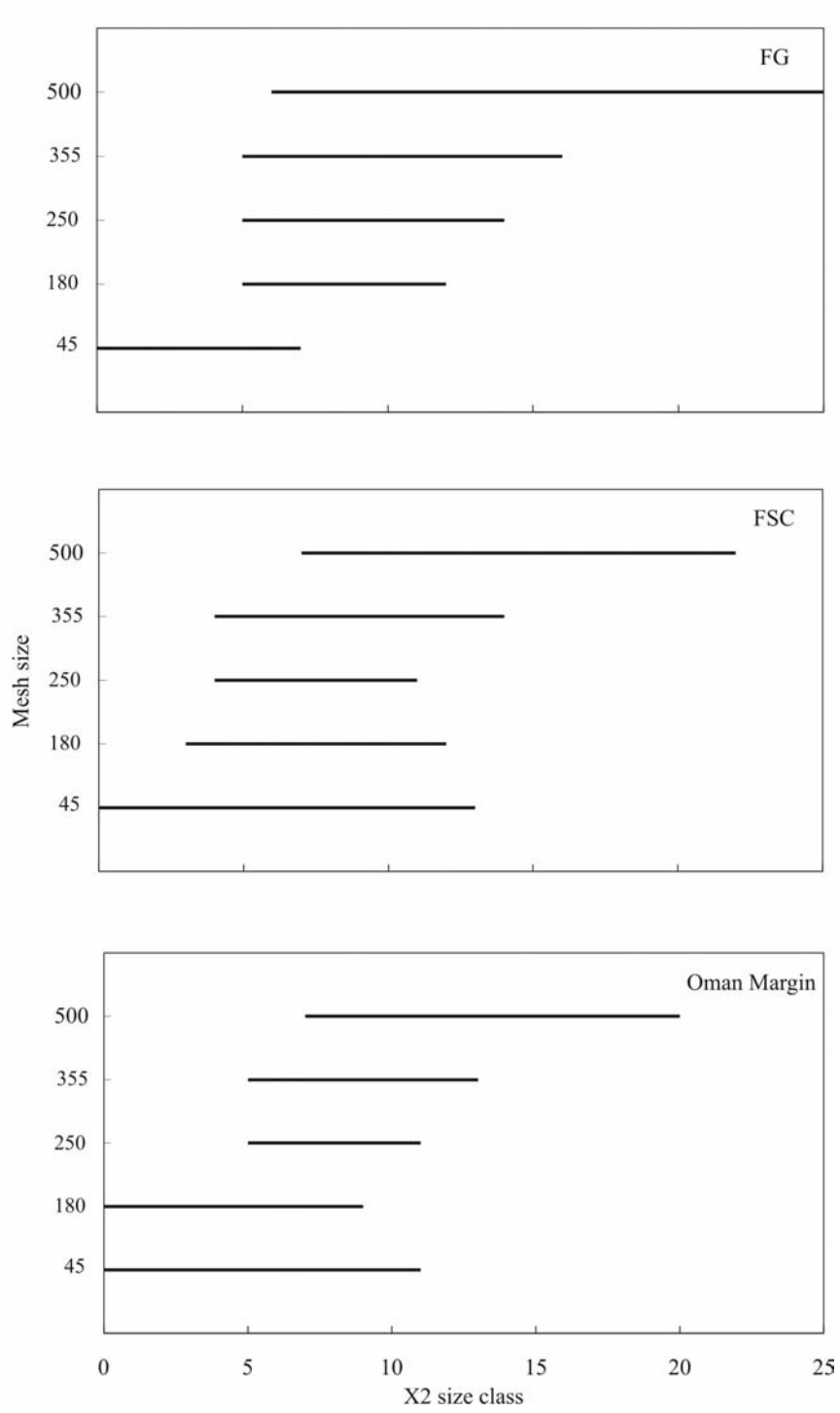


Figure 3.5. Graphical presentation of the range of body sizes covered by the mesh sizes (μm) used in the study.

### 3.4 Sample limitations

Sample size is always a compromise between covering as large surface area as possible and the time constraints associated with sorting these samples. The density of larger organisms is reduced in comparison to smaller ones and consequently greater sample sizes are required to estimate their abundance and biomass reliably. At inappropriate (small) sample sizes the retention of these larger individuals becomes random and the estimates of their contribution to the rest of the community are similarly unreliable. This can be demonstrated through a hypothetical community (Gerlach et al., 1985) where the total biomass of organisms is assumed to amount to 10 g $m^{-2}$. This surface area could then contain 100 individuals of 0.1 g, 10 individuals of 1 g or one individual of 10g. A sample size of 1 $m^2$ would hence provide reliable estimates of the smaller individuals but in order to obtain more accurate estimates of the larger ones the sample size would have to be increased. However, time constraints associated with sorting smaller individuals from increased sample sizes is not cost-effective and improvements in the reliability of abundance and biomass estimates are small. This has generally resulted in the collection of separate samples for different faunal size fractions but it is clear that the limitations at the larger end need to be recognised and accounted for in the analysis.

The faunal sediment samples are often sieved through a mesh to reduce the amount of sediment and inorganic debris. As with surface areas and sample sizes, different mesh sizes are used to target specific faunal size fractions. An inherent property of sieving is that it is never a 100 % efficient in retaining only the targeted individuals. A given mesh size typically retains some individuals that “should” have passed as organisms adhere to other retained particles or the mesh itself (the shape of the organisms may

be important). This means that sieved samples always contain organisms that are not reliably represented in the resulting extract. The use of variable and overlapping mesh and sample size accounts for this limitation at all but the smallest mesh size, where the analysis must consider this bias.

### 3.5 Analytical methods

A wide variety of statistical methods were used to analyse the data sets ranging from simple descriptive statistics (e.g. abundance, biomass, average individual size) to multivariate analyses of assemblages. The statistical methods are generally described within the appropriate chapters but an overview of some of the more specific methods are given below. The statistical procedures were carried out by using “Minitab version 14”, “SigmaPlot version 8” and “Primer version 5” software.

One of the main aims of this study was to characterise the shape of the biomass size spectra at the three study locations. This generally involved investigating whether the shape of the spectra conformed more to a unimodal or bimodal distribution pattern by testing if the individual size classes were significantly different from one another. In all cases the analysed data consisted of five replicate data sets hence providing appropriate power to conduct all of the applied statistical techniques and to have confidence that the generated results were reliable and not susceptible to Type I or II errors.

### 3.5.1 Kernel Density Estimation

Manly (1996) investigated the possibility of estimating the precise locations of troughs and peaks in biological size distribution data by utilising a technique he called "bump hunting" or Kernel Density Estimation. This technique involves comparing the properties of observed sample distributions with computer generated samples taken with different number of modes. In other words, the location and number of modes in size distribution data can be determined by using smoothed bootstrap re-sampling to see if the observed spectra are consistent with a continuous null distribution of increasing number of modes. The location and the number of modes can be defined when the observed and model distributions are consistent (bootstrap test not significant at 5% probability level). However, it has been suggested that the underlying assumptions of this statistical approach are not met when the test is run for averaged distributions (e.g. mean data from replicates) or for manipulated distributions such as biomass size spectra (Leaper et al., 2001). Consequently this approach was not adopted in the current study.

### 3.5.2 Unplanned multiple comparison test – Games-Howell method

The Games-Howell is an approximate test of equality of means when the data are found to be inherently heteroscedastic (inequality of variances among the samples; Sokal & Rohlf, 1995). The method performs unplanned comparisons between pairs of means using a studentized range with specially weighted average degrees of freedom and a standard error based on the averages of the variances of the means.

The minimum significant difference, $MSD_{ij}$, between any pair (*i, j*) of means is given by the following expression (Games & Howell, 1976):

$$MSD_{ij} = Q_{\alpha[k,\, v^*]} \, (s^2_{yi} + s^2_{yj})^{1/2} \qquad (3.1)$$

where

$$v^* = (s^2_{yi} + s^2_{yj})^2 \,/\, \{[(s^2_{yi})^2/(n_i-1)] + [(s^2_{yj})^2/(n_j-1)]\}, \qquad (3.2)$$

k = number of samples and

$\alpha$ = the significance level

$s^2_y$ = variance of the means (sample variance/number of observations).

The critical value $Q_{\alpha[k,\, v^*]}$ is obtained from the table of the stundentized range (Sokal & Rohlf, 1995). The actual difference between any pair of means is compared to its relevant MSD value.

### 3.5.3 Multivariate analysis

Multivariate analysis is based on comparing the similarity of two or more samples. Similarity can be defined as the extent to which the samples share their components. Multivariate techniques are thus based on similarity coefficients calculated between pairs of samples. These can then be used to either classify the samples into similar groups (clustering) or to "map" them on an ordination plot so that the distances between the different samples reflect the differences in their composition.

A commonly used measure of similarity between two samples is the Bray-Curtis coefficient of similarity (Clarke & Warwick, 1994). The measurement of similarities

can be biased by a small number of highly abundant components. To account for this, and to obtain a better reflection of the overall community composition, the data can be transformed so that less emphasis is given to the highly abundant components. The data transformation techniques range from square root to logarithmic to presence/absence transformations with fourth root (or double square root) transformation probably being the most commonly used method. In the current study all the multivariate analyses were performed on untransformed (actual) data sets.

#### *3.5.3.1 Cluster analysis*

Cluster analysis is based on the principle that samples within a group (or a cluster) are more similar to each other than samples outside the group. Hierarchical methods group together samples that are most similar in terms of their community composition forming further clusters at increasingly lower level of similarity until all samples are connected. The results can be displayed as a dendrogram with one axis representing the samples and the other defining the similarity levels.

#### *3.5.3.2 Non-metric multi-dimensional scaling*

Non-metric MDS produces a map of the samples based on their dissimilarity so that samples that are most dissimilar are plotted furthest apart. These MDS plots are produced by an iterative procedure that constructs MDS plots from successive runs until an optimal solution is reached. After each run the dissimilarity between each sample is plotted against their distance on the MDS plot and a regression line is fitted to these points. The goodness of fit of this line is referred to as “stress” with low stress

values corresponding to a closer fit. The procedure is repeated until the lowest stress value is obtained. Hence the stress value effectively reflects how well the multi-dimensional relationships among the samples are represented on a two dimensional plot. Stress values of less than 0.05 give an excellent representation whilst values exceeding 0.3 indicate a fit little better than randomly placed data.

*3.5.3.3 Analysis of similarities*

Analysis of similarities (ANOSIM) is a non-parametric test that helps to determine if a significant difference exists between two or more samples. The test operates on a dissimilarity matrix that is generated by comparing the differences (distances) between any two replicates (samples being compared must consist of replicate measurements). ANOSIM summarises the differences in composition between pairs of samples into a single measure that is compared to test the hypothesis that there is more difference in composition from sample to sample as opposed to replicate to replicate within one sample (i.e. ANOSIM is an analogue to analysis of variance).

# 4. BENTHIC COMMUNITY DESCRIPTION

## 4.1 Introduction

The primary aim of this chapter is to provide an overview of the benthic communities in terms of abundance, biomass and taxonomic identity of the constituent organisms. Abundance and biomass values have been reported for the community as a whole as well as for the commonly used faunal size fractions of meio- and macro-fauna and intermediate meso-fauna. Meiofauna has been defined as the collection of organisms that passed through a 500 μm mesh but were retained on 45 μm mesh. Macrofaunal fraction consists of organisms retained on the 500 μm mesh (excluding retained megafauna that was not sampled reliably) whilst mesofaunal fraction has been compiled by combining the individuals from 180, 250 and 355 μm fractions.

It is a common procedure that smaller organisms typically classified as meiofauna (e.g. nematodes, harpacticoids and ostracods) are excluded from the analysis of larger size fractions as they are not thought to be retained adequately on the coarser mesh sizes. This approach was also adopted in this chapter for meso- and macro-faunal fractions to make comparisons with previous studies more compatible. However, the subsequent chapters have not excluded any organisms from the analysis based on their taxonomic identity (or any other criteria) to comply with the non-taxonomic approach outlined in chapter 1.

## 4.2 Abundance

The total abundance at the three study sites varied from 690,125 ind. $m^{-2}$ (FG) to 441,361 ind. $m^{-2}$ (FSC) and 1,042,754 ind. $m^{-2}$ (OM; table 4.1, figure 4.1). At all locations meiofaunal size range contributed the most to the total abundance (84-99%). The densities of macrofaunal size fractions varied from 6,551 ind. $m^{-2}$ to 2,609 ind. $m^{-2}$ and 4,244 ind. $m^{-2}$ for FG, FSC and OM, respectively.

In terms of taxonomic composition, nematodes dominated the meiofaunal size range at all locations (table 4.2). They also contributed the most towards the total densities. This was particularly true at the OM site where nemtodes accounted for 99 % of all individuals. Similarly polycheates accounted for most of the individuals in the macrofaunal size range at all three locations. At the FG and FSC locations a number of different polychaete families were recorded with Amphinomidae, Capitellidae and Nereidae dominating the FG site and Paraonidae, Capitellidae and Aricidae dominating the FSC site. At the OM locations the polychaetes consisted almost exclusively of Ampharetidae with some representatives of Spionidae (e.g. *Minuspio* spp. and *Paraprionospio* spp.). All polychaetes from the OM site were characterised by enlarged gill structures that are thought to represent an adaptation to the reduced oxygen levels (Lamont & Gage, 2000).

The same polychaete families also dominate the mesofaunal fraction at the OM site. At the FG site the intermediate size group consisted predominantly of small bivalves (Veneroidae), gastropods (Philinidae) and polychaetes (Opheliidae). The abundance of this size group was more than an order of magnitude greater than at the other two locations and the increased numbers of small individuals may have represented a

recent spatfall event. The abundance of mesofaunal size range at the FSC site was relatively evenly distributed between polychaetes, crustacean, nemerteans and sipunculids.

Table 4.1. Summary of abundance values (ind. $m^{-2}$) at the three study locations (values in brackets refer to standard deviations; n=5).

| | FG | | FSC | | OM | |
|---|---|---|---|---|---|---|
| **Meiofauna** | 576,800 | (204,554) | 431,800 | (257,463) | 1,033,000 | (246,554) |
| **Mesofauna** | 106,774 | (50,530) | 6,951 | (2,244) | 5,509 | (4,706) |
| **Macrofauna** | 6,551 | (1,703) | 2,609 | (265) | 4,244 | (2,218) |
| **Total** | 690,125 | (251,845) | 441,361 | (257,682) | 1,042,754 | (246,774) |

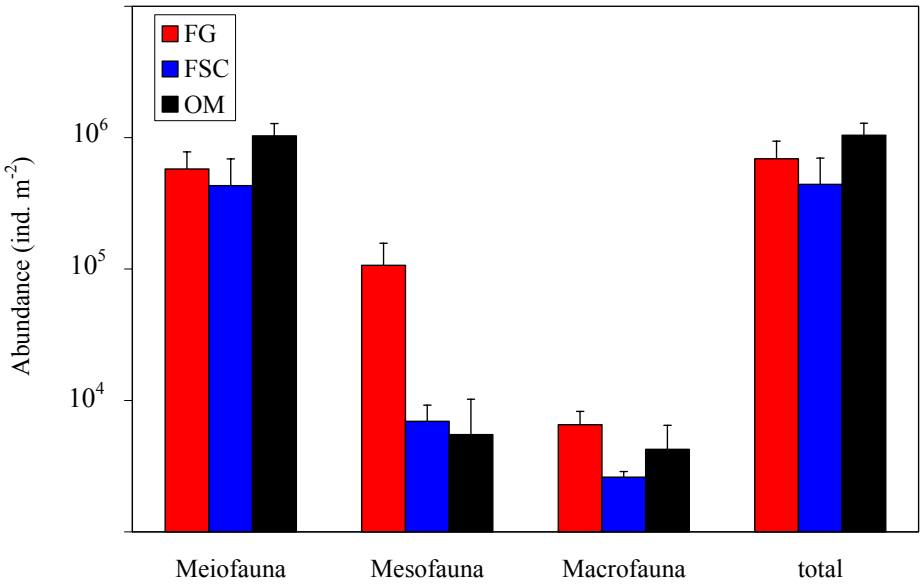


Figure 4.1. Abundance of the different size fractions at the three study locations (error bars represent standard deviations).

Table 4.2. The dominant taxonomic group in each size fraction in terms of abundance.

| | **FG** | **FSC** | **OM** |
|---|---|---|---|
| **Meiofauna** | Nematoda | Nematoda | Nematoda |
| **Mesofauna** | Mollusca | mixed | Polychaeta |
| **Macrofauna** | Polychaeta | Polychaeta | Polychaeta |
| **Total** | Nematoda | Nematoda | Nematoda |

### 4.3 Biomass

The total biomass was recorded as more than three times higher at the FG location (13.6 g wwt $m^{-2}$) than at the OM site (4.0 g wwt $m^{-2}$; table 4.3). The total biomass at the FSC site was intermediate (10.7 g wwt $m^{-2}$). Macrofauna accounted for most of the total biomass at all locations although meso- and meio-fauna were also major contributors at the FG and OM sites, respectively (figure 4.2). Mesofaunal size fraction contributed relatively little at the OM site. In the meiofaunal size range most of the biomass was attributed to nematodes whilst polychaetes generally dominated the biomass distributions in all other size fractions (table 4.4).

### 4.4 Abundance-biomass curves

The abundance-biomass comparison (ABC) method was developed by Warwick (1986) as a technique to detect the effects of pollution on benthic macrofaunal communities. It is based on k-dominance curves (Lambshead et al., 1983) that plot cumulative abundance on the y-axis against species rank on the x-axis. The ABC method superimposes dominance plots for species abundance and biomass and the relative positions of these curves serve as an indicator of the degree of disturbance at the sampling site. In undisturbed environments biomass is dominated by few larger species that are represented by relatively few individuals and consequently the biomass curve is positioned above the abundance curve across the x-axis. Conversely, in disturbed environments the community is dominated by smaller individuals that are present in high numbers and the abundance curve is positioned above the biomass curve.

Table 4.3. Summary of biomass values (g wwt $m^{-2}$) at the three study locations (values in brackets refer to standard deviations; n=5).

| | FG | FSC | OM |
|---|---|---|---|
| **Meiofauna** | 0.63 (0.20) | 0.70 (0.25) | 1.13 (0.98) |
| **Mesofauna** | 3.55 (2.23) | 0.16 (0.04) | 0.15 (0.12) |
| **Macrofauna** | 9.37 (2.92) | 9.86 (3.78) | 2.72 (1.86) |
| **Total** | 13.55 (4.77) | 10.73 (3.97) | 4.00 (2.65) |

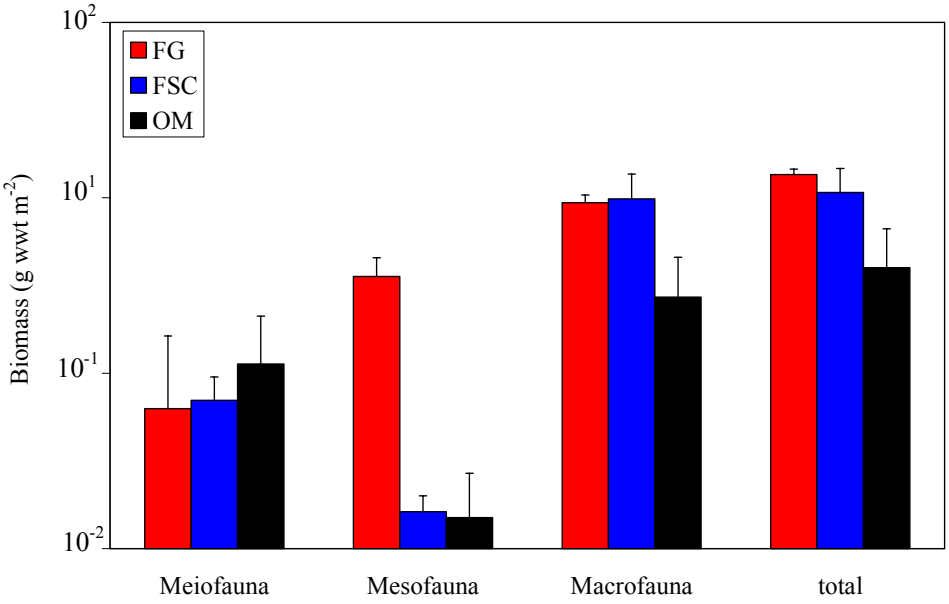


Figure 4.2. Biomass of the different size fractions at the three study locations (error bars represent standard deviations).

Table 4.4. The dominant taxonomic group in each size fraction in terms of biomass.

| | **FG** | **FSC** | **OM** |
|---|---|---|---|
| **Meiofauna** | Nematoda | Nematoda | Nematoda |
| **Mesofauna** | Polychaeta | mixed | Polychaeta |
| **Macrofauna** | Polychaeta | Polychaeta | Polychaeta |
| **Total** | Polychaeta | Polychaeta | Polychaeta |

The ABC method was applied to the current data sets. The size classes represented the species and they were ranked in order of decreasing biomass and abundance and the results were plotted and superimposed as described above. Warwick (1986) had stated that this method may not be applicable to meiobenthic organisms, as they do not necessarily show an obvious size difference between the organisms inhabiting disturbed and undisturbed habitats. Consequently the analysis was generally limited to macrofaunal size range (> 500 μm) but plots were also presented for the data sets as a whole.

The macrofaunal ABC plots for the FG and OM sites showed that the abundance and biomass curves overlaid one another throughout the size classes (figure 4.3). This indicates moderate disturbance at these two sites. As already noted the FG site is subjected to both extensive oil and gas industry activities and heavy trawling pressure (Jennings et al., 1999). The benthic environment at the OM site is not subjected to any obvious anthropogenic stress and the disturbance indicated by the ABC plots perhaps reflects the reduced oxygen levels and increased downward flux of organic material as outlined in chapter 2. At the FSC site the biomass curve was positioned above the abundance curve indicating a stable and undisturbed sediment environment.

The ABC plots produced for the data set as a whole displayed a trend of decreasing abundance diversity (fewer size classes contributed more to the total abundance). At the FG and OM sites the abundance curves were positioned above the biomass curves throughout the plots and at the FSC site the two curves overlaid one another (figure 4.4). This clearly reflected the inclusion of meiofaunal organisms in the analysis as

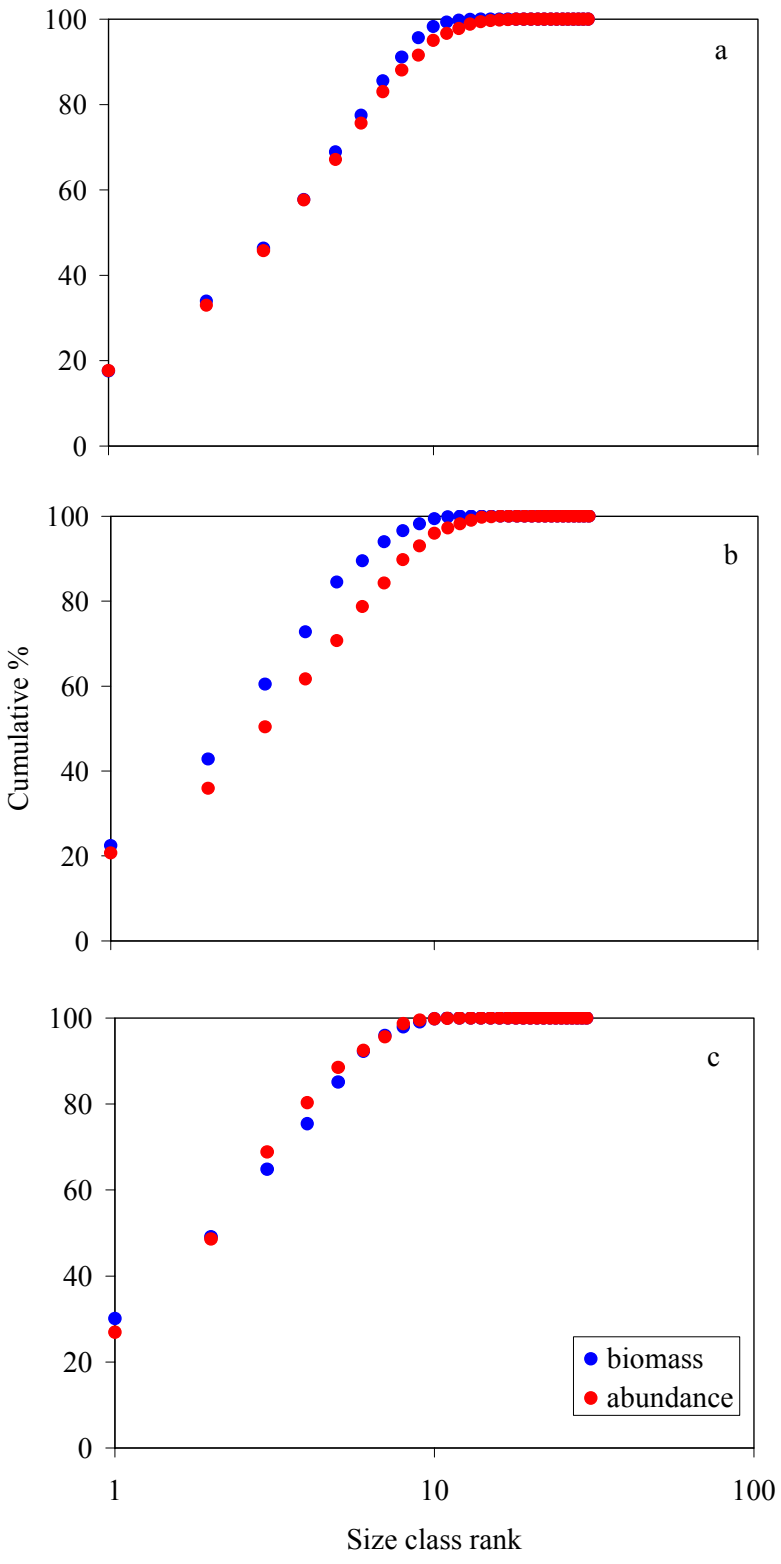


Figure 4.3. ABC plots for the macrofaunal size fraction (> 500 µm) at the (a) FG, (b) FSC and (c) OM locations.

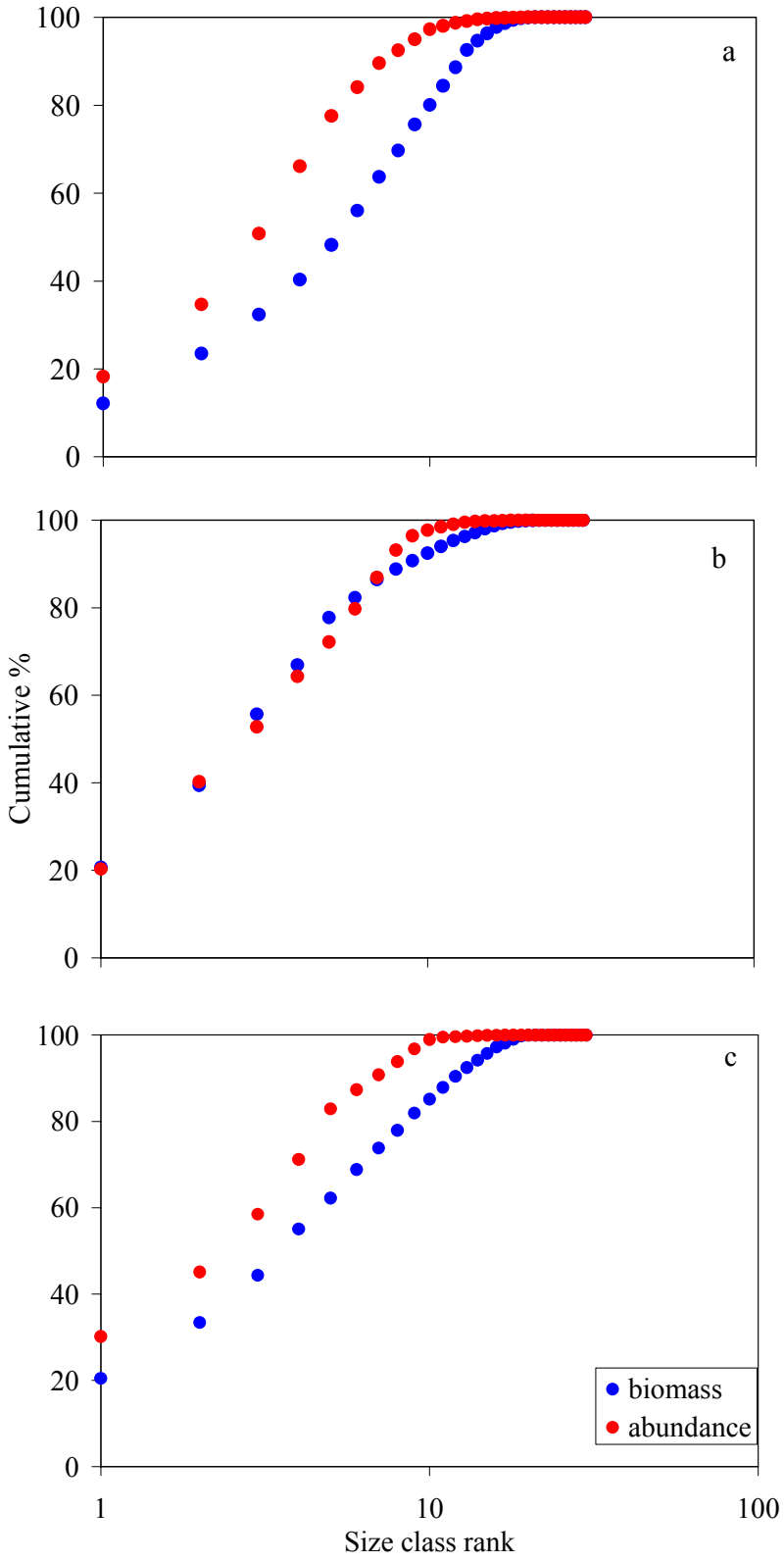


Figure 4.4. ABC plots for all the data at the (a) FG, (b) FSC and (c) OM locations.

the increased proportion of smaller body sizes combined with high overall numeric dominance led to the observed trends. As stated by Warwick (1986), it is unclear how well the community-wide ABC plots (e.g. including all size fractions) reflect the degree of disturbance in benthic communities.

### 4.5 Comparison with previous studies

Macrofaunal abundance at the FG site has been reported to vary from 2,429 to 6,362 ind. $m^{-2}$ (McIntyre, 1961; Hartwig et al., 1983; De Wilde et al., 1986). The estimate from the current study (6,551 ind. $m^{-2}$) is slightly higher but of the same order as the previously determined values. The abundance of meiofauna has been reported to range from 900,000 to 2,700,000 ind. $m^{-2}$ (De Wilde et al., 1986; Faubel et al., 1983) with the current estimate of 580,000 ind. $m^{-2}$ representing a slightly lower value.

The biomass estimate of the macrofaunal size fraction (9.4 g wwt $m^{-2}$) compares favourably with the range of values reported previously (5.6 – 42.8 g wwt $m^{-2}$; McIntyre, 1961; Hartwig et al., 1983; De Wilde et al., 1986). The estimate of 42.8 g wwt $m^{-2}$ included individuals of the large bivalve species *Arctica islandica* that were not observed in the current study. Excluding *A. islandica*, De Wilde et al. (1986) reported a biomass value of 14.4 g wwt $m^{-2}$ for the macrofaunal size fraction. The meiofaunal biomass in this study was somewhat lower than previously reported values (1.2-8.4 g wwt $m^{-2}$; De Wilde et al., 1986; Faubel et al., 1983) probably reflecting the lower abundances at this size fraction. In general, polychaetes and nematodes dominated the biomass and abundance in all studies of macro- and meio-faunal size ranges, respectively.

At the FSC site the abundance of macrofauna (2,609 ind. $m^{-2}$) was very similar to other estimates reported from this site recently (~2,500 ind. $m^{-2}$; e.g. Bett, 2001). However, the biomass estimate in the current study (9.9 g wwt $m^{-2}$) was approximately twice as high as previously published literature values (5.0 g wwt $m^{-2}$; Bett, 2000). In terms of taxonomic dominants, polychaetes and sipunculids have been reported to contribute the most to both total abundance and biomass in all studies.

Levin et al. (2000) reported mean macrofaunal abundance of 12,363 ind. $m^{-2}$ in the core of the OMZ (400 m) off the coast of Oman. This was about three times the estimate from the current study (4,244 ind. $m^{-2}$). Similarly Levin et al.'s biomass estimate (15.0 g wwt $m^{-2}$) was reported as more than five times higher than in this study (2.7 g wwt $m^{-2}$). Levin et al. (2000) stated that the macrofaunal size fraction was largely dominated by Spionidae and Cirratulidae polychaetes. Although representatives of these taxa were also observed in this study, the samples were largely dominated by smaller Ampharetidae polychaetes. The lower abundance coupled with smaller body size of Ampharetidae may have accounted for the lower biomass estimate. Cook et al. (2000) provided estimates of mean nematode abundance at the same location as Levin et al. as 1,700,000 ind. $m^{-2}$, which was also higher than the current meiofaunal abundance estimate of 1,033,000 ind. $m^{-2}$ (OM meiofauna consisted almost exclusively of nematodes).

The benthic communities at FG, FSC and OM sites are generally similar to those previously described for these locations. The observed deviations are likely to reflect natural variations and may be related to different sampling times (seasonality),

slightly different geographic locations (e.g. Oman Margin) and small-scale variation in environmental conditions (e.g. sediment and hydrodynamic conditions).

# 5. BENTHIC SIZE SPECTRA

## 5.1 Introduction

Body size structure is an important attribute of any community. As a number of physiological processes are closely linked to individual body size, the community size structure may provide an insight into community functioning. Consequently the understanding of size distributions forms an important tool in describing, comparing and making predictions about marine ecosystems (Rasmussen, 1993). This chapter concentrates on characterising the benthic communities in terms of their biomass and abundance size structures. These basic patterns and relations will then serve as a foundation for the subsequent chapters that utilise the size spectra in testing the hypothesis of body size miniaturisation in the deep-sea benthos (chapter 6), estimating the benthic secondary production (chapter 7) and developing a size-based simulation model (chapter 8).

Sheldon et al. (1972) were the first to describe the size structure of aquatic communities in detail. Their observations indicated that pelagic size structure was characterised by an even biomass distribution across the size classes. In other words, organisms ranging in size from bacteria to whales, all contributed an equal amount of biomass within their $\log_2$- scaled size classes. These results were further analysed in terms of energy transfer models that incorporated size-dependent metabolism and constant predator-prey size ratios and the results suggested a slightly decreasing biomass trend with increasing body size (Kerr, 1974; Platt & Denman, 1978). The original work of Sheldon et al. (1972) has subsequently served as a basis for a number

of studies that have applied the size spectral approach to a wide range of marine environments.

For example, the application of spectral methods to benthic metazoan communities resulted in a bimodal distribution with the peaks corresponding to meio- and macro-fauna, respectively (Schwinghamer, 1981; Warwick, 1984). This observed size distribution pattern was claimed to be conservative in nature and was widely accepted as confirmation that the previously operationally defined components of meio- and macro-fauna represented functionally distinct entities as well (Giere, 1993). The bimodal pattern was observed for both biomass and species size spectra alike, although subsequent research efforts on biomass distributions have often failed to reproduce these results suggesting that the dichotomy in biomass distributions may not be as conservative a feature of benthic communities as first thought (Strayer, 1986; Drgas et al., 1998; Duplisea & Dragas, 1999; Duplisea, 2000).

The first objective of this chapter is to present the results for the biomass and abundance size spectral analyses carried out for the meio-, meso- and macro-fauna from three environmentally contrasting habitats: a deep-water location in the Faroe-Shetland Channel (FSC; 1600 m), a shallow-water location on the Fladen Ground, North Sea (FG; 150 m) and a mid-slope oxygen minimum zone location on the Oman Margin, Arabian Sea (OM; 500 m). The results will help to improve our current understanding of the benthic communities: for instance, a bimodal size distribution would provide further evidence for the claims that meio- and macro-fauna represent two functionally distinct components of benthos. Conversely, a continuous body size distribution lacking a distinct biomass trough would suggest that either the two faunal

groups are only operationally defined entities along a common biomass continuum or that biomass and abundance spectra are not suitable measures of the possible distinctions.

The second objective involves the comparison of the three sampling locations and the investigation of how environmental factors influence the shape of the body size distributions. Several studies have investigated the effect of habitat architecture (Schwinghamer, 1981; Duplisea & Drgas, 1999; Leaper et al., 2001), organic enrichment (Schwinghamer, 1988; Raffaelli et al., 2000), predation (Raffaelli et al., 2000), trawling (Duplisea et al., 2002) and reduced oxygen levels (Vanaverbeke et al., 2003; Quiroga et al., 2005) on benthic size structure although some of these studies have only considered a subsection of the benthic community (e.g. meio- or macro-fauna or an individual taxonomic component such as nematodes).

The influence of environmental conditions on the body size distribution patterns was assessed by comparing the FG and FSC sites to examine if community size structure changes with increasing water depth. The second comparison was established between the oxygen minimum zone location in the Arabian Sea and the two well-oxygenated NE Atlantic sites allowing the examination of how benthic community size structure is influenced by the reduced ambient oxygen concentrations coupled with the increased flux of organic material from the overlying surface waters.

## 5.2 Methods

As noted in chapter 1, biomass size spectra can be constructed by using several techniques. This section briefly summarises the types of spectra and the statistical procedures applied in the analysis. More detailed descriptions of the statistical methods are provided in chapter 3.

Regular size spectra have been constructed for biomass and abundance data by using X2 geometric groupings of organism wet weight (in g) on the *x*-axis and $\log_{10}$ wet biomass or abundance on the *y*-axis. Each body size class is twice the size of the class below ranging from the smallest organisms in class 0 (0.02-0.04 μg) to the largest in the size class 29 (10-20 g). Due to the heteroscedastic nature of the data, Games-Howell unplanned multiple comparison test is used to test for significant differences in the total biomass amongst the different size classes.

Relative biomass and abundance spectra are also constructed by converting the data within the X2 size classes into percentages. This allows a direct visual and statistical (ANOSIM) comparison of the shapes of the spectra between the different study locations. The biomass distributions from the current study are also compared to the data provided by Schwinghamer (1981). Instead of using X2 geometric wet weight classes on the *x*-axis, Schwinghamer expressed the size classes in terms of equivalent spherical diameters on a $\log_2$ scale. Consequently the data from the current study have also been reallocated into ESD size classes (e.g. 250-500 μm, 500-1000 μm etc).

Cumulative frequency size spectra have been constructed for both biomass and abundance. The cumulative abundance size spectra are particularly useful in gauging differences in the individual body size distributions between the different sites and these are presented and discussed in greater detail in chapter 6 that concentrates on body size miniaturisation in the deep-sea.

Regression analyses have been carried out on the regular size spectra although the differential width of the size classes can complicate this analysis. Because of the logarithmic scaling, the smaller size classes contain organisms of similar sizes (e.g. size class 4: 0.3-0.6 μg) whereas the larger size classes consist of organisms with a wider size range (e.g. size class 29: 10-20 g). Platt and Denman (1978) suggested that dividing the total biomass by the width of the size class will help to overcome this problem and called the resulting biomass distribution a normalised size spectrum. Consequently regression analyses have also been carried out on the normalised biomass size spectra.

## 5.3 Results

The size range of taxa varies over 10 orders of magnitude ranging from the smallest organisms in class 0 (0.03 μg; for all three sites) to the largest in class 29 (15 g), 22 (0.1 g) and 20 (0.03 g) for FG, FSC and OM, respectively. The investigation of benthic body size structure is inevitably subjected to artifacts (see chapter 3). The biomass decrease in size classes 1-4 (rounded shapes of the spectra; e.g. figure 5.1) represented the limitations associated with sieving at the smallest mesh size. The increased variability at the largest size classes could be attributed to unreliable sampling of the larger organisms (sampled surface area too small). Consequently the reliable parts of the spectra extended from size class 5 to size class 20.

The general shapes of the regular biomass spectra are observed to be similar at all three sites. All spectra are characterised by biomass increasing more rapidly through the smaller size classes with the rate of increase slowing at the larger end (figures 5.1, 5.2 & 5.3). At the FG and FSC sites a slight decrease in biomass is evident between the size classes 12 and 15. At the OM site similar decrease in biomass can be observed between size classes 10 and 13. FG location is characterised by local biomass maximum around size class 10. This is mainly attributed to the increased abundance of small bivalves (Veneroidea), gastropods (Philinidae) and polychaetes (Opheliidae). Although some signs of bimodality could be observed in the regular biomass size spectra, particularly at the OM site, none of the size classes across the reliable parts of the spectra are found to be significantly different from one another (G-H unplanned comparison).

The abundance spectra at the FG and FSC locations are characterised by a common trend of constant abundance at the smallest size classes followed by a more rapid decrease between size classes 8 and 15 (figures 5.4 & 5.5). The decreasing trend in faunal densities continues at higher size classes although at a slower rate than at the intermediate body sizes. At the FG location the presence of increased numbers of small bivalves, gastropods and polychaetes is again detected as a local abundance maximum around size class 10. The shape of the OM site combined abundance spectrum follows an approximately similar pattern although a high degree of variability can be observed between the individual replicates (figure 5.6).

The shapes of the biomass and abundance spectra can be compared for the three study locations (figures 5.7 & 5.8). As differences exist between the total biomass present at each site (elevations of the spectra along the *y*-axis), the biomass recorded at any size class is expressed as a percentage of the total thus resulting in the construction of relative biomass size spectra allowing a direct comparison between the sites. This analysis reveals that FG and FSC locations appear visually similar and the major deviation between the two sites is observed around size class 10 where the local biomass maximum is attributed to the increased number of smaller organisms as discussed above. The OM spectrum displays more variability with local biomass maximum observed at size classes 9 and 15. ANOSIM analysis reveals that the shape of OM biomass spectrum is significantly different from the other two locations ($p < 0.01$). The relative biomass distributions at the FG and FSC sites also differ significantly from one another ($p < 0.05$). These results are further reflected in the cluster analysis and the resulting MDS plots (figure 5.9). The relative abundance spectra produce similar trends to those observed in the relative biomass distributions.

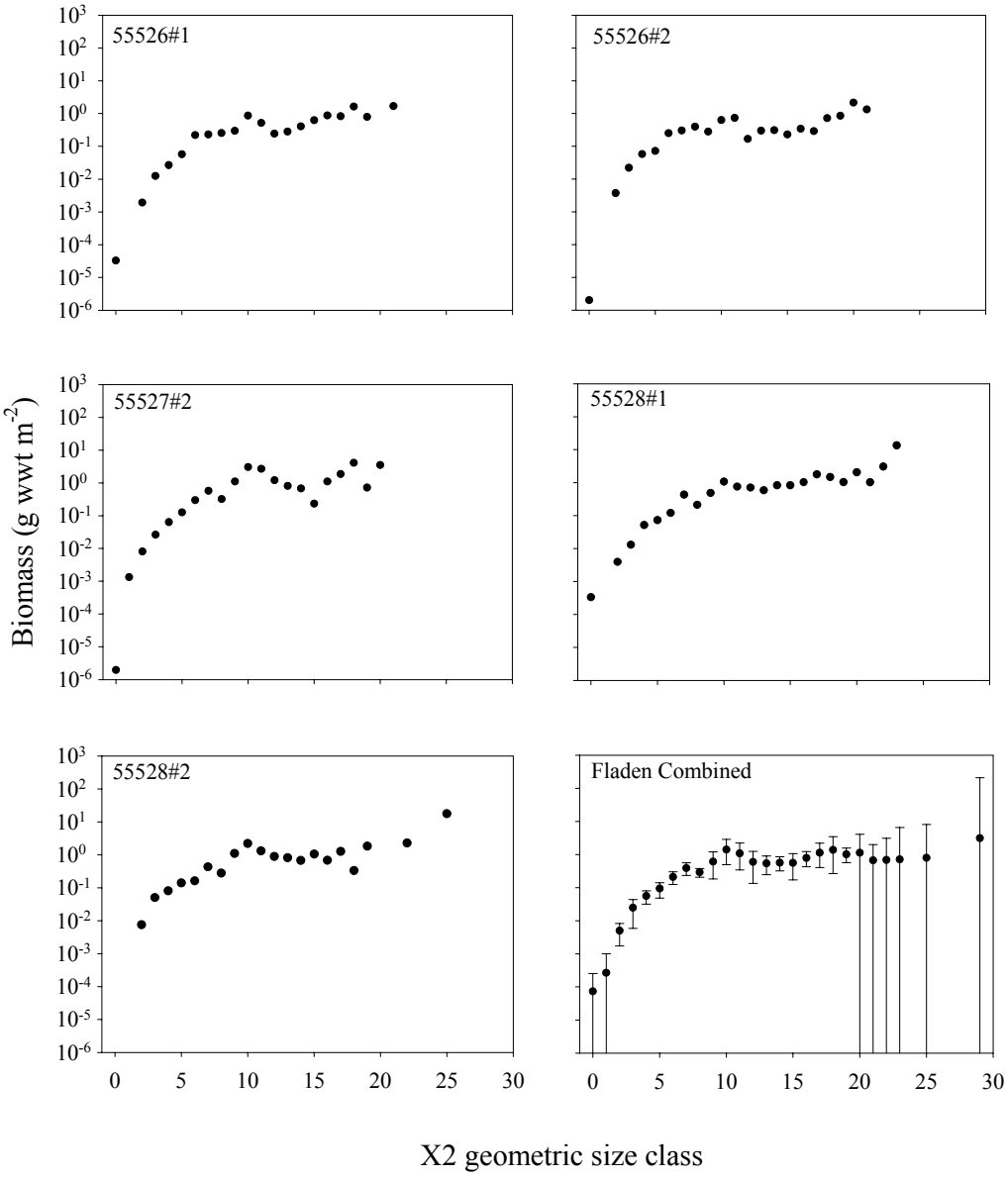


Figure 5.1. Regular biomass size spectra for the five replicate samples from the FG location and the combined spectrum plotted with 95 % confidence intervals.

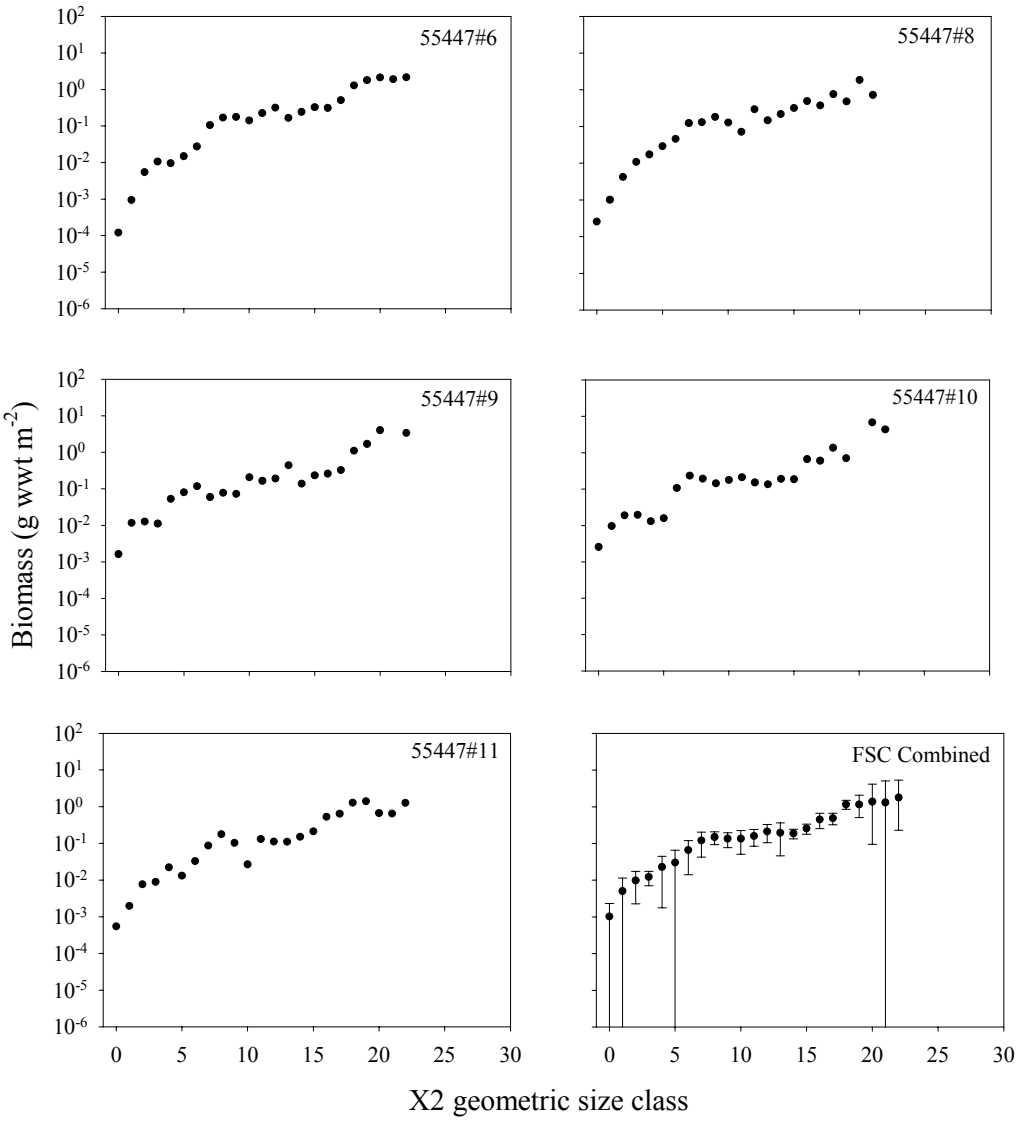


Figure 5.2. Regular biomass size spectra for the five replicate samples from the FSC location and the combined spectrum plotted with 95 % confidence intervals.

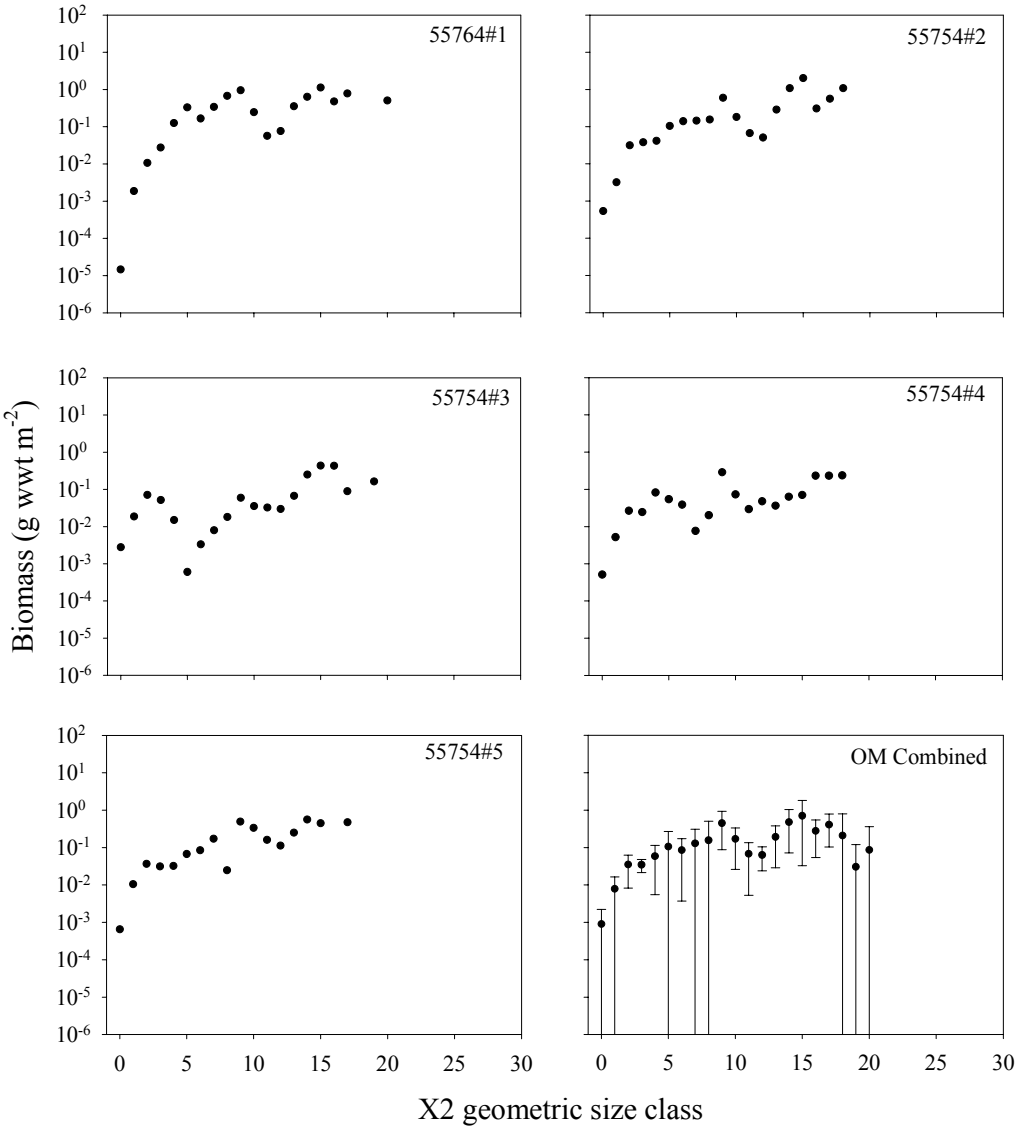


Figure 5.3. Regular biomass size spectra for the five replicate samples from the OM location and the combined spectrum plotted with 95 % confidence intervals.

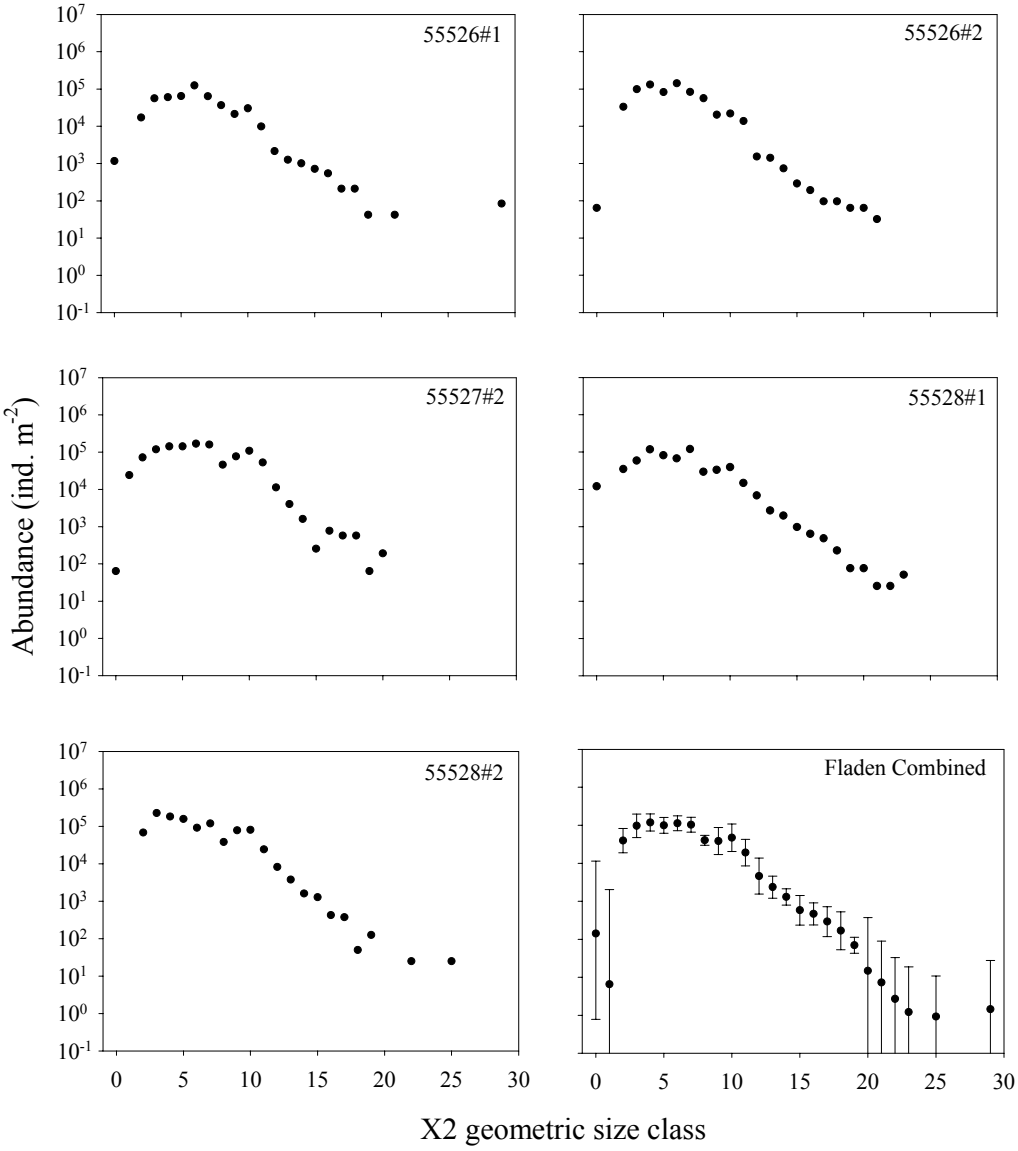


Figure 5.4. Regular abundance size spectra for the five replicate samples from the FG location and the combined spectrum plotted with 95 % confidence intervals.

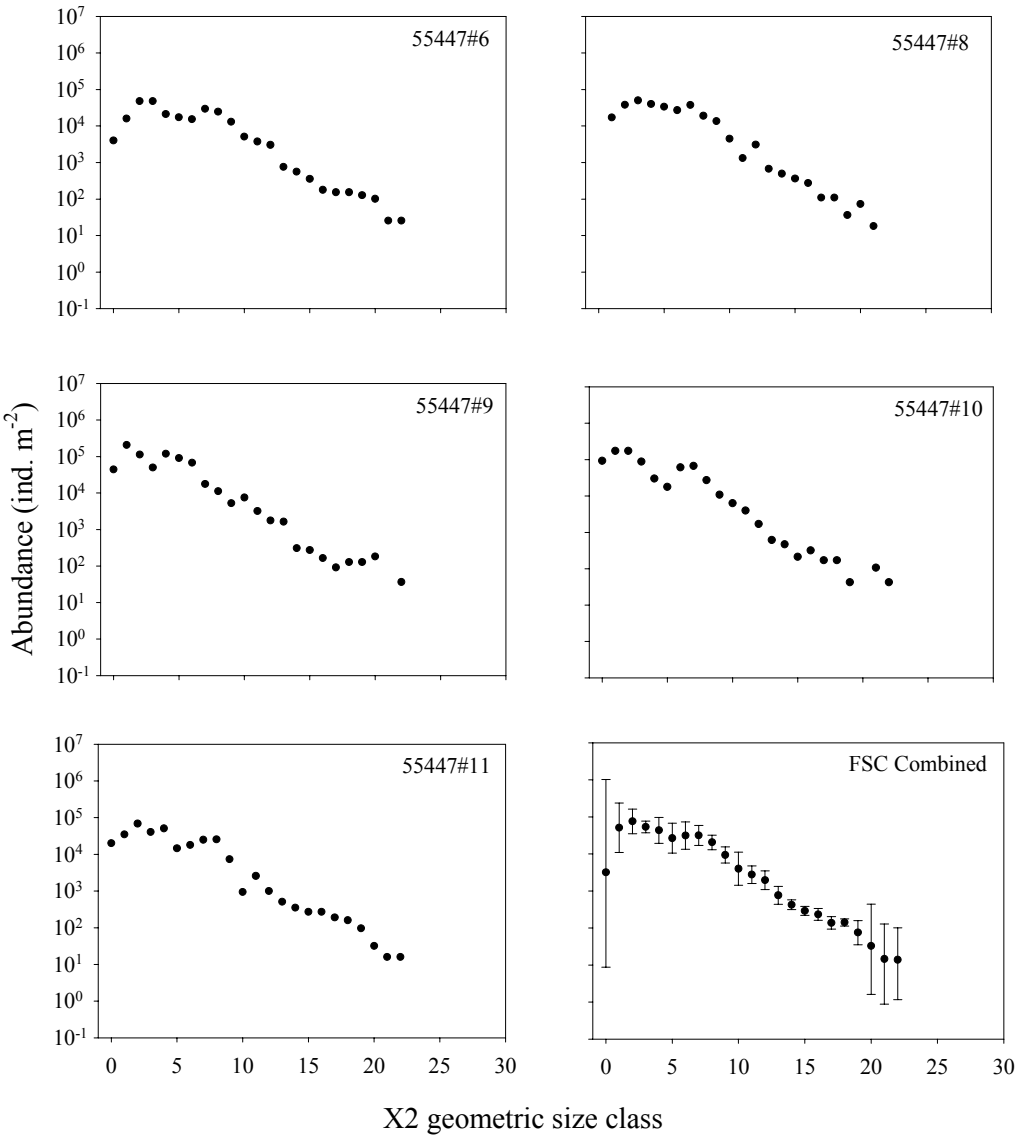


Figure 5.5. Regular abundance size spectra for the five replicate samples from the FSC location and the combined spectrum plotted with 95 % confidence intervals.

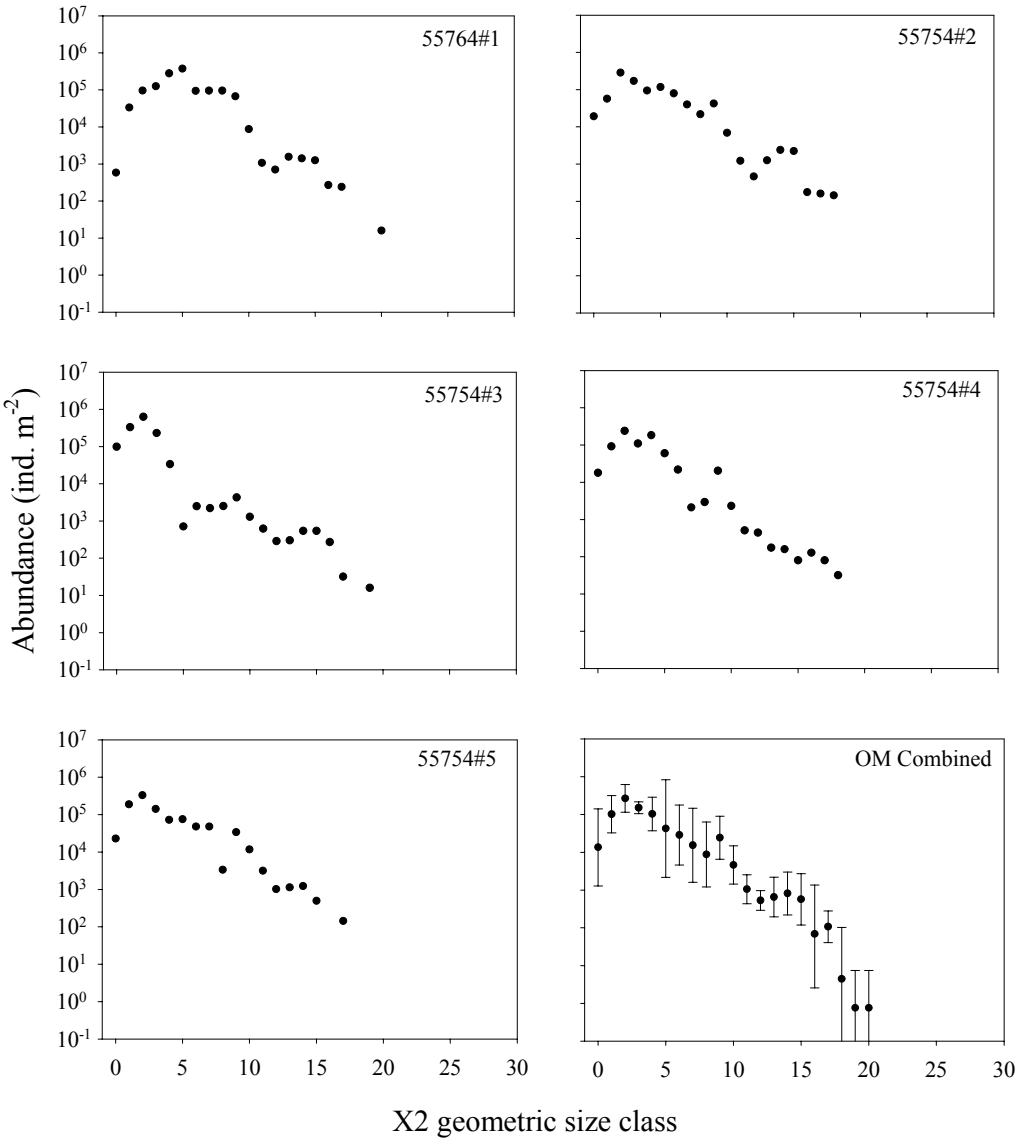


Figure 5.6. Regular abundance size spectra for the five replicate samples from the OM location and the combined spectrum plotted with 95 % confidence intervals.

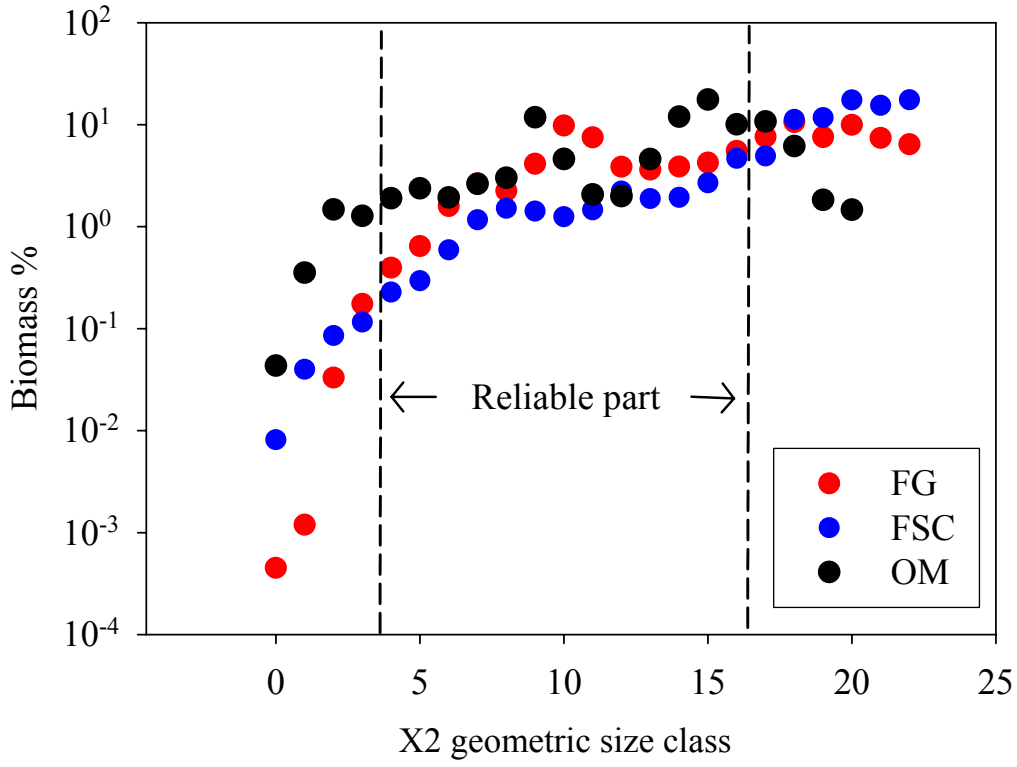


Figure 5.7. Relative biomass size spectra for the three sampling locations. The reliable part of the spectrum is marked on the graph (see text for details).

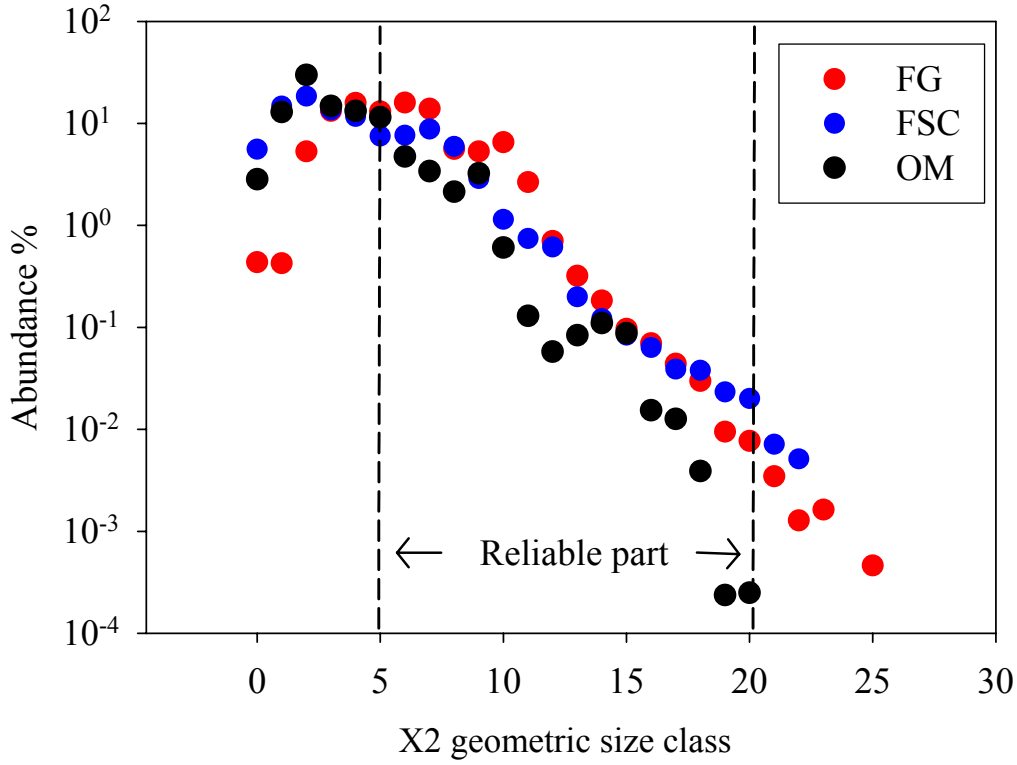


Figure 5.8. Relative abundance size spectra for the three sampling locations. The reliable part of the spectrum is marked on the graph (see text for details).

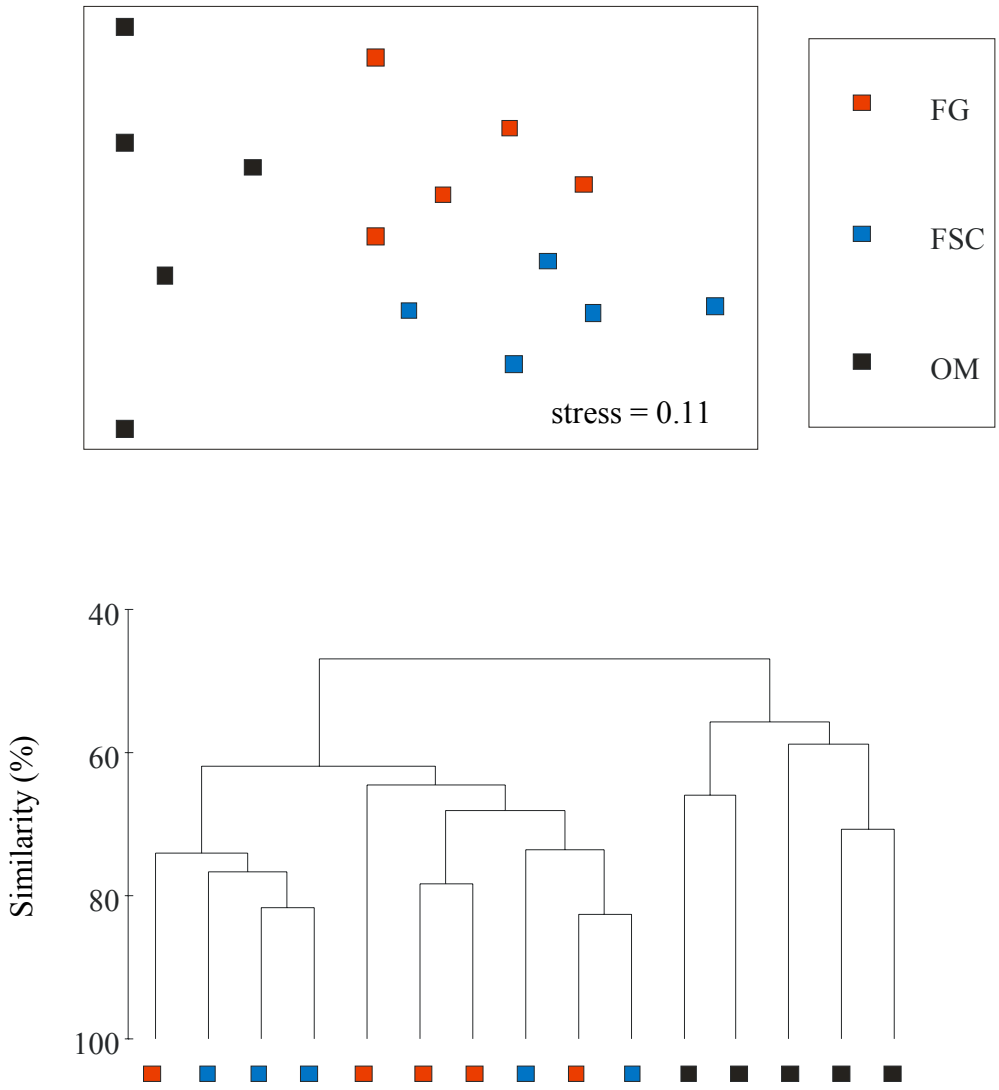


Figure 5.9. MDS ordination and dendrogram presentation of the standardised biomass data from the three study locations. Hierarchical clustering was based on Bray-Curtis similarities derived from untransformed data.

A comparison with the Schwinghamer (1981) data can be carried out by plotting biomass against ESD size classes and then standardising these data to percentage values (figure 5.10). The biomass distributions are similar for the smallest and largest size classes but at the intermediate body sizes the current study sites do not show evidence of the biomass trough observed in the Schwinghamer data. This difference in the relative biomass distribution is statistically quantified by ANOSIM that showed the shape of the Schwinghamer data to differ significantly from the other three locations ($p < 0.05$). The clustering of the four data sets on MDS plots separate the Schwinghamer data from the other locations (figure 5.11). The shapes of the FG, FSC and OM biomass spectra were also found to be significantly different from one another ($p < 0.05$) and they form separate clusters on the MDS plots.

The error bars (data distribution) in the original Schwinghamer data were observed to be particularly large across the reported biomass troughs. When the size spectra in the current study were plotted individually on an ESD scale with their respective 95 percent confidence intervals, the bimodality was not evident (figure 5.12). Furthermore the confidence limits at the current study locations were observed to be smallest across these size classes implying that the reliable parts of the ESD spectra range from 125 μm to 4-8 mm approximately corresponding to the reliable range on the X2 scale.

The cumulative biomass size spectra display similar differences between the three sites (figure 5.13). The distributions of the FG and in particular the OM site spectra resemble the typical sigmoid shape where biomass is accumulated most rapidly at

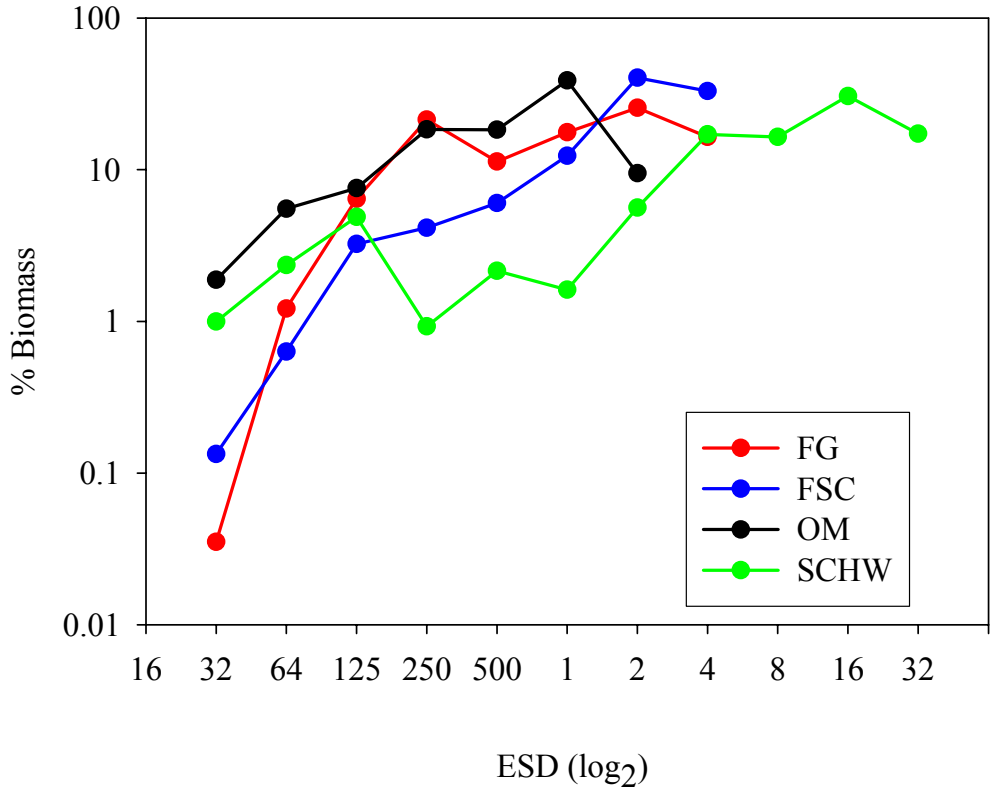


Figure 5.10. Relative ESD biomass size spectra for the three sampling locations and the Schwinghamer data (1981).

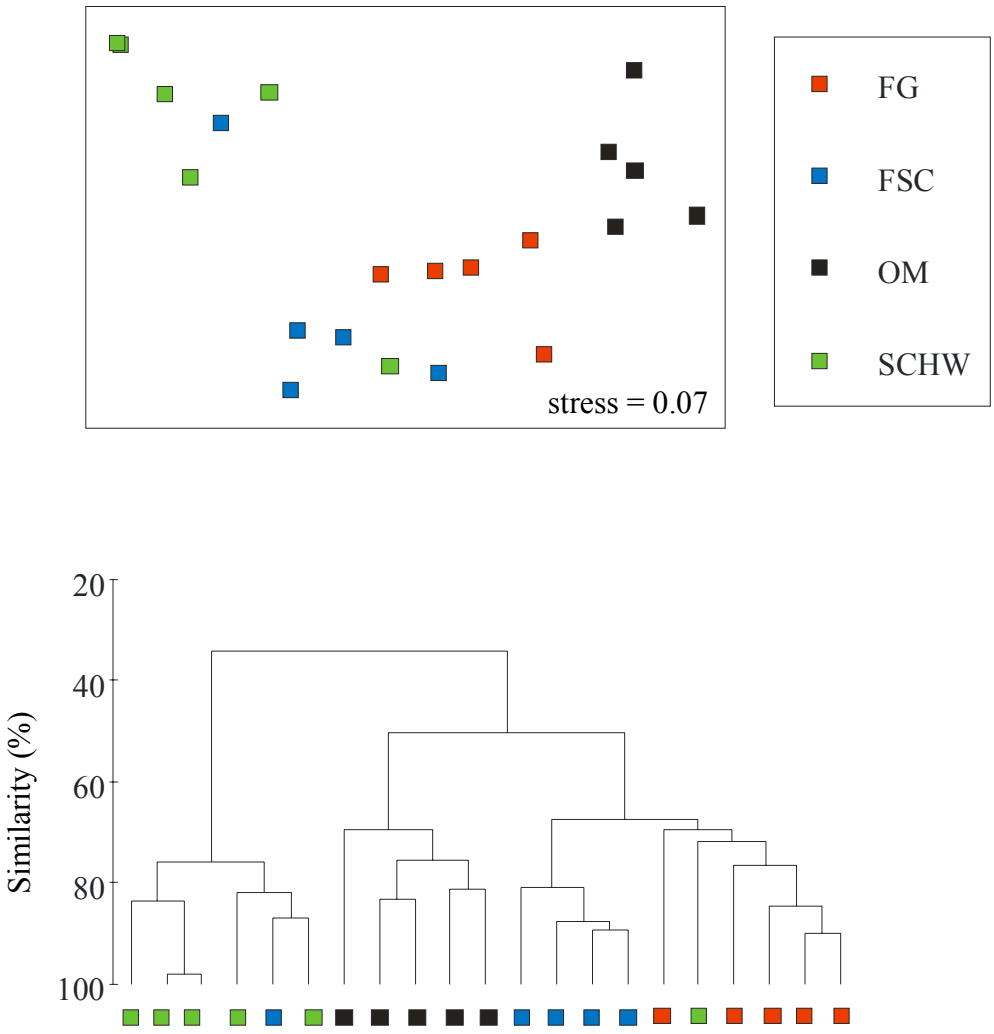


Figure 5.11. MDS ordination and dendrogram presentation of the standardised biomass data from the three study locations and the Schwinghamer data (1981). Hierarchical clustering was based on Bray-Curtis similarities derived from untransformed data.

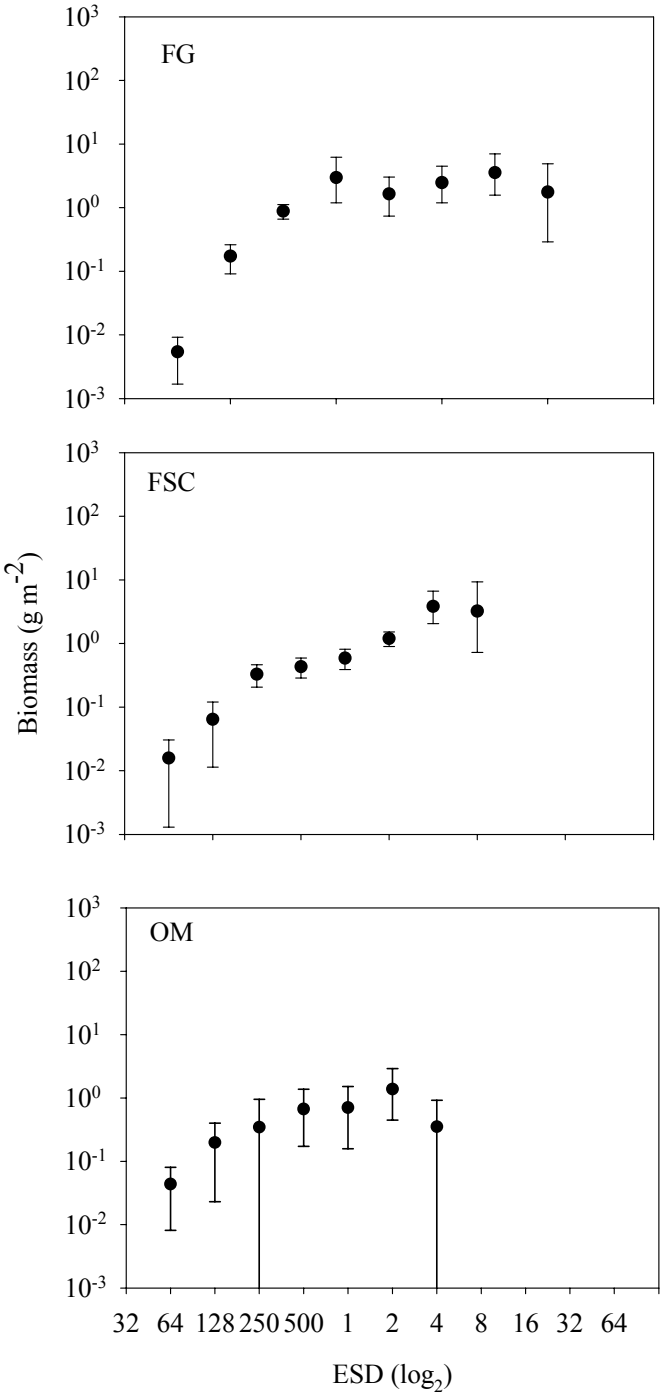


Figure 5.12. ESD biomass size spectra for the three sampling locations with the 95 % confidence intervals.

intermediate size classes with both extremes displaying slower rates of increase. The steepest parts of the accumulation curves for the FG and OM locations fall between size classes 17-21 and 13-17, respectively. The shape of the FSC site curve follows an exponential mode where the largest size classes seem to contribute the most to the total biomass. The cumulative biomass size spectra of the three study locations shift along the *x*-axis with OM spectrum clearly falling on the smallest size classes. The FG spectrum extends the furthest into the larger size classes with the FSC spectrum positioned in between, although this trend is somewhat masked by the relatively small biomass contribution of the intermediate size classes (9-19) at the FSC site. Similar general trends are observed in the cumulative abundance spectra where FSC and OM spectra both display a shift towards smaller body sizes with the FG spectrum extending into larger size classes (figure 5.14).

The regression analyses have been carried out on regular biomass and abundance spectra where both body size (mean weight of each size class) and the total biomass are plotted on $\log_{10}$-scale (figure 5.15). All regressions were found to be significant ($p < 0.01$). The resulting slopes for the biomass distribution vary from 0.185 for FG, 0.258 for OM and 0.322 for FSC. The slope of the FSC regression is found to be significantly different from the slope at the FG site ($p < 0.01$). All the other slopes are not significantly different from one another. The slopes for abundance distribution were recorded as –0.674 for FSC, -0.734 for OM and –0.806 for FG. Again all regressions are significant ($p < 0.01$) and significant differences are observed only between the slopes of FSC and FG locations ($p < 0.01$). Regression analyses have also been carried out for the normalised biomass size spectra ($p < 0.01$) and the slopes for the three locations were recorded as –0.69, -0.82 and –0.97 for FSC, FG and OM,

respectively, with FSC being significantly different from the other two sites ($p < 0.05$; figure 5.16).

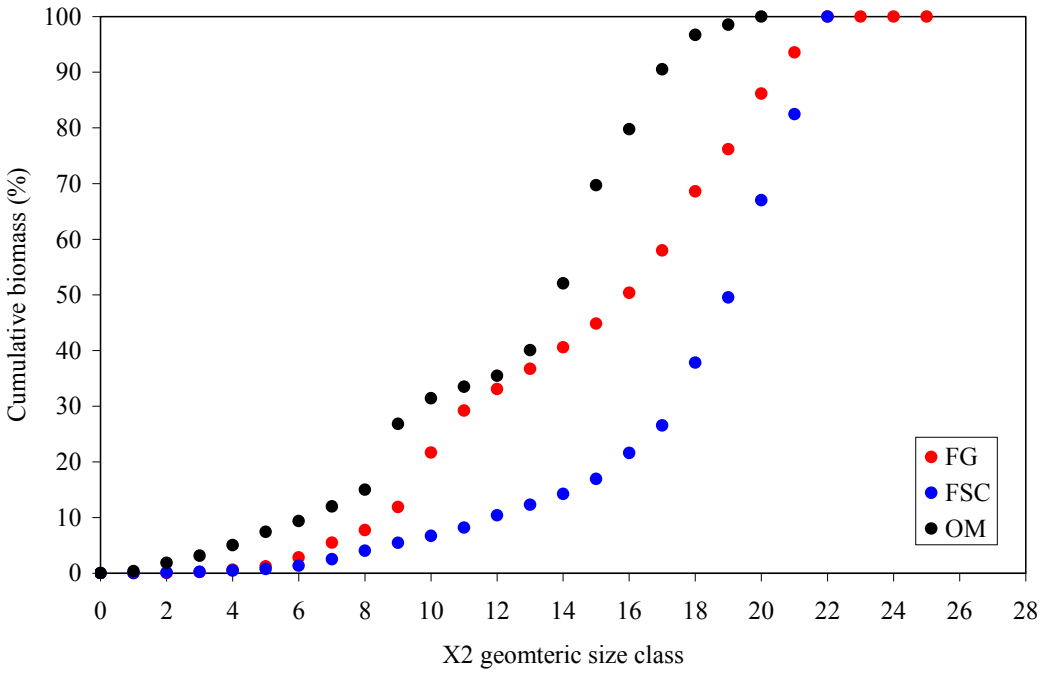


Figure 5.13. Cumulative biomass size spectra for the three study locations.

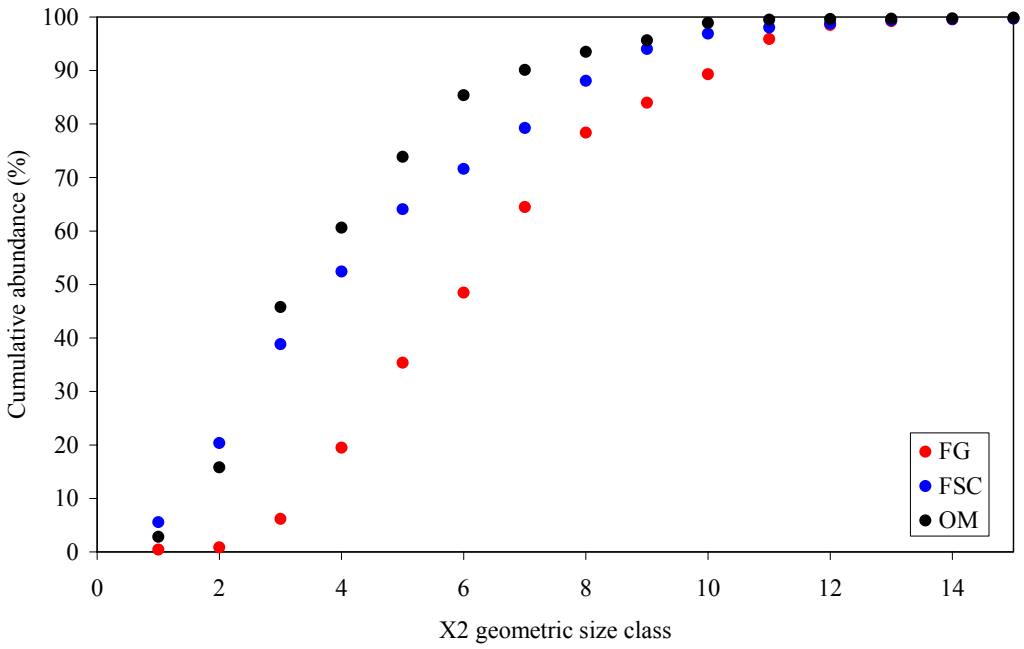


Figure 5.14. Cumulative abundance size spectra for the three study locations. Only the smaller end of the spectrum is displayed to allow a closer inspection of the smaller size classes.

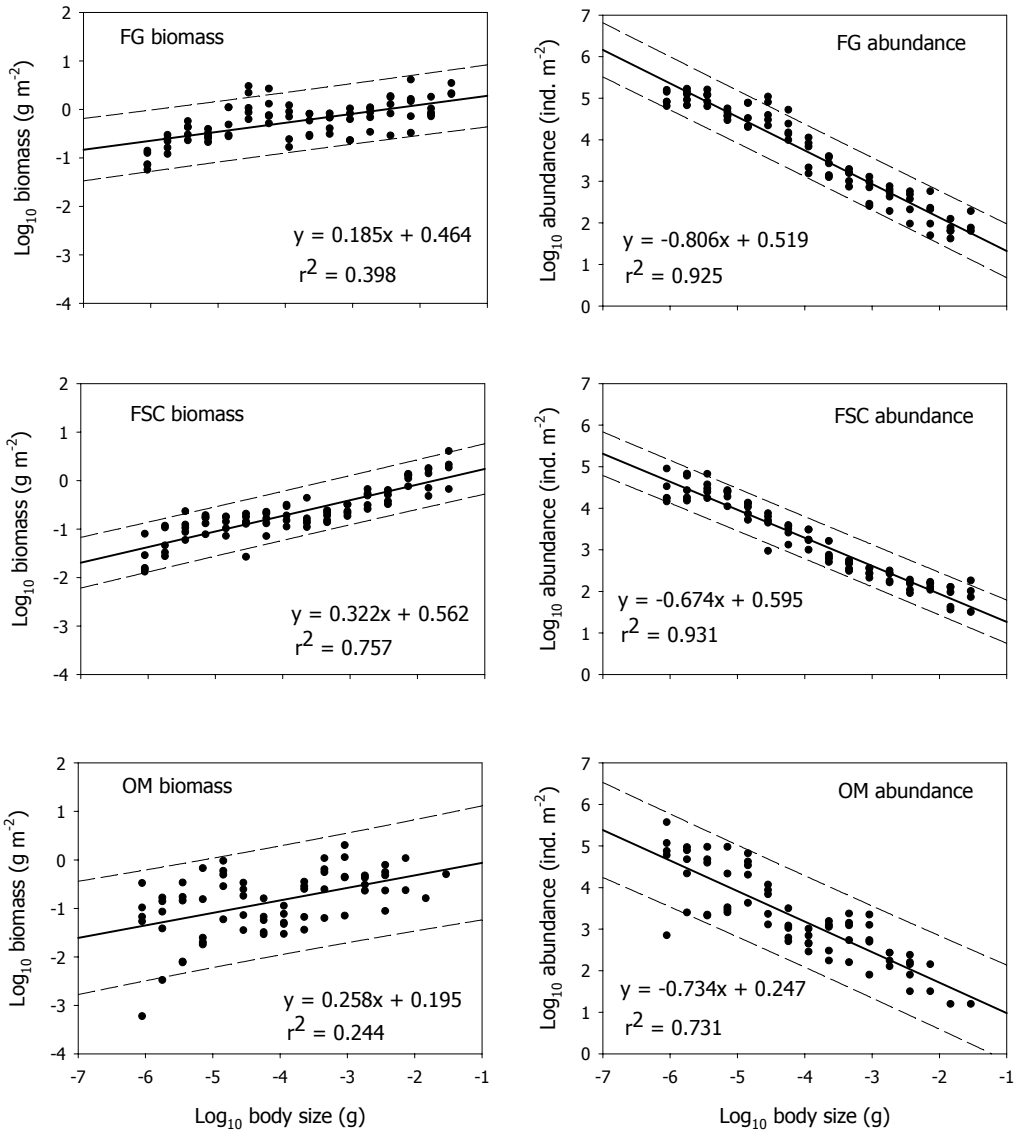


Figure 5.15. Ordinary least squares regression analysis for biomass and abundance at the three study locations. The broken lines represent 95 % prediction intervals. All regressions are significant ($p<0.01$).

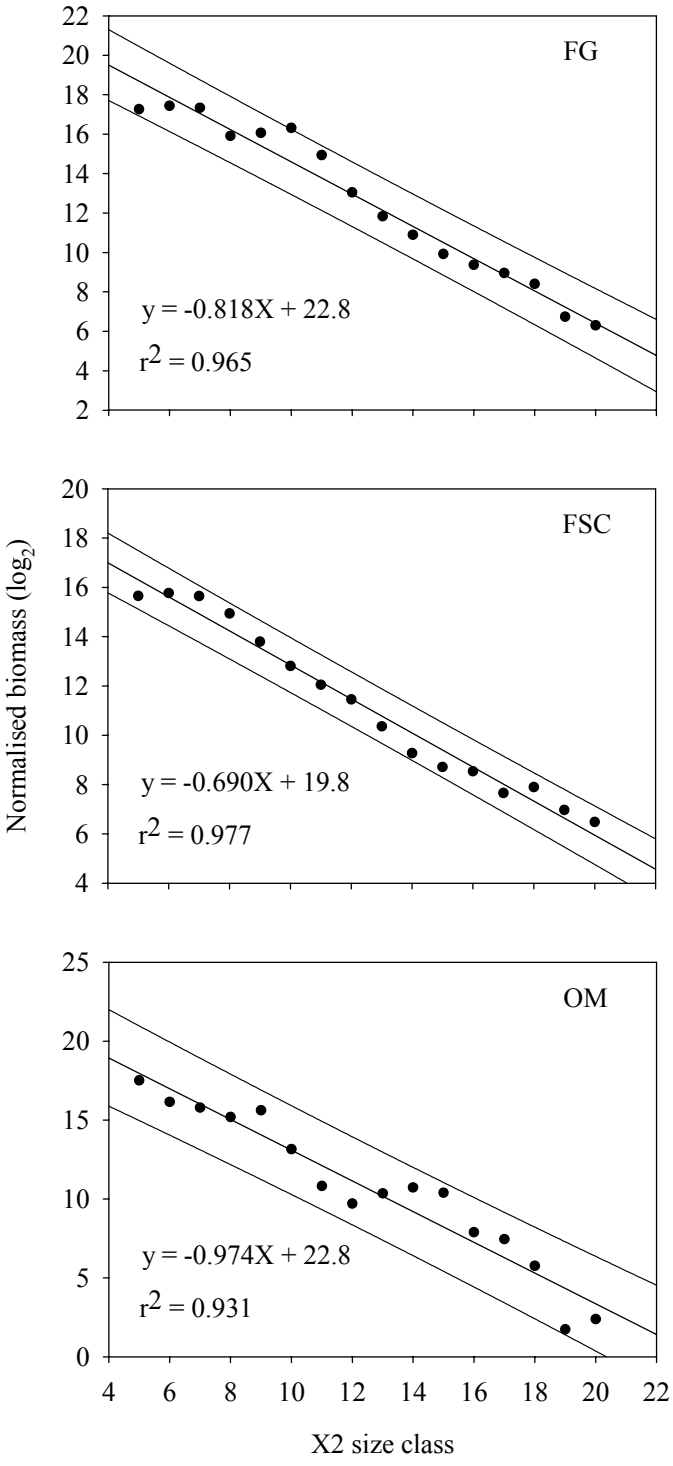


Figure 5.16. Normalised size spectra for the three study locations.

## 5.4 Discussion

### 5.4.1 Shape of the spectrum

The biomass size spectra were observed to follow the same general pattern for all three study locations. The steepest increase in biomass occurred at the smaller size classes (0-10) followed by a shallower trend at the larger end of the spectrum. This pattern could be partly attributed to the sampling limitations resulting in the rounding of the spectra at the smaller size classes and increased variability at the larger end. Visually all three biomass spectra displayed small local biomass minima at intermediate size classes. For FG and FSC sites these minima occurred over the same body size range as the biomass trough reported by Schwinghamer (1981, 1983, 1985). At the OM site the local minimum was more pronounced and occurred at slightly smaller size classes. Despite these small-scale variations, there were no statistical differences detected between the size classes at any of the sites across the reliable part of the spectra.

A more direct comparison with the Schwinghamer data (1981) was obtained by plotting the biomass in ESD size classes. This revealed that none of the current study sites showed evidence of dichotomy. Even the OM site that displayed the most pronounced biomass trough in the regular biomass size spectrum appeared to follow a pattern of biomass increasing with body size. The width of each ESD size class is approximately equal to the combined width of three corresponding X2 size classes and hence the reduced resolution associated with ESD size classification resulted in a failure to detect the local biomass minimum apparent on a finer scale. These visual

observations were further quantified statistically as the ANOSIM analysis showed the shape of the Schwinghamer data to be significantly different from the current study sites. The comparison of the error bars across the size classes for the four locations shows that the variability of the Schwinghamer data is particularly large at the size classes associated with the biomass trough (figure 5.12). This may reflect the fact that samples were collected for meiofauna and macrofauna with a "gap" in sampling in between. The apparent biomass trough may thus represent an artificial and conservative feature associated with repeated inadequate sampling of the organisms that fall between the two size groups. An appropriate sampling of the intermediate body sizes at the other three locations resulted in decreased variability across the size spectra and these locations did not display a statistically quantifiable biomass trough. Despite the small local biomass minima observed in some of the spectra, there is no statistically quantifiable evidence that meio- and macro-fauna displayed separate biomass peaks and the biomass data suggest that the two groups are methodically defined components of the same size continuum.

### 5.4.2 Size spectra in wider context

In addition to Schwingahmer's pioneering work, other studies have also provided evidence that benthic biomass size spectra may be characterised by a local biomass minimum effectively separating meio- and macro-fauna into distinct components (Schwinghamer, 1983, 1985; Gerlach et al., 1985; Cattaneo, 1993). Udalov and Burkovsky (2002) carried out a study in the silty-sandy littoral zone of a White Sea estuary with the sampling stations ranging from strongly desalinated to marine conditions. They collected samples for meio-, meso- and macro-fauna and sampled

the most seaward station monthly over the summer period of 1995 (June-September). They detected a gap in the biomass size spectra in June that corresponded to the biomass trough outlined by Schwinghamer (1981). During the following months this gap was first temporarily filled by juvenile macrofauna settling on the seabed (July) and then re-established as the organisms grew and the juvenile macrobenthos merged with the larger adult population (September).

Stead et al. (2005) also reported distinct bimodality in the biomass size spectra of stony stream metazoan communities during early spring and autumn months. However, the rest of the spectra, constructed at monthly intervals for a 14-month period, conformed more to a unimodal pattern. Lack of bimodality has been reported in a number of other studies from fresh- (Strayer, 1986; Ramsay et al., 1997) and brackish-water environments (Drgas et al., 1998; Duplisea & Drgas, 1999; Duplisea 2000).

Since Schwinghamer (1981) first carried out the spectral analysis of benthic body size structures, the bimodal biomass distribution has been widely quoted in general textbooks as evidence that meio- and macro-fauna form two ecologically distinct components of the benthic community (Parsons et al., 1984; Giere, 1993). However, it is clear that the biomass size spectra constructed for a number of marine and limnic environments have not followed a single pattern as has been suggested previously. Possible causes of this apparent variation range from inadequate sample collection and analysis protocols to inherent natural community functions.

### 5.4.3 What causes the variability in the benthic community size structures?

#### *5.4.3.1 Sampling artifacts*

As already discussed, a non-continuous sampling of the benthic fauna is likely to produce a non-continuous size distribution. If samples are specifically collected for meio- and macro-fauna, it is not surprising that reduced biomass levels are observed where there are effectively gaps in the data. The organisms intermediate in size between meio- and macro-fauna need to be sampled by an appropriate combination of sieve mesh- and sample-sizes relevant to those particular body sizes. Lack of such targeted sampling can lead to increased variation in the data. It is also important to recognise and account for the inherent limitations of any sampling protocol associated with mesh- and sample-size at small and large size classes (see also chapter 3).

The choice of sampling gear may also influence the perceived community size structure. For instance, a recent study comparing the performance of a standard deep-sea box corer and a hydraulically-damped megacorer revealed that box corer samples underestimated the macrofaunal abundance by approximately 50 % (Bett et al., submitted). This apparent loss of individuals in the box corer samples was attributed to the bow wave effect associated with the deployment of this sampler. Bett et al. (submitted) also reported that there was a tendency for smaller species to be more abundant in the megacorer samples implying that they are more likely to be influenced by the bow wave effect. Similar influence can be expected for other sampling devices that present a high resistance as they pass through the water column. It is likely that at least some of the variability observed in the biomass distribution patterns in the past can be accounted for by the inadequate collection and/or analysis

of the benthic samples. In the current study the emphasis was on obtaining high-quality sediment samples and analysing these with a combination of relevant sieve mesh sizes and sample surface areas.

*5.4.3.2 Community processes as source of variation*

Another source of variation in the observed biomass size spectra patterns may arise as a result of the natural processes within benthic communities. Warwick (1984), investigating *species* rather than *biomass* size spectra, explained the observed bimodality as a consequence of the macrobenthos having a planktonic life phase. According to Warwick (1989), meiobenthos are regarded as being the evolutionary oldest faunal component forming a highly efficient consumer unit due to their high species diversity and variety of narrowly specialised feeding mechanisms. Most macrofaunal species with planktotrophic development produce eggs, and hence hatching larvae, that fall in the same size category as meiofauna. In order to avoid competition and predation these larvae escape to the water column. They do not settle back on the seabed until they are large enough to avoid direct interactions with meiofaunal organisms. This size also corresponds to the claimed biomass and species trough in the size spectra as well as the typical size of holoplanktonic organisms that would cause competition with extended pelagic existence.

Udalov and Burkovsky (2002) also concluded that the bimodal *biomass* pattern resulted from the planktotrophic development of most macrobenthic organisms combined with the relatively small proportion of species with direct development. They demonstrated this pattern to breakdown in the upper reaches of the estuary

where the biomass distribution was observed to be more continuous with biomass increasing with body size. They attributed this altered pattern to the increased presence of taxa with direct development resulting in the meio- and macro-benthos merging into a single unit.

According to this hypothesis, the bimodal biomass distribution should start to breakdown in environments where organisms either display direct or lecithotrophic development modes. Warwick (1989) predicted such environments to include fresh- and deep-water habitats as well as polar regions. Although freshwater studies have produced unimodal biomass size distributions (Strayer, 1986; Morin & Nadon, 1991; Bourassa & Morin, 1995) others have shown signs of bimodality (Poff et al., 1993; Stead et al., 2005). Schwinghamer (1985) showed deep-sea biomass size spectra to follow the bimodal pattern but these results may reflect the sampling techniques and protocols used. To the best of my knowledge, no *biomass* size spectra have been constructed for the benthic infauna as a whole from polar regions. Kendal et al. (1997) constructed *species* size spectra for Arctic communities and these displayed a distinct dichotomy contrary to the hypothesis suggested by Warwick.

Udalov and Burkovsky (2002) also predicted that the observed bimodality is closely linked to seasonality. In temperate latitudes reproductive events (e.g. planktonic life phase and settlement) proceed during the summer months when primary production is at its peak. Conversely, in moderate and tropical latitudes reproduction can be extended over most of the year with a more continuous supply of larvae to the seabed resulting in a more continuous biomass size spectrum.

Both empirical data and theoretical considerations would suggest that biomass distribution patterns are highly dynamic both in space and time. The variability observed in the biomass size spectra would suggest that bimodality is not a conservative or universal feature and if the biomass distributions had to be described by a single, general pattern then the continuously increasing biomass with increasing body size would probably provide the best approximation. This trend was repeatedly observed in the current study although the OM site did show some evidence of bimodality.

Local, small-scale variation and even distinct biomass troughs can arise as a result of processes such as macrofaunal reproduction and its associated patterns. Although these deviations from the continuously increasing biomass distribution can provide some evidence that meio-and macro-fauna are two functionally distinct components of the benthos, biomass size spectra in general are not effective in distinguishing the two groups. This generalisation does not necessarily apply to species size spectra (e.g. Warwick, 1984).

### 5.4.4. The effect of environmental factors on the size spectra

The current study sites allowed a direct assessment of how two major environmental parameters influence the size distributions. Fladen Ground and Faroe-Shetland Channel represented sampling stations of contrasting water depth but otherwise share similar environments. Bathymetry is often related to the amount of organic matter that reaches the seabed with the food concentration decreasing with increasing water depth. As expected, the standing stock at the FSC location was found to be

significantly lower than at the FG site. The aim of this comparison was to determine whether the size spectra of the two sites also differed.

The Oman Margin site samples contrast with the two NE Atlantic stations in terms of ambient oxygen concentrations. Although some studies have investigated the effect of reduced oxygen levels on nematode (Vanaverbeke et al., 2003) and macrofaunal (Quiroga et al., 2005) size spectra, no study has examined the effect of hypoxia on the benthic community as a whole.

*5.4.4.1 Bathymetry*

The regular size spectra of the FG and FSC stations mainly differed in their total biomass levels. The FG site spectrum was elevated in relation to the FSC spectrum but the basic shapes of the two spectra appeared similar. The relative and cumulative size spectra showed that the intermediate size classes (9-19) at the FSC site contributed less to the total biomass. Conversely, the cumulative abundance size spectra showed that the small and intermediate size classes contributed more to the total abundance indicating that the benthic community at the FSC location consisted of predominantly smaller individuals. The spectra displayed a shift towards the smaller body sizes with increasing water depth.

Normalised size spectra and the associated regression analysis have been regularly used to compare the size structures between different sites. In the current study all the regressions over the reliable parts of the spectra were significant ($p < 0.01$) and the residual variations were relatively small ($r^2 = 0.931$ to $r^2 = 0.977$). The slope of the

normalised size spectrum can be used to assess the deviations of the community size structure from the steady-state distribution. When the slope equals –1, the biomass is equally distributed among the size classes. Slope values greater (less negative) than –1 indicate that biomass increases with size. In the current study the slopes at both FG and FSC were greater than –1 (-0.82 and –0.69, respectively) and they were also found to be significantly different ($p < 0.05$). The less negative slope at the FSC site is associated with increase of biomass at the larger size classes.

Although the total biomass is significantly lower at the FSC site, the largest size classes at the two locations contained similar amounts of biomass. This was attributed to the presence of a few larger individuals at the FSC site (Ophiuroidea and Sipunculida at size classes 21-22) that were also found to bias the average individual biomass estimates (see chapter 6). The results of this chapter clearly outline the considerable influence of water depth on the community size structure. The reasons for the apparent shifts are discussed in more detail in chapter 6.

*5.4.4.2 Hypoxia*

The data from the OM site showed the largest degree of variation between the individual replicates. As the sampling and analysis protocols were essentially identical at all locations, this variability can only be attributed to natural causes. The shapes of the biomass and abundance spectra differed from the other two study locations regardless of the method of analysis. The regular biomass size spectra displayed the most pronounced local biomass minimum around size classes 11-12 (76

μg wwt). This was also reflected in the relative biomass spectrum that was found to be significantly different from the FG and FSC spectra.

The benthic community at the OM site consisted almost exclusively of nematodes and polychaetes that are thought to be more tolerant of the hypoxic conditions than, for example, harpacticoids or calcified invertebrates (Levin, 2003). The biomass and abundance dominance was found to switch from nematodes to polychaetes abruptly between size classes 9-10 in all the sample replicates. Although the size classes at the OM site were not found to be significantly different, the taxonomic dominance switch coupled with the apparent biomass trough may represent the functional distinction between meiofauna (e.g. nematodes) and macrofauna (e.g. polychaetes) as suggested by Schwinghamer (1981) and Warwick (1984).

Reduction in the ambient oxygen level is thought to influence individual body size. In reduced oxygen conditions the metazoan benthic fauna have often been reported to consist of smaller-sized organisms with macro- and mega-fauna typically rare or absent (Levin, 2003). Chapelle and Peck (1999) suggested that maximum individual body size might be closely controlled by oxygen availability and McClain & Rex (2001) similarly observed a positive relationship between maximum body size and oxygen concentration for gastropods proposing that this might help to explain the pervasive size-depth relationships among deep-sea taxa. These observations suggested that smaller individuals have an advantage in hypoxic environments by presenting a larger surface area: volume ratio. They may also have greater metabolic flexibility that confers an ability to use food resources in the absence of oxygen (Zehnder, 1988).

However, these analyses did not include fauna from oxygen minimum zones. Organisms permanently inhabiting OMZ sediments may have evolved a different set of responses and adaptations to low oxygen levels from those that are temporarily exposed to hypoxia (Levin, 2003). Within OMZs, Foraminiferans are the only taxa that have shown an obvious decrease in body size with decreasing oxygen concentrations. A number of polychaete and nematode taxa have been shown to display an opposing trend of increasing body size with decreasing oxygen concentration (Levin, 2003). In the current study, individual body size was generally shown to be smaller at the OM than at the FG site and of similar size as the organisms of the deeper FSC location (chapter 6).

The slopes of the *normalized biomass size spectra* regression lines were found to be steeper than those recorded for the other two study sites indicating that biomass decreased with body size at the OMZ location. This shift towards smaller body sizes was also recorded in the cumulative biomass and abundance size spectra. Quiroga et al. (2005), investigating the macrofaunal size structure of an OMZ community off Chile, also reported a steeper gradient of regression lines for the fauna inhabiting the permanently low oxygen environment in comparison to well-oxygenated areas. Their slope for the OMZ macrofauna was recorded as –0.837, which is closer to the slopes recorded for the FG (-0.82) and FSC (-0.69) sites than the OM site in the current study (-0.97). When the OM size spectra were restricted to include only the larger size classes (size class 10 upwards) the slope of the resulting regression line was found to be even steeper (-1.015) thus further deviating from the values reported by Quiroga et al. (2005). Vanaverbeke et al. (2003) constructed nematode size spectra for an oxygen-stressed site on the Belgian continental shelf and reported a single class

biomass peak that was attributed to a particular nematode species (*Sabatieria puncata*) thought to be well adapted to highly polluted conditions. The biomass size spectra constructed at the OM site did not show evidence of any one size class noticeably dominating the biomass distributions. A local biomass maximum was observed at size class 9 but the decrease in biomass was probably attributed more to a switch in taxonomic dominance from nematodes to polychaetes than to a specific meiofaunal taxa.

OMZs are not only characterized by reduced oxygen levels but also by increased food availability that varies inversely with oxygen (Levin et al., 2000). This makes it difficult to distinguish their individual effects on the community structure. The food arriving from the surface waters is often relatively undegraded and may arrive in many forms including phytoplankton cell aggregations or, as observed off the coast of Oman, as jellyfish carcasses. These food parcels land on the seabed randomly creating a small-scale mosaic of food patches. The abundance and biomass distributions of benthic populations may reflect this patchiness hence providing a possible mechanism that can result in the increased variability in the biomass and abundance spectra as observed at the OM site. The OMZ size spectra clearly differed from the size distributions observed at the well-oxygenated sites, the most notable changes being the shift towards smaller body sizes and the pronounced biomass minimum effectively separating nematode and polychaete populations from one another.

5.4.5 Conformation to the metabolic theory of ecology

The metabolic theory of ecology predicts how metabolic rate varies with body size and temperature and consequently how this rate imposes controls on ecological processes at all levels of organization from individuals to ecosystems (Brown et al., 2004). At the heart of this theory is the idea that most biological processes can be scaled to body size according to allometric equations as discussed in chapter 1. The unusual property of these allometric equations is that their scaling exponents can be expressed as multiples of 1/4. These quarter-power (or derivatives of thereof) scaling exponents have been reported for a number of biological processes ranging from metabolic rates to abundance and biomass relations (Peters, 1983).

For example, numerical abundance (N) has been predicted to scale with body size (M) as $N = M^{-3/4}$(Peters & Wassenberg, 1978; Damuth, 1981). Biomass (B) can be derived by multiplying population abundance by individual body mass, implying that population biomass can be expected to increase with body size ($B = M^{-3/4}M = M^{1/4}$). As metabolic rate scales with mass as $M^{3/4}$, it has been predicted that the rate of energy use, calculated as the product of individual rate and population density, is independent of the body size ($M^{3/4}M^{-3/4} = M^0$; Peters & Wassenberg, 1978). This is known as the "energetic equivalence hypothesis" and it generally applies to communities that share a common energy source.

However, it has been suggested that in size-structured communities organisms do not share a common energy source and that the energy available to the larger organisms is constrained by inefficient energy transfer through the food chain (Brown & Gillooly,

2003; Dinmore & Jennings, 2004). This would imply that the quarter-power scaling exponent hypothesis would start to breakdown and, for example, the observed scaling of abundance with body size would be steeper. In such cases the energy transfer efficiency would act as limiting factor (R) and the resulting allometric equation could be expressed as $N = [R]M^{-3/4}$ (Brown et al., 2004). In other words, deviations in the scaling exponents from the expected values could suggest that individuals within communities do not feed from a common food source and that more complex trophic relations prevail.

In the current study the scaling exponents of biomass and abundance relations displayed variations around the expected values of 1/4 and –3/4, respectively (figures 5.15 & 5.17; tables 5.1 & 5.2) although the slopes of biomass and abundance relations derived by ordinary least squares regression models differed significantly ($p < 0.05$) from these theoretically expected values at the FG and FSC locations but not at the OM site.

Geometric mean or Reduced Major Axis (RMA) regressions have been claimed to be more relevant in estimating the functional bivariate relations in biological data where natural variation exceeds the measurement variance (Ricker, 1973; Schwinghamer et al., 1986). Consequently the slopes of biomass and abundance relations were also determined by RMA regressions. Although these slopes were found to be significantly different from the theoretical values for biomass relations at the FG and OM locations and for abundance relations at all locations, the RMA regression models produced similar general trends to those observed with the OLS regression models (figure 5.17).

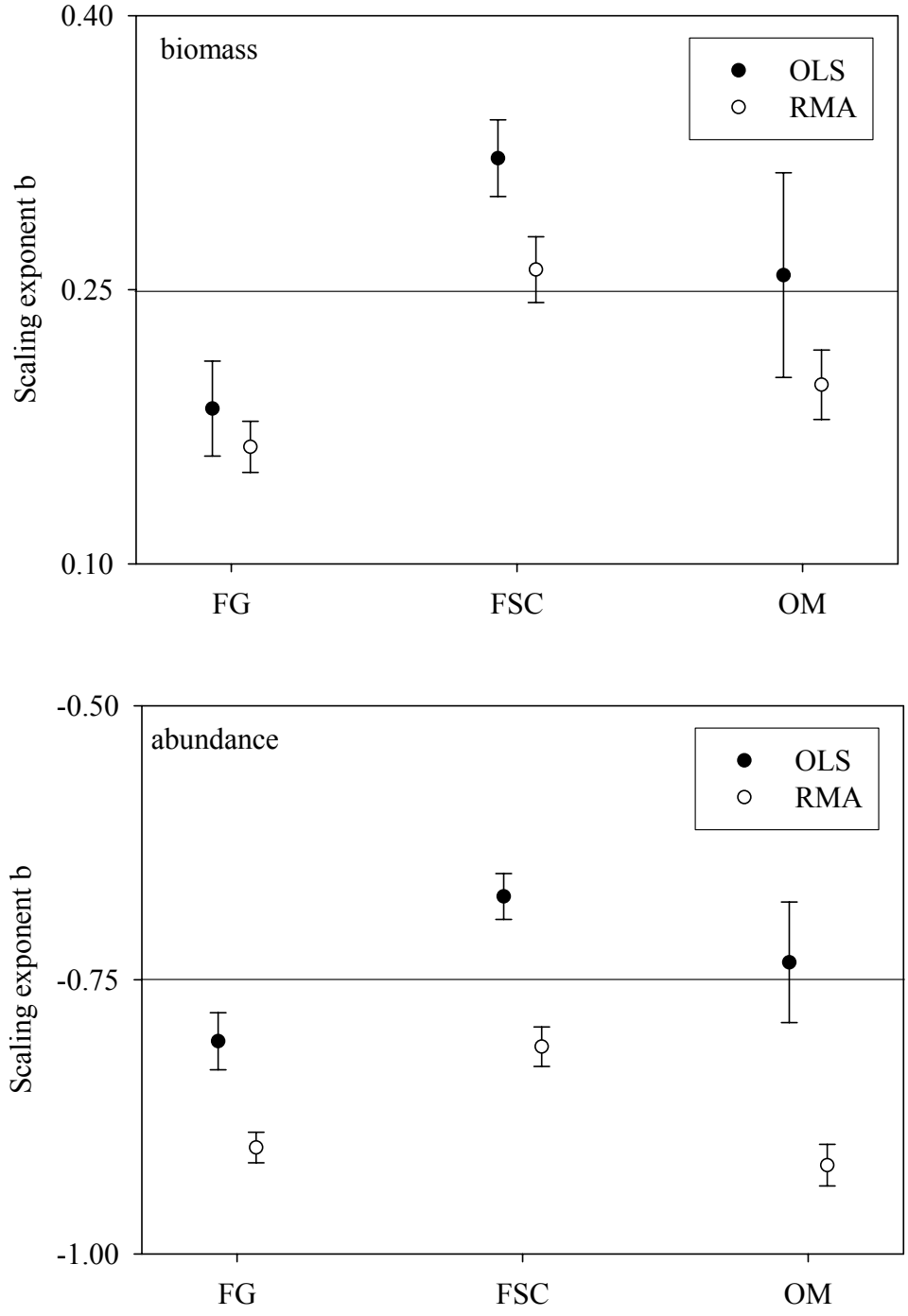


Figure 5.17. Comparison of the scaling exponents from the three study locations to the theoretically expected values of 1/4 and -3/4 for biomass and abundance, respectively. OLS: ordinary least squares regression; RMA: reduced major axis regression (see text for details). Error bars represent standard errors.

Table 5.1. Regression parameters for the regular and normalized biomass size spectra ($Y = \log_{10}a + b\log_{10}X$). All regressions are significant ($p<0.01$). OLS = Ordinary Least Squares regression; RMA = Reduced Major Axis regression; NOLS = Normalised Ordinary Least Squares regression.

| Regression | Location | Slope (b) | Intercept ($\log_{10}a$) | $r^2$ | S.E. slope | S.E. intercept |
|---|---|---|---|---|---|---|
| OLS | FG | 0.185 | 0.464 | 0.398 | 0.026 | 0.107 |
| | FSC | 0.322 | 0.562 | 0.757 | 0.021 | 0.085 |
| | OM | 0.258 | 0.195 | 0.244 | 0.056 | 0.241 |
| RMA | FG | 0.164 | 0.029 | 0.429 | 0.014 | 0.025 |
| | FSC | 0.261 | 0.260 | 0.632 | 0.018 | 0.068 |
| | OM | 0.198 | 0.036 | 0.250 | 0.019 | 0.034 |
| NOLS | FG | -0.818 | 22.77 | 0.965 | 0.042 | 0.555 |
| | FSC | -0.690 | 19.75 | 0.977 | 0.028 | 0.374 |
| | OM | -0.974 | 22.83 | 0.931 | 0.071 | 0.944 |

Table 5.2. Regression parameters for the abundance size spectra ($Y = \log_{10}a + b\log_{10}X$). All regressions are significant ($p<0.01$). OLS = Ordinary Least Squares regression; RMA = Reduced Major Axis regression.

| Regression | Location | Slope (b) | Intercept ($\log_{10}a$) | $r^2$ | S.E. slope | S.E. intercept |
|---|---|---|---|---|---|---|
| OLS | FG | -0.806 | 0.519 | 0.925 | 0.026 | 0.108 |
| | FSC | -0.674 | 0.594 | 0.931 | 0.021 | 0.085 |
| | OM | -0.734 | 0.247 | 0.731 | 0.055 | 0.236 |
| RMA | FG | -0.903 | 0.020 | 0.981 | 0.014 | 0.025 |
| | FSC | -0.811 | 0.060 | 0.961 | 0.018 | 0.066 |
| | OM | -0.919 | -0.043 | 0.965 | 0.019 | 0.034 |

Although the scaling exponents generally approximated the values predicted by the metabolic theory and the energy equivalence hypothesis, the slopes were still statistically different in most cases. These results can possibly be explained by the fact that benthic communities show some evidence of size-structured feeding relations and that the predicted scaling exponents must be corrected for the appropriate limiting resource (R). In this scenario all benthic organisms do not feed from a common food pool but are instead characterised by size-structured food webs with larger predators feeding on smaller prey. The reduction in available energy with increasing body mass supports fewer larger organisms and this is depicted by the steeper abundance – body size regression lines. However, benthic infaunal communities, may not necessarily display size structured food chains as, for example, larger bivalves may be filter feeding directly on the same organic matter as the smaller organisms (Dinmore & Jennings, 2004). Dinmore and Jennings (2004) predicted the slopes of abundance – body mass relationships by using a simple model that accounted for the energy transfer efficiency between different trophic levels (as identified by stable isotope analysis). Their results suggested that the slopes of empirical benthic size spectra were consistent with their theoretical predictions based on the trophic structure and energy transfer efficiency.

### 5.4.6 Summary

The data presented in this chapter suggest that biomass size spectra do not separate meio- and macro-fauna as two functionally distinct units. The biomass distribution patterns could be generally described as a continuously increasing function of body

size and as such they do not conform to the bimodal trend reported by Schwinghamer (1981). The current data and other previously published reports (e.g. Duplisea & Drgas, 1999; Udalov & Burkovsky, 2004; Stead et al., 2005) suggest that variable biomass distribution patterns may arise as a result of spatial and temporal variation or inappropriate sampling and analysis protocols. Body size spectra do appear to reflect changes in environmental conditions and generally approximated the theoretically expected patterns as outlined by the metabolic theory of ecology (Brown et al., 2004).

# 6. BODY SIZE MINIATURISATION IN THE DEEP-SEA

## 6.1 Introduction

Benthic organisms generally depend on food originating from the overlying surface waters. As both the quantity and the quality of food decrease with water depth and distance from the shore (Rowe & Staresinic, 1979, Suess, 1980) the benthic standing stock can also be expected to follow the same trend. Deep-sea organisms have been suggested to adapt to these decreased food levels in one of two ways. Some taxa [gastropoda (Clarke, 1960); isopoda (Wolff, 1962); amphipoda (Thurston, 1979)] have been shown to increase in size (gigantism), potentially allowing them to forage further in search of limited food resources. On the other hand meio- and macro-faunal communities have shown trends towards body size miniaturisation with increased water depth. Thiel (1975) formulated a hypothesis stating that 'associations governed by constantly limited food availability are composed of smaller individuals on average' and attributed this to the fact that food limitation does not allow the higher energy consumption of larger organisms on a local scale (Thiel, 1979).

Subsequent studies attempting to test this hypothesis have produced conflicting results with some studies providing support (Carey, 1981; Gage, 1977; Soetaert & Heip, 1989; Soltwedel et al., 1996) and others contradicting it (Shirayama, 1983; Smith & Hinga, 1983; Tietjen, 1989). The variable sampling and sorting methods used in these studies may in part explain some of these contradicting results. For example,

Shirayama (1983) and Polloni et al. (1979) outlined the need to compare samples that were both spatially and temporally consistent, relevant and reliable. Most of the studies have also attempted to analyse benthic size structure in terms of average individual biomass values, although potentially more information can be revealed by using body size spectral methods.

With access to appropriate, high quality sample sets, this chapter aims to investigate the body size miniaturisation of benthic infaunal assemblages with increasing water depth. It primarily focuses on comparing the two NE Atlantic study sites with contrasting water depths (Fladen Ground 150 m; Faroe-Shetland Channel 1600 m) although the data from the Arabian Sea OMZ location are also considered. The relative merits and limitations of using average individual biomass and spectral methods are discussed.

## 6.2 Methods

The simplest way to compare body sizes between the study sites is to use 'average individual biomass' (AIB), sample biomass divided by sample abundance (e.g. Bett & Gage, 2000). As the samples were sieved through a nest of mesh sizes, the data can be analysed in three different ways: (1) the overall sample total combining all the sieve fractions (500, 355, 250, 180, 45 μm) together (i.e. >45 μm), (2) separate fractions including only the specimens retained on that particular sieve mesh (i.e. largest fraction >500 μm, next fraction <500μm but >355 μm etc.), and (3) cumulative fractions giving the notional catch as if each sieve had been used on its own

(e.g.>500, >355, >250, >180 and >45 μm). Total sample AIB values were calculated for all three data 'treatments' as a mean value of the five replicates from each site.

A more detailed method of gauging potential differences in benthic size structure between the study sites is the construction of body size accumulation curves. All specimens were assigned to a body size class and the cumulative percentage of individuals present in each size class was plotted. The relative differences between the replicates and the sites were assessed using the Analysis of Similarities (ANOSIM) routine provided by the PRIMER software (Clarke & Green, 1988; Warwick & Clarke, 1991). As applied here, ANOSIM tests were based on analyses of dissimilarity matrices generated by summing the differences between the cumulative percentages of any two replicates. For example, for Fladen Ground samples the cumulative percentage in each size class of replicate one was deducted from the respective cumulative percentage of replicate two. The absolute differences were then summed and the resulting value was used as a measure of dissimilarity between the two replicates. The procedure was repeated for all the replicates at all the sites to produce the dissimilarity matrices. This approach was used for the data set as a whole and for major taxonomic (Polychaeta, Crustacea and Nematoda) groups separately where possible. The dissimilarity matrices were also used to plot Multi-Dimensional Scaling ordination maps where the distance between the replicates or sampling sites represents the degree of dissimilarity (replicates most dissimilar to one another plotted furthest apart).

## 6.3 Results

The mean absolute abundance and biomass values recorded at Fladen Ground were higher than those observed at the deeper FSC site (table 6.1). The highest overall abundance levels were recorded at the Oman Margin site and were coupled with the lowest biomass values reflecting the fact that this site is mainly dominated by small nematodes. At all sites, polychaetes dominated the macrofauna and nematodes the meiofauna in terms of numbers and biomass. At the Fladen Ground site high numbers of bivalves (Veneridae), gastropods (Philinidae) and polychaeta (Opheliidae) were recorded in the smaller sieve fractions (180-355 μm). Although some smaller macrofauna were found at the FSC site, the relative numbers were low in comparison to the Fladen Ground location. Apart from a few small bivalves, the Oman Margin site fauna consisted almost exclusively of nematodes and polychaetes.

The overall body size (measured as AIB for all the sieve fractions combined) did not differ significantly between the Fladen Ground and FSC sites (figure 6.1 - accumulative 45 μm fraction; figure 6.2 – all combined). Inspection of the accumulated fractions (figure 6.1) reveals that the average individual biomass at the FSC site was higher in most of the sieve fractions. However, the individual fractions displayed an opposing trend with average body size at Fladen Ground being larger at intermediate mesh sizes (figure 6.2). These observations imply that it is the presence of the largest individuals (>500 μm) at the FSC site that contribute considerably to the observed AIB values. If the organisms retained on the 500 μm sieve are excluded from the analysis, average individual biomass is found to be significantly larger in all the sieve fractions from the Fladen Ground site (figure 6.3). The AIB at the Oman

Margin site was generally found to be the lowest of the three locations in most of the sieve fractions, regardless of whether these fractions were considered individually or cumulatively (figures 6.4, 6.5 & 6.6). The influence of the particularly small AIB in the 500 μm fraction was reflected as reduced AIB in all the subsequent accumulative fractions as well (figure 6.4). When the largest fraction (500 μm) was removed from the data set, the AIB of the OM site seemed visually closer to the other two sites although significant differences were still detected between the three sites (figure 6.6).

Table 6.1. Summary statistics of benthic community abundance, biomass and average body size at shallow-water (Fladen Ground, 150m), deep-water (FSC, 1600m) and OMZ (OM, 500 m) sites based on 5 replicate sets at each location. (AIB, average individual biomass; p, probability result of Kruskal-Wallis-test comparison between the sites).

| Parameter | Units | Fladen Ground | FSC | Oman Margin | p |
|---|---|---|---|---|---|
| Macrofauna abundance > 500 μm | ind/$m^2$ | 8,403 | 2,988 | 4,932 | 0.022 |
| Total abundance | ind/$m^2$ | 801,426 | 471,422 | 1,057,381 | 0.039 |
| Total biomass | g(wwt)/$m^2$ | 15.0 | 11.0 | 4.1 | 0.012 |
| AIB total | g(wwt)/$m^2$ | $1.9x10^{-5}$ | $2.7x10^{-5}$ | $3.9x10^{-6}$ | 0.006 |
| AIB < 500 μm | g(wwt)/$m^2$ | $6.6x10^{-6}$ | $2.8x10^{-6}$ | $1.3x10^{-6}$ | 0.005 |

The problem of randomly retaining larger specimens in benthic samples is not uncommon. At the largest sieve fraction the presence of larger individuals is closely related to the surface area covered by the sampling device. Consequently, the analysis of benthic samples is always a function of the area covered and the mesh size used. The presence of random larger individuals can easily skew the results of the analysis and often in macrobenthic work a larger mesh size may be used to try to remove this effect (e.g. use of 2 mm mesh on top of a 500 μm mesh). As a larger mesh size was not used in the current study it is possible that the presence of few larger individuals may mask the real trends in the data set and consequently their exclusion may be justified to reveal the true underlying pattern in size distribution. In fact, at the FSC location the larger size classes contained specimens of sipunculids and ophiuroids that contributed considerably to the total biomass but had a relatively small influence on the overall abundancies.

Figure 6.7 shows the overall body size cumulation curves for each replicate from the three study sites. All of the FSC and most of the OM curves lie above the Fladen Ground ones over most of their range. This depicts an obvious shift in the distribution of body sizes between the three sites, with the FSC and OM communities being clearly dominated by smaller organisms. The OM site data were further characterised by a high degree of variability as depicted by the wide spread of the accumulation curves over the size range. The body size distributions (i.e. the shape and position of the curves) were statistically tested by using ANOSIM and the Fladen Ground site was found to be significantly different from the other two sites ($p < 0.01$). There was no significant difference between the FSC and the OM sites. The MDS plots similarly showed the replicates from the FG site to cluster away from the FSC and OM

locations (figure 6.11). The analysis of major taxa showed that both nematodes (all three sites) and crustaceans (FG and FSC only) followed the same trend and that again there were significant differences between the sites (figures 6.8 & 6.9; $p < 0.01$). Polychaetes displayed an opposing trend (figure 6.10) with a higher proportion of smaller individuals encountered at the Fladen Ground site than at the other two locations ($p < 0.01$). Again FSC and OM were not siginificantly different from one another. These differences were also detected on the resulting MDS plots (figure 6.11).

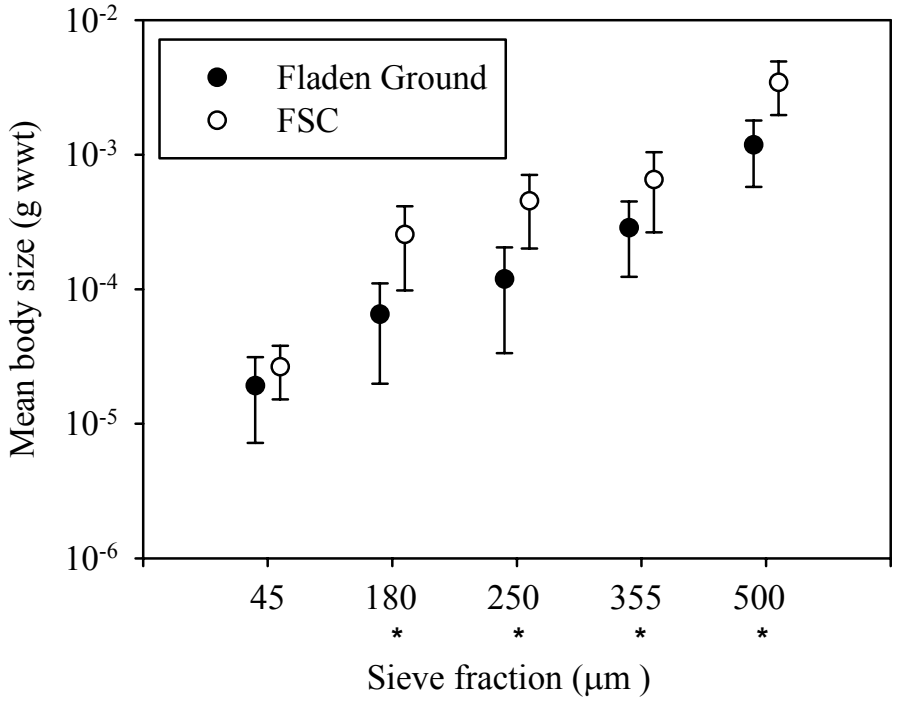


Figure. 6.1. Mean body size for the accumulative sieve fractions. * denotes a significant difference between the two sites (MANN-WHITNEY U $p < 0.05$; error bars are 95% CI).

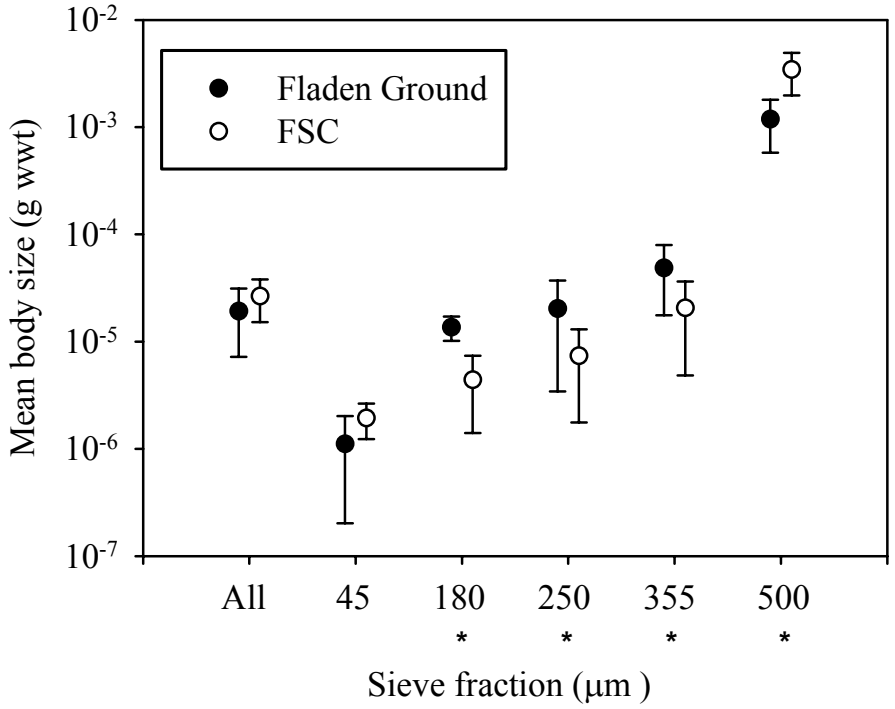


Figure 6.2. Mean body size for the individual sieve fractions. * denotes a significant difference between the two sites (MANN-WHITNEY U $p < 0.05$; error bars are 95% CI).

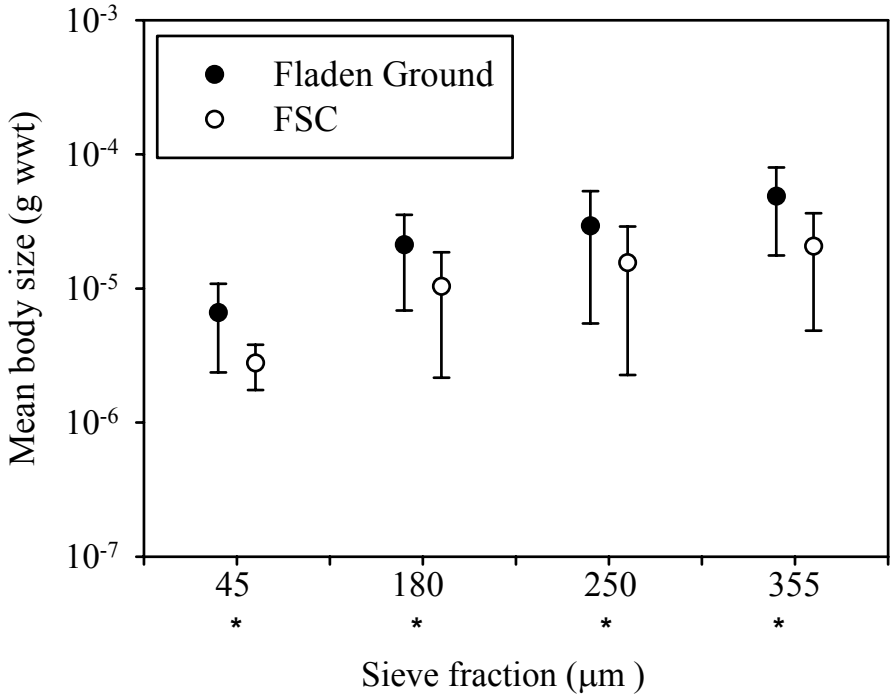


Figure 6.3. Mean body size for the accumulative sieve fractions (excluding the 500 μm). * denotes a significant difference between the two sites (MANN-WHITNEY U $p < 0.05$; error bars are 95% CI).

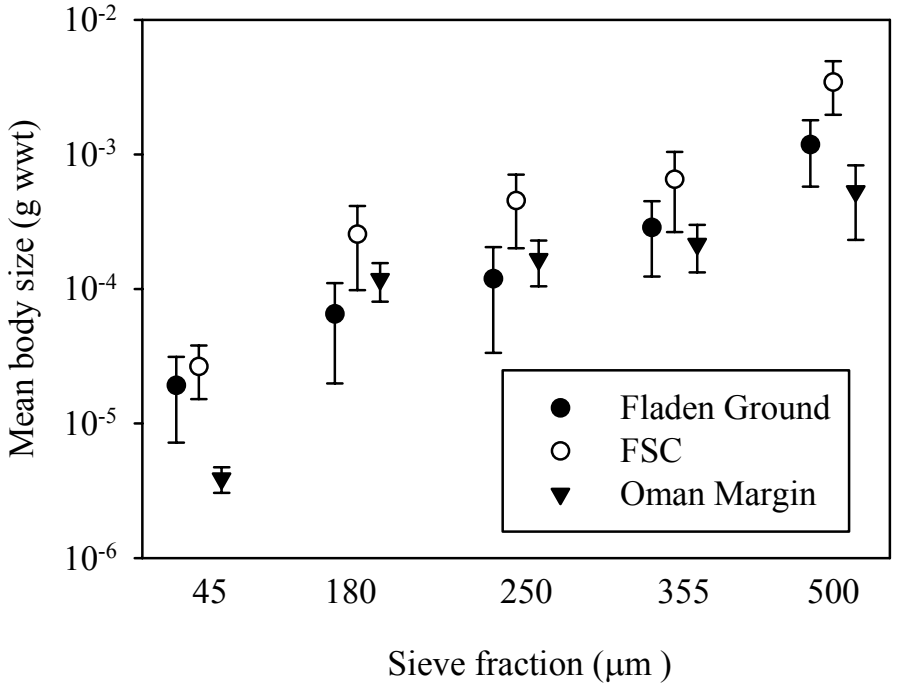


Figure 6.4. Mean body size for the accumulative sieve fractions (error bars are 95% CI; there are significant differences in all sieve fractions: Kruskal-Wallis test $p < 0.05$).

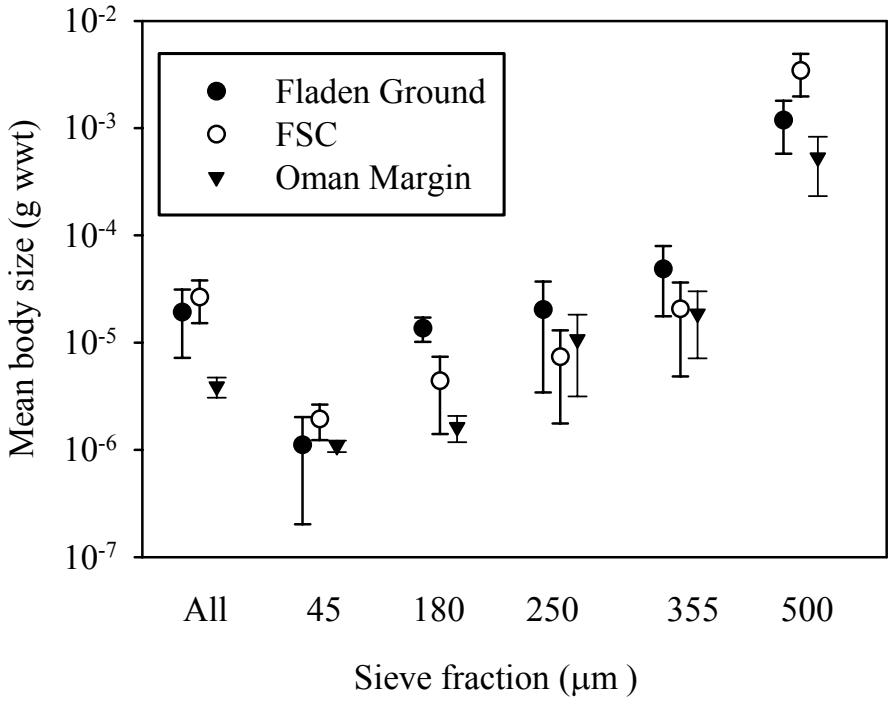


Figure 6.5. Mean body size for the individual sieve fractions (error bars are 95% CI; there are significant differences in all sieve fractions: Kruskal-Wallis test $p < 0.05$).

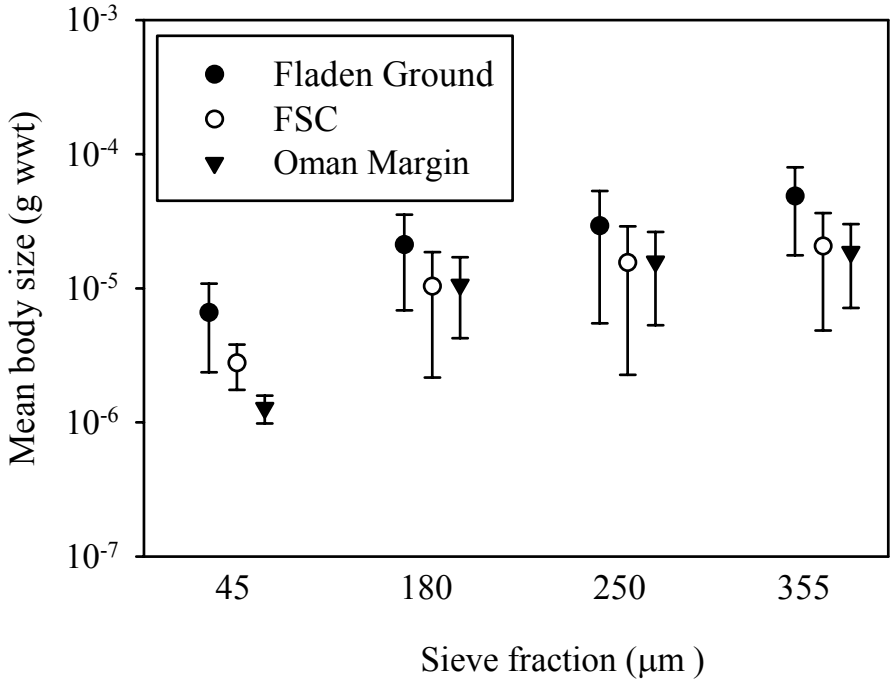


Figure 6.6. Mean body size for the accumulative sieve fractions (excluding the 500 μm; error bars are 95% CI; there are significant differences in all sieve fractions: Kruskal-Wallis test $p < 0.05$).

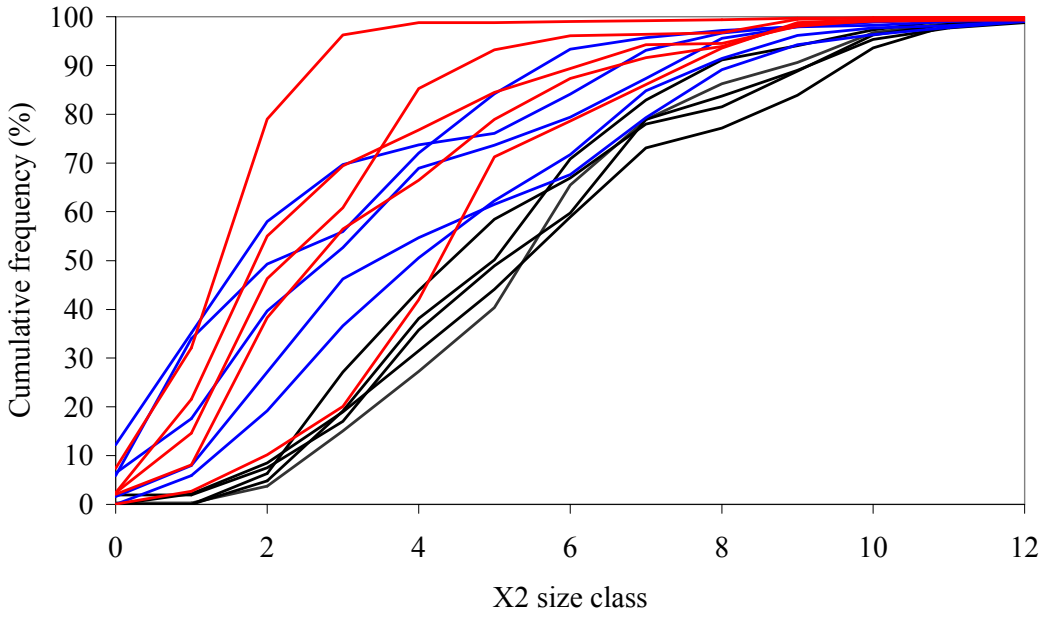


Figure 6.7. Body size accumulation curves for the overall data set (black line: FG; blue line: FSC; red line: OM).

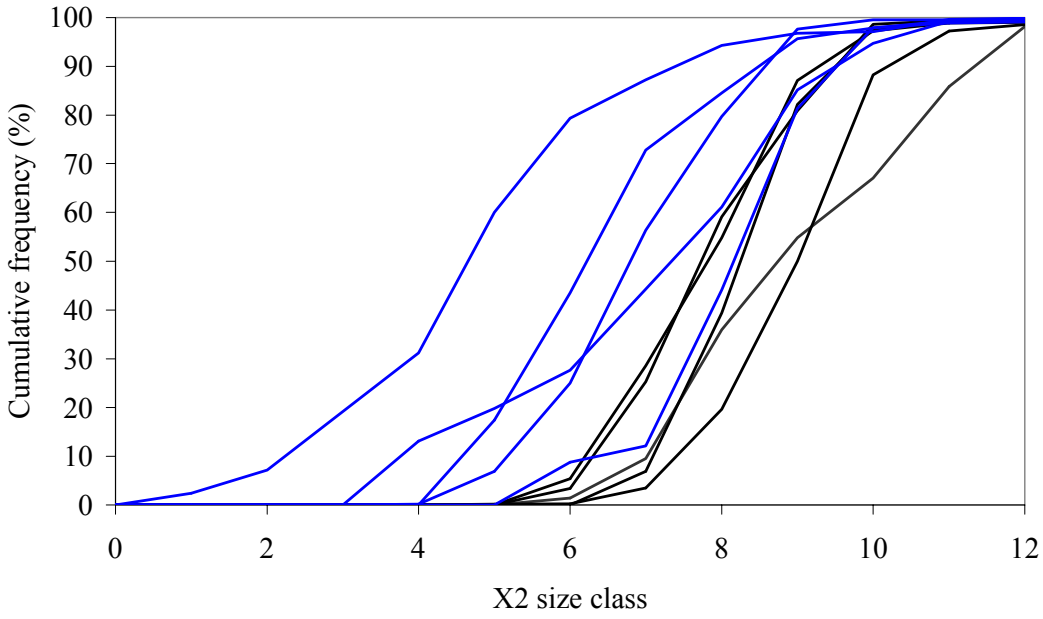


Figure 6.8. Body size accumulation curves for the Crustacea (black line: FG; blue line: FSC).

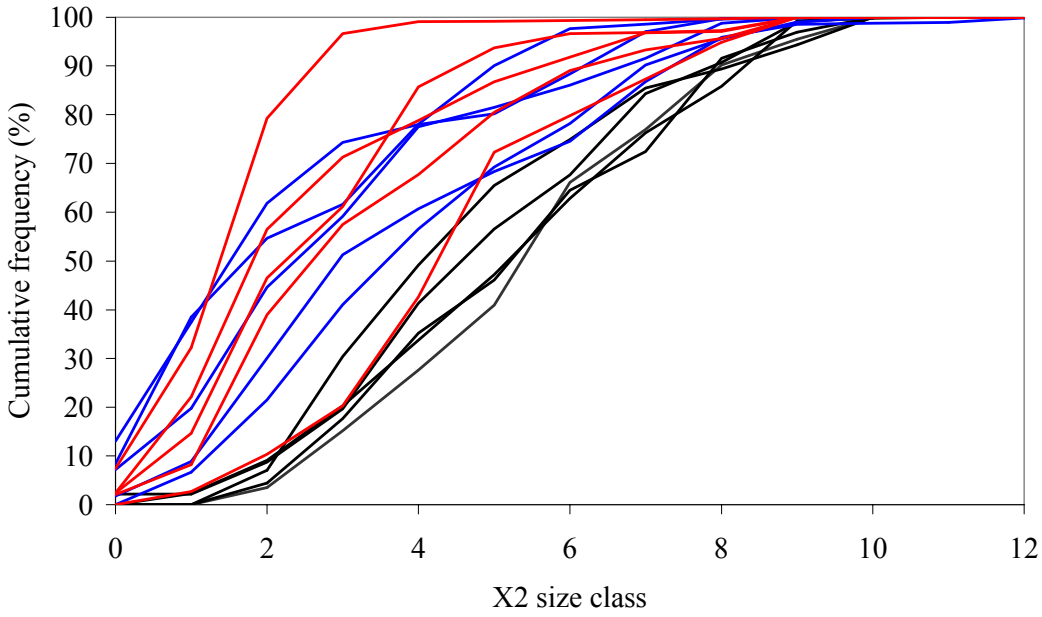


Figure 6.9. Body size accumulation curves for the Nematoda (black line: FG; blue line: FSC; red line: OM).

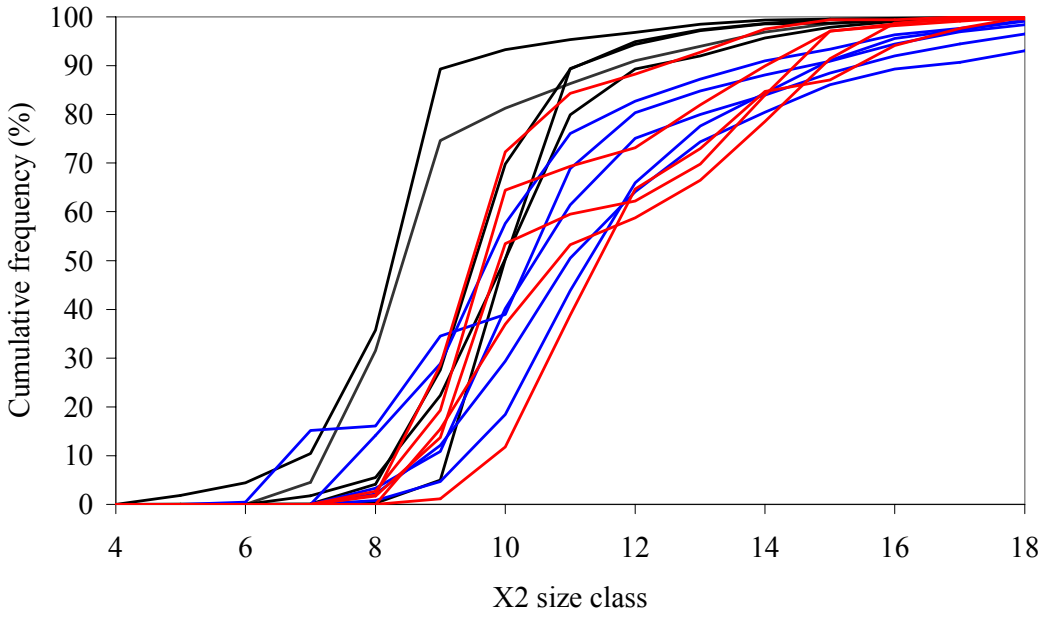


Figure 6.10. Body size accumulation curves for the Polychaeta (black line: FG; blue line: FSC; red line: OM).

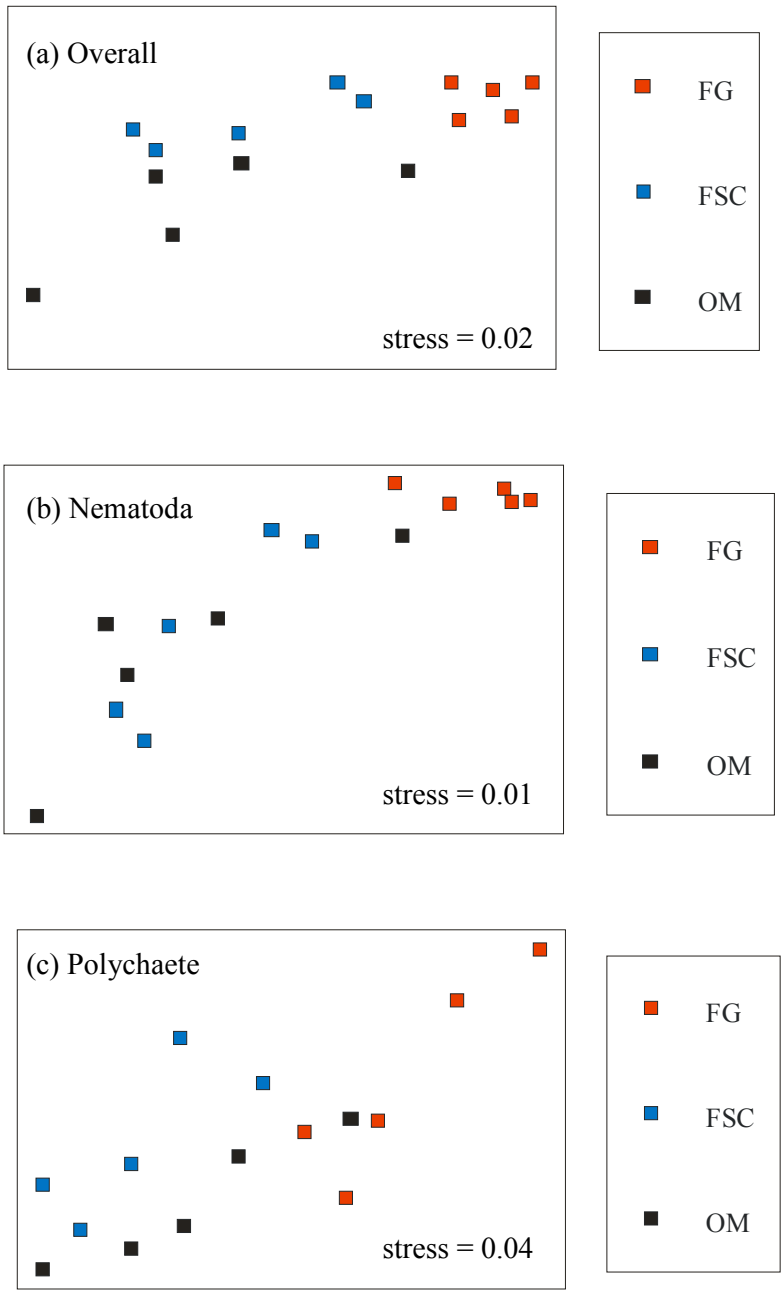


Figure 6.11. MDS plots for the three sampling sites based on the dissimilarity matrices generated by summing the differences between the cumulative percentages of any two replicates (see text for details); (a) Overall data set, (b) Nematoda and (c) Polychaeta.

## 6.4 Discussion

As outlined in the introduction, the emphasis on the discussion of body size miniaturisation in the deep-sea is mainly on the comparison of the two NE Atlantic sites (FG and FSC). Although the data from the Oman Margin site are also introduced and put into context, it is perhaps simpler to try to demonstrate the observed trends between the other two sites separately as the differences in their environmental characteristics resulted largely from the contrasting water depths (e.g. not further complicated by reduced oxygen levels).

Most of the studies that have previously attempted to test Thiel's (1975) hypothesis have used average individual size to try to gauge changes in the underlying body size structure. The fact that these studies have provided contradictory results is not surprising considering the complexity and the limited value of AIB data. By definition average values consider all the individuals in the sample and thus can be highly sensitive to the presence of extreme data points. These can potentially mask the true trends in underlying size structure, as rare large individuals have little influence on body size accumulation curves but can have a marked effect on AIB values. For example, in the present study the inclusion of larger individuals from the 500μm fraction at the deeper site was enough to skew the average values to the point that the body sizes appeared larger on all other sieve fractions. The body size accumulation curves clearly depicted a significant shift towards smaller body sizes at the deeper site and only by excluding the largest organisms from the analysis were the AIB values able to reflect this trend. This clearly highlights the limited value of attempting to reduce benthic body size distributions to a single average value.

The comparison of the body size accumulation curves for major taxa produced contradicting results. Nematodes and crustaceans followed the trend of the data set as a whole, whereas polychaetes displayed smaller body sizes at the Fladen Ground site. The deviation of the polychaete body size structure from the general trend may have resulted from either different taxonomic composition and the associated recruitment histories or the degree to which the two sampling sites are subjected to habitat disturbance. For example, high numbers of small polychaetes (Opheliidae) and molluscs (Veneridae, Philinidae) were encountered at the Fladen Ground site, suggesting that a relatively recent settlement event had taken place. The occurrence of large spat falls relatively late in the season is not unusual as, for example, Philinidae gastropods have been recorded to spawn throughout the summer with the larval settlement time typically more than 30 days (Hansen & Ockelmann, 1991; Wilson, 2000). There was no evidence of recently settled juvenile macrofauna at the deeper FSC site.

The sampling location at Fladen Ground is also subjected to disturbance by extensive oil industry activity and offshore fisheries whilst the FSC location represents a relatively undisturbed deep-sea environment. Environmental disturbance (e.g. pollution) has been shown to result in smaller body sizes of macrobenthic organisms, whereas meiobenthos may not display an obvious size difference between conservative and opportunistic species (Warwick, 1986). It is possible that the trends observed in the size accumulation curves of the major taxa reflected the increased disturbance levels at the FG sampling site. If this is the case the observed shift in the

body size distributions with depth may be even more pronounced in undisturbed habitats.

The reasons for the observed size miniaturisation patterns remain unclear. Rex and Etter (1998) stated that the size related adaptations to the environmental conditions in deep-sea benthos should be examined at species level with the measurements standardised to similar species assemblages and common growth stages. Although a species-level approach could help to elucidate some of the factors responsible for the size-depth patterns, it is difficult to extend this approach to community level as it is not realistic to expect the benthic communities to have a consistent taxonomic composition over a broad bathymetric range. Thiel's original hypothesis (1975) about body size miniaturisation in deep-sea environments applied to benthic assemblages as a whole and hence a different approach may help to determine some of the causative factors at this level. One alternative is to use the non-taxonomic approach adopted in this study that assumes organisms of similar size to respond similarly to environmental constraints.

Thiel (1975) argued that the causative agent is the limited food supply, which results in smaller body sizes on average. He explained this by comparing the advantages of being either small or large in a food-limited environment. Although the cost of maintaining a given biomass of smaller organisms is higher than that required to maintain the same biomass of larger organisms, the high individual food demands of larger animals and the requirements to maintain a critical population density for reproduction generally favours smaller body sizes. This hypothesis generally applies to infauna (e.g. meio- and macro-fauna) that feed on the sediment locally. Organisms

(e.g. some megafauna) with broader home ranges can display increased body sizes with water depth as they benefit from reduced vulnerability to local extinction and are able to feed over larger areas hence utilising their metabolic advantage (Thiel, 1979; Rex & Etter, 1998).

With the exception of hydrothermal vents and cold seeps, the main food source for benthic communities is generally the organic matter synthesised in the overlying surface waters (Sokolova, 2000). The amount of organic matter reaching the sea floor is often a function of water depth with the organic content decreasing with increasing bathymetric depth (Rowe, 1971). The flux of organic material to the seafloor is not easy to determine and data for the two study sites are scarce. As most of the organic material that reaches the sea floor is utilised by the fauna (Gage & Tyler, 1991; Cole et al., 1987), the standing stock of benthos is a good indirect measurement of this flux. Although primary production at the two study sites has been reported to be similar (~ 1 g C m-2 d-1; Cadée, 1986; Riegman & Kraay, 2001), there are differences in the benthic biomass levels (table 6.1). Using Suess' (1980) equation linking primary production of organic carbon in surface waters to particulate organic carbon flux to depth it can be estimated that the FSC site receives about 10% of the organic input that reaches the Fladen Ground site. Although the Suess equation has been criticised (Lutz et al., 2002) and there may be additional organic inputs to the North Sea (Austen et al., 1991), it may nevertheless be reasonable to suggest that there is an order of magnitude difference in the organic matter flux to the two study sites. It is therefore conceivable that food limitation may act as a contributing factor in controlling the optimal body size of benthic communities resulting in smaller body size distribution observed at the FSC site in the current study.

A number of other environmental factors have been suggested to explain differences in body size structure between contrasting habitats and perhaps the most obvious one in the analysis of benthic communities is that of sediment grain size distribution. For instance, Schwinghamer (1981) hypothesised that sediment granulometry determined the size distributions of infaunal organisms and that shifts would occur in the size spectra in response to changes in particle size composition but subsequent studies have frequently provided contrary evidence (Warwick, 1984, Duplisea & Drgas, 1998, Leaper et al., 2001). Similarly, Chapelle and Peck (1999) suggested that individual body size may be correlated with dissolved oxygen concentration but in this study both the bottom water oxygen levels and the particle size distribution of sediments were very similar suggesting that the differences in size distributions between the two NE Atlantic stations did not result from variations in these parameter values and that other factors such as temperature, hydrodynamics and predation may also influence the observed size structures.

If the hypothesis proposed by Chapelle and Peck (1999) is true for benthic infauna in general, then it would be expected that the organisms sampled at the core of the OMZ at the Oman Margin site should display signs of decreased body size, particularly at the largest sieve fraction (500 μm). This trend is observed in the current study where the overall body size distribution was significantly smaller at the Oman Margin location (figure 6.7 (a)). Although the body size distribution of the Oman Margin polychaetes was found to be significantly larger than at the FG, no significant differences were detected between the deeper FSC and the OM locations (figure 6.7 (b)). These findings imply that the body size of the benthic infauna at the OM site

may be controlled by the oxygen availability as suggested by Chapelle and Peck. However, OMZ areas are often characterised by other environmental gradients, such as sediment organic content, that may also influence the size distributions and therefore make it difficult to distinguish the effect of individual gradients (Levin et al., 2000).

Benthic environments within the OMZ areas are typically characterised by a high sediment organic content as a result of the reduced mid-water consumption of the organic matter sinking from the highly productive euphotic zone (Levin et al., 2000). It is possible that the reduced size distribution at OM site in comparison to FG location reflects the low oxygen concentration within the OMZ. However, it is also equally possible that the increased food availability counteracts this effect allowing the existing organisms to attain larger body sizes than otherwise expected. Although it is probable that both processes influence the body size distribution at the OM site, it is very difficult to assess their individual contributions.

The results from this study are effectively based on data from only two sampling stations located on the continental margin and slope and so their implications must be interpreted with caution. The construction of size spectra for a number of stations across a bathymetric gradient are required to further assess the existing hypothesis concerning the size-depth patterns. Overall the results from the two locations appeared to follow the pattern of smaller organisms dominating the deeper sediment environment with food availability acting as one possible control.

# 7. BENTHIC SECONDARY PRODUCTION AND ENERGY FLOW

## 7.1 Introduction

Productivity can be defined as the rate at which assimilated matter is converted into body mass. For steady-state systems the amount of biomass produced equals the amount eliminated and hence production forms a central component of energy flow and organic matter recycling within the ecosystem (Tumbiolo & Downing, 1994). For instance, benthic organisms play an important role in mass and energy transfer between different parts of the system. In many cases this is represented by directly linking primary producers to higher predators (e.g. demersal fish). The role of benthos in redistributing and recycling organic matter and nutrients is also unequivocal. The measurement of secondary benthic production and the understanding of the controls that influence it are therefore essential in comprehending ecosystem functioning and dynamics (Tumbiolo & Downing, 1994).Unfortunately the process of measuring production and energy transfer dynamics at community level is difficult and the size-based approach discussed in the previous chapters can offer an attractive alternative to producing first approximations.

Secondary production is classically quantified by using techniques such as the increment summation method, the removal summation method, the instantaneous growth method or estimation of production by the Allen curve (e.g. Hynes-Hamilton & Coleman, 1968; Waters, 1977; Crisp, 1984). However, these techniques often

require repeated measurements of abundance and biomass of known population cohorts. These data requirements make it a difficult task to establish at community or ecosystem level due to time constraints and the difficulty of associating rare species to particular cohorts (Sprung, 1993). Consequently, ecologists have developed indirect estimation methods such as empirical models that attempt to predict secondary production from more easily obtained community parameters such as individual body size (Brey et al., 1996).

Banse and Mosher (1980) and Schwinghamer et al. (1986) produced allometric scaling equations that predicted production as a function of body mass. These models were essentially based on the hypothesis that a negative exponential relation exists between body size and metabolic rate (Peters, 1983). However, metabolic rate and production of benthic organisms is also influenced by other controls such as temperature and resource availability (Brown et al., 2004). The rates of biological processes are known to increase exponentially with temperature and the quantity and quality of food is thought to decrease with water depth in marine benthic ecosystems (Rowe, 1971). Consequently, Tumbiolo and Downing (1994) improved the earlier empirical relations by considering the effects of temperature and water depth on the production of marine invertebrates. The resulting allometric relation predicts annual production (P) as a function biomass (B) in g dwt $m^{-2}$, maximum individual size ($W_m$) in mg dwt, temperature (T) in ˚C and water depth (d) in meters:

$$\log_{10}P = 0.18 + 0.97\log_{10}B - 0.22\log_{10}W_m + 0.04T - 0.014T\log_{10}(d + 1) \quad (7.1)$$

Multivariate analysis carried out by Tumbiolo and Downing (1994) showed that, corrected for temperature and depth variations, secondary production varied with body mass as $W_m^{-1/4}$ across a number of different environments as predicted by the metabolic theory of ecology (Brown et al., 2004).

Production can also be empirically related to respiration over a broad range of body sizes (Humphreys, 1979). Schwinghamer et al. (1986) calculated annual respiration (R) of meio- and macro-fauna from annual production (P) using the relations derived for benthic invertebrates by Banse (1979) and Banse and Mosher (1980). This relation was expressed in kcal $m^{-2}$ $y^{-1}$ (kcal $m^{-2} \approx cm^3$ $m^{-2} \approx$ g wwt $m^{-2}$; Schwinghamer 1981, Schwinghamer et al., 1986):

$$\text{Log}_{10}R = 0.367 + 0.993\text{log}_{10}P \qquad (7.2)$$

The body size-based estimates of community production and respiration enable the determination of benthic energy demand on a larger scale. The aim of this chapter is to use biomass size spectra in conjunction with these empirically derived allometric equations (eqs 7.1 & 7.2) to provide estimates of secondary production at the three study sites. Production estimates are compared across the sampling sites and the relative contributions of the various size classes to total production are assessed. This approach helps to highlight potential gaps in our current understanding of material and energy transfer dynamics at community level hence providing focus and direction for the future research efforts in this area.

## 7.2 Methods

Annual production and respiration estimates were derived for the size classes encompassing the reliable part of the biomass size spectrum (chapter 5). The allometric formula developed by Tumbiolo and Downing (1994) was used to estimate production at the three study sites (eq 7.1). This model predicts benthic secondary production as a function of two powerful and easily measurable variables of community structure: biomass and maximum individual body size. Due to the non-taxonomic approach of the current study the maximum individual body size was substituted for maximum body size at each size class. As this modification is not strictly analogous to the original parameter, it may have an influence on the resulting production estimations. However, it was felt that the method could still be trialled and the early results showed that the production estimates derived from this approach appeared to agree reasonable well with other independently obtained community production estimates (see discussion). The model outlined by Schwinghamer et al. (1986) was used to derive estimates of community respiration from the production values (eq 7.2).

Based on these estimations a number of benthic production size spectra (BPSS) were constructed. The regular BPSS were plotted by determining the total production (g wwt) in each size class. The relative BPSS standardised the production estimates to percentages that were also plotted as a cumulative percentage spectra.

In addition to considering the size classes on their own, an alternative approach was adopted where size classes were combined together to form three groups. The

combination of size classes followed the approach introduced by Schwinghamer et al. (1986) with meio- and macro-fauna representing the smaller and larger ends of the metazoan size spectrum, respectively. A third group (mesofauna) was added to represent the intermediate body sizes and thus the meiofaunal group included size classes 5-7 (< 180 μm ESD), the mesofaunal group size classes 8-12 (180-500 μm ESD) and the macrofaunal group size classes 13-20 (> 500 μm ESD). The production, biomass and respiration values were presented as summed totals for each group. The analysis also allowed the derivation of estimates for P:B ratios by dividing the estimated annual production by the observed biomass in each group.

## 7.3 Results

Total annual production was found to be highest at the FG site (42.2 g $m^{-2}$ $y^{-1}$), with the FSC (13.4 g $m^{-2}$ $y^{-1}$) and OM (13.8 g $m^{-2}$ $y^{-1}$) locations having lower values (table 7.1, figure 7.1). Annual production and respiration of meio- and meso-fauna decreased with water depth, but at the deepest site (FSC) the production of macrofauna was higher than at the intermediate OM site. However, these trends may reflect variations in environmental parameters other than water depth. For instance, the OM site is strongly characterised by permanently low oxygen concentrations and increased downward flux of organic carbon.

The increased production and higher standing stock at the shallower FG site in comparison to the FSC location probably reflected two factors. First, the incoming flux of organic carbon at this location is expected to be higher than at the deeper FSC site (Rowe, 1971; Suess, 1980). In other words food availability may limit the production proportionally more at the FSC site resulting in lower standing stock. The second factor is related to temperature, which influences the rates of biological processes. The deeper FSC site is characterised by water temperatures that are nearly 10 degrees below those recorded at Fladen Ground and consequently the production rates can be expected to be lower.

Differences in temperature and water depth can also help to explain the fact that the total annual production at the OM site was similar to FSC despite the total biomass being significantly lower (table 7.1). As already outlined, water depth in the Tumbiolo and Downing model is included to reflect the flux of organic material to the seabed.

Table 7.1. Estimated values of annual production and respiration presented together with measured biomass values (all in g wwt $m^{-2}$). Values in parenthesis are standard deviations. Meio-, meso- and macro-fauna defined as groups that combine the original X2 size classes (see text for details).

| | | **FG** | **FSC** | **OM** |
|---|---|---|---|---|
| Meiofauna | P | 6.5 (1.7) | 1.8 (0.7) | 3.0 (2.9) |
| | B | 0.7 (0.2) | 0.2 (0.1) | 0.3 (0.3) |
| | P:B | 9.3 (0.2) | 8.3 (0.4) | 9.3 (0.5) |
| | R | 14.9 (3.8) | 4.2 (1.7) | 7.1 (6.7) |
| Mesofauna | P | 21.4 (12.4) | 3.7 (0.8) | 5.2 (4.0) |
| | B | 4.3 (2.7) | 0.8 (0.2) | 1.0 (0.7) |
| | P:B | 5.0 (0.2) | 4.7 (0.2) | 5.4 (0.2) |
| | R | 49.3 (28.2) | 8.6 (1.8) | 12.0 (9.1) |
| Macrofauna | P | 14.4 (5.4) | 7.9 (1.9) | 5.6 (3.9) |
| | B | 8.0 (3.3) | 5.7 (1.8) | 2.6 (1.9) |
| | P:B | 1.8 (0.2) | 1.4 (0.1) | 2.1 (0.2) |
| | R | 33.2 (12.5) | 17.3 (4.0) | 12.7 (8.7) |
| Total | P | 42.2 (18.6) | 13.4 (2.1) | 13.8 (9.8) |
| | B | 13.0 (5.8) | 6.7 (1.8) | 3.9 (2.6) |
| | R | 97.5 (42.5) | 30.1 (4.3) | 31.8 (22.2) |

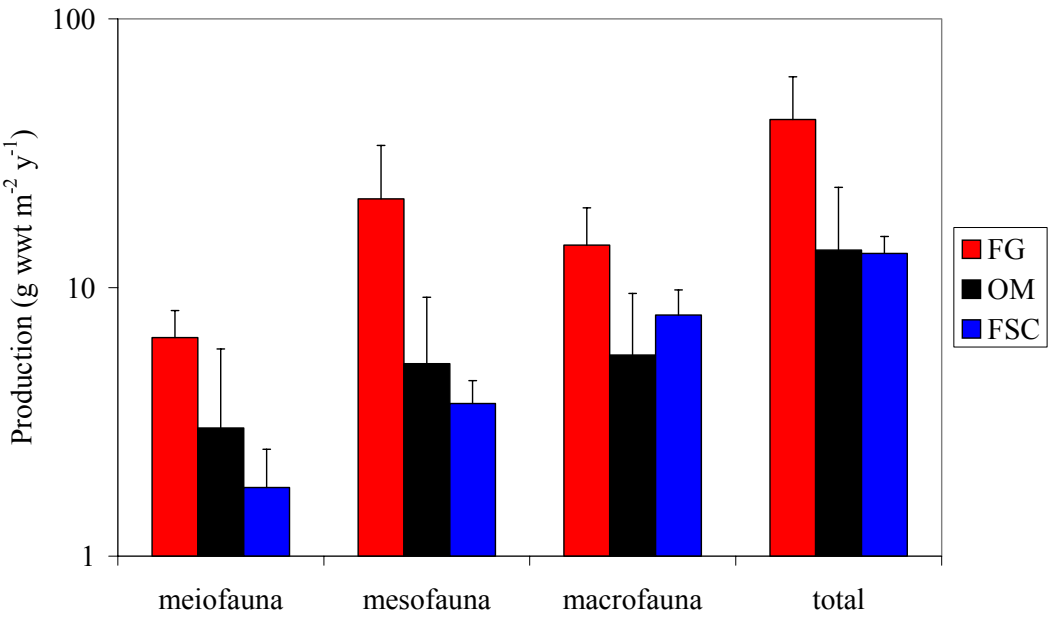


Figure 7.1. Estimated annual production at the three study locations (error bars represent standard deviations).

Although an increased flux of organic carbon was expected as a result of reduced water depth and the associated increase in quantity and quality of the food, the flux at the OM site is not simply a function of water depth. The hydrodynamics associated with monsoon seasons result in increased surface primary production and as the water column between 100-1000 m is typically devoid of oxygen, and hence pelagic organisms, the organic matter sinking from the surface arrives on the seabed relatively undegraded. The increased surface production coupled with minimal mid-water consumption results in increased input of food to the seabed. Consequently the Suess formula (1980) probably underestimates the sedimentation rate of organic carbon at this location.

At the FSC site macrofauna contributed more than 50 % to the overall production while at the other two sites these values were closer to 30-40 % (table 7.1). This pattern was also evident in the regular and relative benthic production size spectra where the largest size classes were shown to contribute the most towards total production at the FSC site (figures 7.2 & 7.3). In contrast, meiofauna accounted for a larger proportion of production at the OM site (22 %) than at the other two locations (FG 15 %; FSC 13 %). The cumulative production percentage spectra also showed that meio- and meso-faunal size classes contributed more at the OM and FG sites (figure 7.4).

The production size spectra of the FG location displayed a distinct peak around size class 10 (figures 7.2 & 7.3) reflecting the increased numbers of small bivalves, gastropods and polychaetes at this site. As the biomass size spectrum did not have a temporal component (i.e. the biomass size spectrum represent a snapshot in time), it is

difficult to assess how these organisms will influence both biomass distribution and production as they grow larger. It is reasonable to expect that these juveniles are subjected to higher mortality rates through increased predation and competition pressures. Consequently, the estimate of annual production at the FG site may have been overestimated. The OM site production size spectrum also reflected the trends observed in the biomass distributions. The bimodality is evident, with distinct production peaks corresponding to high densities of nematodes and polychaetes in the meio- and macro-faunal size ranges, respectively.

P:B ratios were derived for the three size groups from the estimated production and the observed biomass values. The P:B ratios were very similar at all three sites within each size group. However, differences were observed between meio-, meso- and macro-fauna (figure 7.5). Meiofaunal P:B values approximated 9 at all study locations. This is in close agreement with previously published estimates (Giere, 1993) indicating a biomass turnover time of about 1.5 months. Macrofaunal P:B ratios were close to 2 with an associated turnover time of about 6 months. Mesofaunal P:B values were observed to be intermediate. In all three groups, P:B ratios were lowest at the deepest (FSC) location implying the longest turnover times.

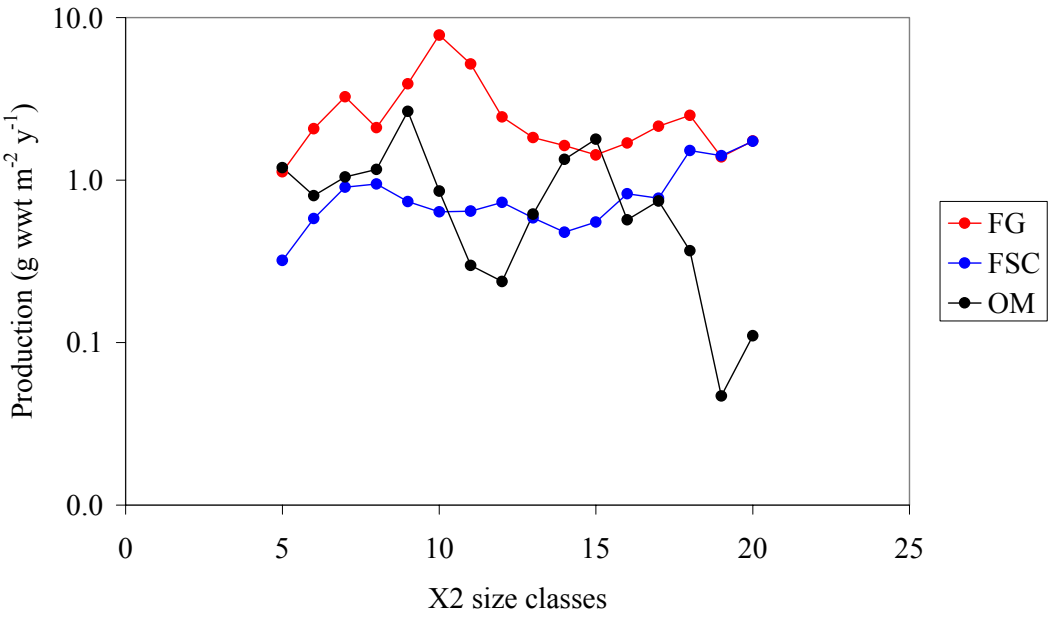


Figure 7.2. Regular benthic production size spectra for the three study locations.

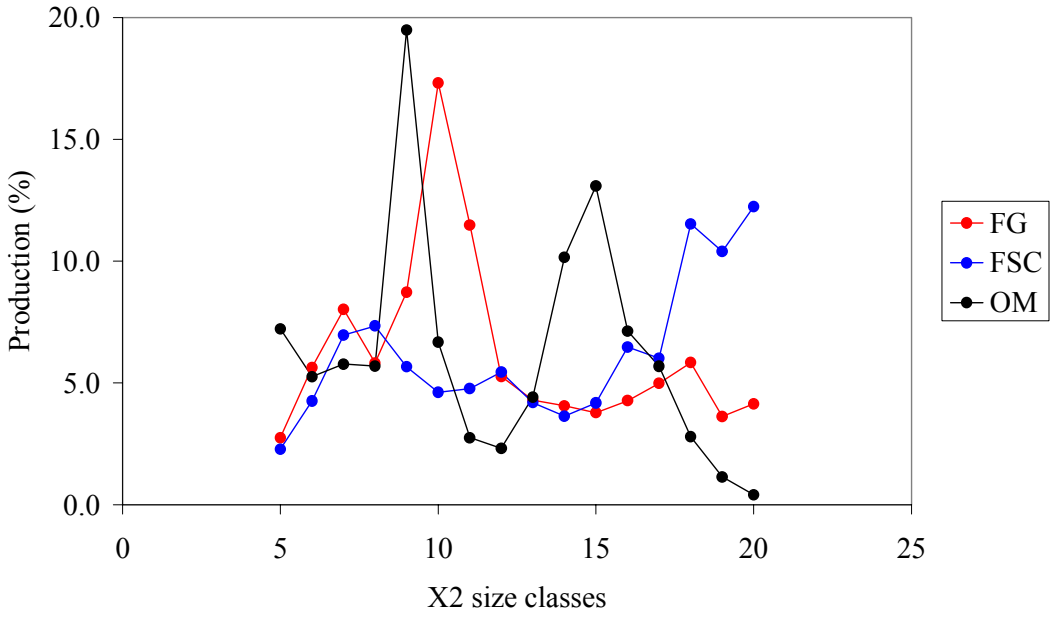


Figure 7.3. Relative benthic production size spectra for the three study locations.

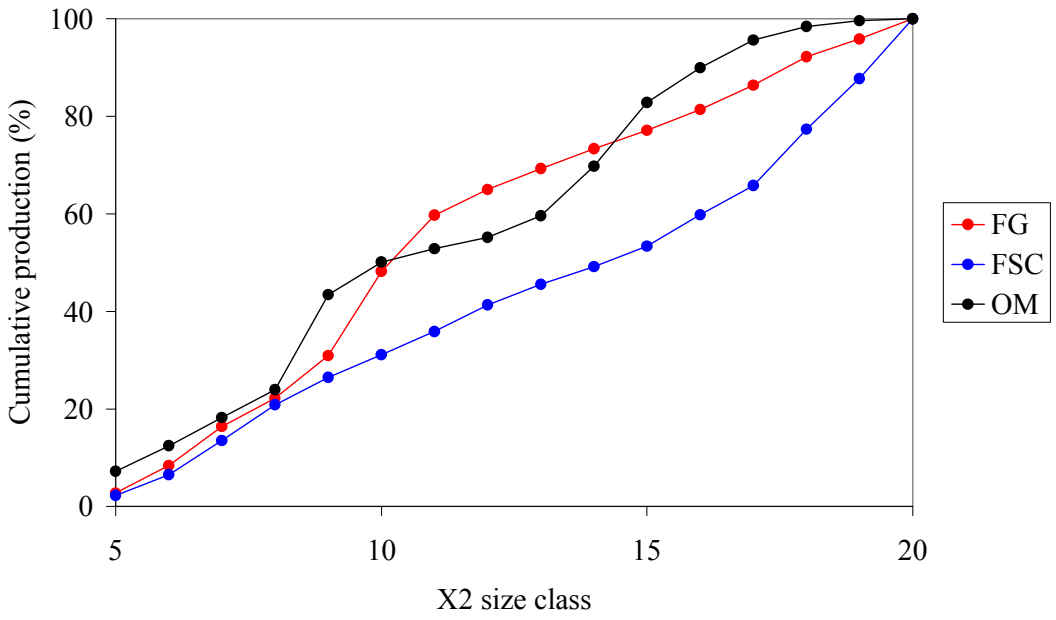


Figure 7.4. Cumulative benthic production size spectra for the three study locations.

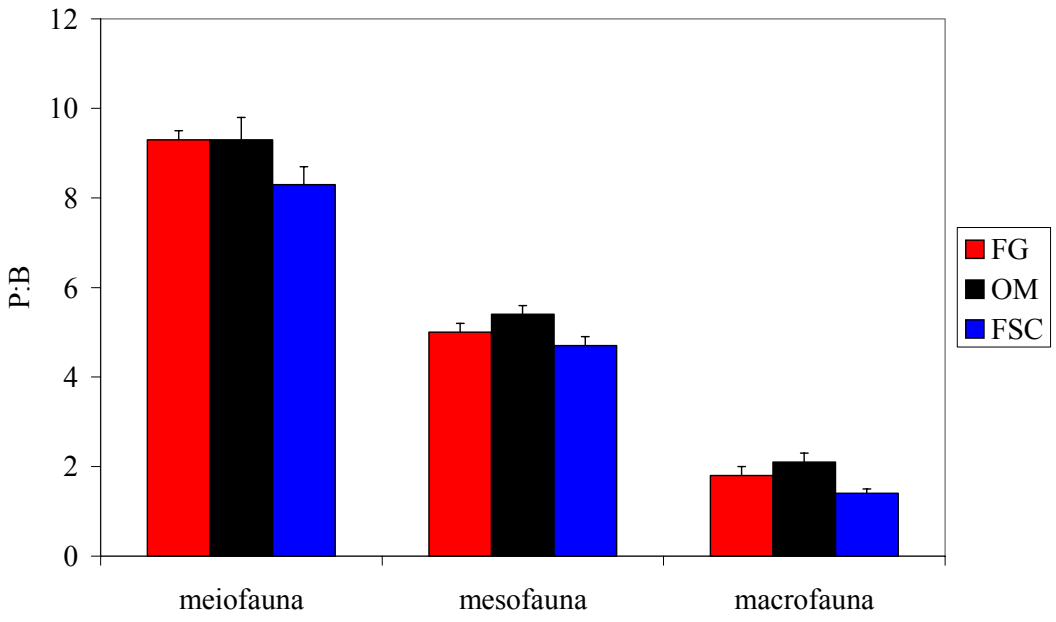


Figure 7.5. P:B ratios at the three study locations (error bars represent standard deviations).

## 7.4 Discussion

### 7.4.1 Context and limitations

Production values can be expressed in a number of different units ranging from grams wet weight to grams organic carbon making the comparison between different studies complicated (Saiz-Salinas & Ramos, 1999). Assuming a dry-to-wet weight ratio of 0.25 and that benthic organisms are approximately 40 % organic carbon by dry weight (Rowe, 1983), the annual production of benthic metazoan infauna at the current study sites ranged from 4.2 g C $m^{-2}$ $y^{-1}$ at the FG location to 1.3 g C $m^{-2}$ $y^{-1}$ at the FSC site and 1.4 g C $m^{-2}$ $y^{-1}$ at the OM site. These production estimates are of the same order and compare favourably with previous production estimates from a wide variety of environments. For example, annual production estimates have been reported to range from 5.3 g C $m^{-2}$ $y^{-1}$ at Fladen Ground (De Wilde et al., 1986), 0.3 – 11 g C $m^{-2}$ $y^{-1}$ in the Antarctic settings (Arntz et al., 1994; Brey & Gerdes, 1997; Saiz-Salinas & Ramos, 1999) to 25 g C $m^{-2}$ $y^{-1}$ in temperate estuarine habitats (Warwick & Price, 1979).

The use of allometric equations in estimating community production represents an indirect and simplistic method that incorporates several conversions, approximations and assumptions (e.g. decrease of food availability with increasing water depth; bioenergetic similitude of organisms of the same size etc). The numeric estimates obviously reflect these approximations and assumptions and should be interpreted with caution. When the limitations of the allometric production estimation techniques are acknowledged and accounted for, this approach can be useful in providing broad conclusions about the community and ecosystem energy flows as well as offer some

perspective on shifts in secondary production patterns across environmental gradients (Saiz-Salinas & Ramos, 1999).

### 7.4.2 Input flux versus energy demand

The flux of organic material to the seabed was estimated from a formula that expresses it as a function of surface primary production and water depth (Suess, 1980). At the FG location the annual amount of organic carbon arriving on the seafloor was estimated to be in the range of 53-79 g C $m^{-2}$ $y^{-1}$ (chapter 2). The energy demand of meio-, meso- and macro-fauna can be determined by assuming that the total production represents a given fraction of the consumed organic carbon. Thus based on their production estimate (4.2 g C $m^{-2}$ $y^{-1}$) and 20 % energy conversion efficiency (Ankar, 1977) the total energy demand amounts to 21.1 g C $m^{-2}$ $y^{-1}$ indicating that the downward flux of organic carbon is sufficient to support the estimated production of benthic metazoan infauna at this location.

The downward flux of organic carbon at the deeper FSC site was estimated as 5.2-7.8 g C $m^{-2}$ $y^{-1}$. The energy demand of meio-, meso- and macro-fauna at this station amounted to 6.7 g C $m^{-2}$ $y^{-1}$ implying that these fauna account for most of the organic carbon arriving from the surface.

The organic carbon flux at the OM site was estimated as 37 g C $m^{-2}$ $y^{-1}$ with the energy demand of the metazoan infauna representing approximately 6.9 g C $m^{-2}$ $y^{-1}$. As at the FG site, the influx of organic material exceeds the carbon demands of the organisms investigated in this study.

As discussed earlier, the incoming carbon flux determined by using the Suess equation (1980) may underestimate the true flux at the OM site. This was highlighted during the field sampling program when dense aggregations of scyphomedusan jellyfish, *Crambionella orsini* (Vanhöffen 1888), were observed in the surface waters of the study area. Similarly, high numbers of dead jellyfish carcasses in varying stages of decay were observed on the seabed at depths varying from 350 to 3300 metres. At the deepest stations jelly detritus was observed as patches measuring several metres in diameter (Billett et al., submitted). These patches were estimated to cover approximately 17 % of the sediment surface presenting a standing stock as great as 78 g C $m^{-2}$. This value is more than twice the estimated annual downward organic carbon flux as determined by the Suess equation. The sinking jellyfish carcasses may therefore represent a significant pathway of organic carbon from the surface to the deep sea. Although these events are probably episodic, they still serve to highlight the complexity of the OM system. The influence of these rapid inputs of organic material on benthic community structure and production are largely unknown.

### 7.4.3 Partitioning of production

The incoming flux of organic material varies in composition and not all of it can be utilised as food by benthic organisms. This results in part of the carbon being buried into sediments. The total amount or organic material utilised by benthos depends on the community composition and whether the community is limited by food availability. For example, at the FG and OM sites the comparison of input fluxes and energy demands would suggest that a large proportion of the organic carbon is either

utilised by organisms other than the benthic metazoans considered in this analysis (i.e. micro- and mega-fauna) or removed from the system in the form of carbon burial. Schwinghamer et al. (1986) showed that microorganisms (e.g. bacteria) accounted for most of the secondary production (81-92 %) within the benthic communities at an intertidal site in the Bay of Fundy, Canada. It is of course very likely that at the current study sites smaller organisms (and megafauna) not included in these estimations also utilised some of the organic carbon.

*7.4.3.1 Microorganisms and protozoans*

A number of studies have investigated the influence of seasonally deposited phytodetritus on the deep-sea protozoan and metazoan communities and reported the metazoan density and biomass levels to be similar before and after the food arrival (Gooday et al., 1996), while foraminiferans have shown an increase in both density and biomass in response to phytodetritus arrival (Gooday & Lambshead, 1989). Other protists (Turley et al., 1988) and bacteria (Lochte, 1992) have been shown to respond similarly to increased phytodetritus levels. Pfannkuche (1985) also reported bacterial biomass to double after sedimentation of particulate organic matter but detected no change in the biomass of the meio-, macro- or mega-fauna.

The apparent lack of response by metazoans has been attributed to the fact that protozoans may be better competitors as a result of their higher growth rates. Foraminiferans specifically can employ a highly mobile network of granuloreticulate pseudopodia that constitute an extremely efficient system for accumulation of food particles hence providing a competitive edge over metazoan organisms (Travis &

Bowser, 1991; Bernard & Bowser, 1992). Gerlach et al. (1985) assessed the role of foraminiferans in both benthic biomass and metabolic size spectra and found that they played a significant role in the smaller size classes.

At the FG location a large number of Foraminiferan tests were observed in the sorted sediment samples. In some size fractions (180-355 μm) these tests were particularly abundant closely agreeing with the observations recorded by previous studies at this location (McIntyre, 1961; De Wilde, 1986). Although it is difficult to estimate what proportion of the observed tests contained live individuals, it is clear that foraminiferans constitute a significant part of the benthic community at this site. Similarly calcareous foraminiferans have been reported to be particularly abundant in the core of the Oman Margin OMZ (Gooday et al., 2000).

It is then possible that foraminiferans significantly contribute to annual production at the FG and OM sites. Although some foraminiferans were present at the deepest sampling site (FSC), their numbers in the sorted samples were negligible in comparison to those observed at the FG location. The low numbers of this highly effective consumer unit at the deeper site may have either allowed metazoans to realise the production niche that was occupied by foraminiferans at the shallower station or the microorganisms may represent a link between the newly arrived organic material and the higher trophic levels. Either way this would represent a potential shift in the partitioning of production among size groups at the two stations and may have further implications for the rates of nutrient recycling.

*7.4.3.2 Larger organisms*

At the opposite end of the size range, the reliable parts of the biomass- and production- size spectra did not include large macro- and mega-fauna. For instance, the biomass dominance of a relatively large bivalve, *Arctica islandica*, at the FG location is well documented in a study by De Wilde et al. (1986). As *Arctica islandica* typically feeds on the organic matter either directly from the overlying water column or as it settles on the sea bed, it is also likely to be an efficient consumer of the incming flux.

7.4.4 Energy budgets

The speculative nature of benthic production and organic matter flux estimates derived from the Tumbiolo & Downing and Suess equations are reflected in the following energy budgets. As the size-dependent approach generally predicts the average behaviour of all organisms in one size category, it may not be accurate in providing production estimates for a particular species. For instance, deviations from the average trend may arise at more specific levels as a result of decreasing transfer efficiency with increasing number of trophic levels. Nevertheless, these energy budgets are likely to be indicative of broader trends that exist within the benthic ecosystem and provide a convenient method for producing bulk estimates at the community level.

*7.4.4.1 Fladen Ground energy budget*

Previous studies have estimated the surface primary production at the FG site as ~ 90 g C $m^{-2}$ $y^{-1}$ (Steele, 1974) of which approximately 25 % or ~25 g C $m^{-2}$ $y^{-1}$ is assumed to reach the seabed (Hartwig et al., 1983). More recent estimates of surface primary production are in the region of 200-300 g C $m^{-2}$ $y^{-1}$ (the annual global production maps with SeaWiFS; http://marine.Rutgers.edu/opp/swf/ Production/results/ all2_swf.html). Assuming that a similar proportion of surface production reaches the seabed (25 %), the flux would approximate 50-70 g C $m^{-2}$ $y^{-1}$, which is close to the value obtained from the Suess formula (53-79 g C $m^{-2}$ $y^{-1}$). The energy demand of meio-, meso- and macro-fauna amounted to 21.1 g C $m^{-2}$ $y^{-1}$ leaving approximately 30 g C $m^{-2}$ $y^{-1}$ for other size groups and burial.

DeWilde et al. (1986) reported the biomass of large bivalve *Arctica islandica* as 3.6 g C $m^{-2}$. Assuming that *A. islandica* together with other larger species account for 5.0 g C $m^{-2}$ of biomass and that they have P:B ratios approximating 1 (i.e. they reproduce biomass equal to their own body weight in a year; DeWilde et al., 1986), then it can be assumed that at least 25 g C $m^{-2}$ $y^{-1}$ of the organic matter arriving on the seabed is accounted for by the smaller organisms such as bacteria and foraminiferans (ignoring carbon burial). If these microorganisms are assumed to have an energy conversion efficiency of 50 % (Ankar, 1977), their annual production would add to about 12.5 g C $m^{-2}$ $y^{-1}$.

Combining the estimates of annual production for the size groups results in total production of 21.7 g C $m^{-2}$ $y^{-1}$ with microorganisms accounting for 12.5 g C $m^{-2}$ $y^{-1}$ (58 %), meiofauna for 0.7 g C $m^{-2}$ $y^{-1}$ (3 %), mesofauna for 2.1 g C $m^{-2}$ $y^{-1}$ (10 %),

macrofauna for 1.4 g C $m^{-2}$ $y^{-1}$ (6 %) and megafauna for 5 g C $m^{-2}$ $y^{-1}$ (23 %; table 7.2).

*7.4.4.2 Faroe-Shetland Channel energy budget*

Given that the calculated energy demand of metazoan infauna (6.7 g C $m^{-2}$ $y^{-1}$ for meio-, meso- and macro-fauna) accounts for most of the incoming organic carbon (5.2-7.8 g C $m^{-2}$ $y^{-1}$) this may suggests that the FSC site is characterised by sequential carbon utilisation. The micro- and mega-fauna at the FSC site also ultimately depend on the incoming organic material as their food source and consequently carbon must be passed through the trophic levels to support the existence of all size fractions. Due to the lack of information on the biomass of microorganisms at the FSC location (bacterial biomass in a similar environment on the Voring Plateau has been reported as 0.9 g C $m^{-2}$; Koster et al., 1991), it is only possible to estimate the production of metazoan organisms. The production of meio-, meso- and macro-fauna was estimated as 1.3 g C $m^{-2}$ $y^{-1}$. Megafaunal biomass for epibenthic organisms (> 5 cm in size) has been estimated as 0.15 g C $m^{-2}$ (Jones et al., submitted) and it can be assumed that the smaller mega-fauna contribute approximately 0.05 g C $m^{-2}$. Assuming a P/B ratio of 1 for the megafaunal size fraction, their annual production can be estimated as 0.20 g C $m^{-2}$ $y^{-1}$ and their annual carbon demand as 1.0 g C $m^{-2}$ $y^{-1}$. The total metazoan benthic production at the FSC site can hence be estimated as 1.6 g C $m^{-2}$ $y^{-1}$ with meiofauna accounting for 12 % (0.2 g C $m^{-2}$ $y^{-1}$), mesofauna for 24 % (0.4 g C $m^{-2}$ $y^{-1}$), macrofauna for 52 % (0.8 g C $m^{-2}$ $y^{-1}$) and megafauna for 12 % (0.2 g C $m^{-2}$ $y^{-1}$; table 7.2).

*7.4.4.3 Oman Margin energy budget*

No megafauna were observed in the core of the oxygen minimum zone during the field sampling program. As the annual organic carbon demand of the meio-, meso- and macro-fauna is relatively small (6.9 g C $m^{-2}$ $y^{-1}$) in relation to the organic carbon flux, it is the microorganisms that seem to utilise most of the newly arrived carbon (~30 g C $m^{-2}$ $y^{-1}$; ignoring carbon burial see below). Again assuming 50 % energy conversion efficiency, the production of microorganisms can be estimated to amount to 15 g C $m^{-2}$ $y^{-1}$ and the total production to be 16.4 g C $m^{-2}$ $y^{-1}$. The microorganisms hence represent 91 % of the total production with meiofauna accounting for 2 % (0.3 g C $m^{-2}$ $y^{-1}$), mesofauna for 3 % (0.5 g C $m^{-2}$ $y^{-1}$) and macrofauna for 4 % (0.6 g C $m^{-2}$ $y^{-1}$; table 7.2).

As with the FG location, these results suggest that microorganisms account for the vast majority of benthic production at the OM site with the smaller P/B ratios and shorter biological turnover times possible resulting in increased rate of nutrient recycling further fuelling the high surface production at this site. However, microorganisms are unlikely to utilise all of the excess carbon as proposed above. Instead some of this carbon is probably buried into sediments and effectively removed from the system. The sediment environments below oxygen minimum zones have been suggested to act as sinks for carbon arriving from the overlying water column and atmosphere (Cowie, 2005). In the Arabian Sea this may be particularly true as large amounts of organic material in the form phytodetritus or other pelagic particles

(e.g. jellyfish carcasses) sink through the water column and are deposited on the seabed.

### 7.4.5 Respiration

Respiration can be described as the summed power expenditure of all metabolic processes thus representing the total carbon demand of the organisms (Peters, 1983). Total respiration should therefore approximate total energy demand (in terms of carbon) for food limited steady state systems. Annual respiration of the meio-, meso- and macro-fauna was determined from their production estimates by using the empirical relation derived by Schwingamer et al. (1986; eq 2). These amounted to 9.8 g C $m^{-2}$ $y^{-1}$ for the FG site, 3.0 g C $m^{-2}$ $y^{-1}$ for the FSC site and 3.2 g C $m^{-2}$ $y^{-1}$ for the OM site. Corresponding figures for the benthic community as a whole can be estimated by including megafauna in equation 7.2 and by assuming that the annual respiration of the microorganisms equals their annual production (Schwinghamer et al., 1986). These estimates amounted to 33.6 g C $m^{-2}$ $y^{-1}$ for the FG site, 3.5 g C $m^{-2}$ $y^{-1}$ for the FSC site and 18.2 g C $m^{-2}$ $y^{-1}$ for the OM site (table 7.2).

In situ experiments at the FG site have reported respiration values of 7.2 g C $m^{-2}$ $month^{-1}$ during the summer months when biological activity is high (DeWilde et al, 1986). Based on these monthly values and assuming reduced biological activity during the winter months, DeWilde et al. (1986) estimated annual respiration to be in region of 50-70 g C $m^{-2}$ $y^{-1}$, which is closer to the estimated flux of the organic carbon at the FG site and the value derived from the empirical equation of Schwinghamer et al. (1986).

Table 7.2. Energy budgets for the three study sites (all units g C $m^{-2}$ $y^{-1}$). Values in brackets refer to estimated production.

| | | FG | FSC | OM |
|---|---|---|---|---|
| **Organic carbon demand (production)** | **Microorganisms** | 25.0 (12.5)* | - | 30.0 (15.0)* |
| | **Meiofauna** | 3.3 (0.7) | 0.9 (0.2) | 1.5 (0.3) |
| | **Mesofauna** | 10.7 (2.1) | 1.9 (0.4) | 2.6 (0.5) |
| | **Macrofauna** | 7.2 (1.4) | 4 .0 (0.8) | 2.8 (0.6) |
| | **Megafauna** | 25.0 (5) | 1.0 (0.2) | - |
| | **Total** | 71.2 (21.7)* | 7.8 (1.6) | 36.9 (16.4)* |
| | **Carbon flux** | 50-70 | 5.2-7.8 | 37.0 |
| | **Respiration** | 33.6 | 3.5 | 18.2 |

* In reality microorganisms probably account for a smaller proportion of the "excess" organic carbon and some of it is lost from the system in the form of carbon burial.

### 7.4.6 Summary

The body size-based approach in estimating community production and energy flow can provide additional insights into the system dynamics on scales that would be difficult to establish by any other means. The results from this analysis showed that, in general, the estimated carbon demand at the three locations was supported by the estimated flux of incoming organic material. The total infaunal production varied from 42 g wwt $m^{-2}$ $y^{-1}$ at the FG location to approximately 14 g wwt $m^{-2}$ $y^{-1}$ at the FSC and the Arabian Sea (OM) sites. The downward flux of organic matter at the FG and OM sites exceeded the estimated carbon demand of the included infauna and further analyses suggested that microorganisms and megafauna account for some of the incoming organic carbon. This was in contrast to the energy budget estimated for

the FSC location where the incoming flux approximately equalled the energy demands of meio-, meso- and macro-fauna.

A part of the incoming organic carbon at all three locations will not or cannot be utilised as a food source and this fraction is consequently buried. The carbon burial rate at FSC location is probably low, whereas at the FG and particularly at the OM site, where the incoming flux of organic material exceeds the estimated energy demand of the benthos, the rate may be significantly higher.

# 8. MODELLING BENTHIC BODY SIZE STRUCTURE

## 8.1 Introduction

Modelling benthic communities is often limited by the lack of quantitative information on many of the biological processes. This probably reflects the relative complexity associated with sampling and obtaining empirical estimates for the biological functions of benthic organisms. Further complications can be attributed to the high degree of uncertainty in these measurements due to natural variation and the difficulty of extrapolating species-specific measurements to community level processes (Blackford, 1997). Consequently fewer benthic community models exist in comparison to those developed for pelagic environment (Ebenhöh et al., 1995).

One approach to modelling the benthos is to use the underlying size structure. This approach is based on the idea that individual body size is closely related to most biological functions (Peters, 1983; Schmidt-Nielsen, 1984; Brown et al., 2004). It also assumes that organisms of the same size behave similarly in terms of bioenergetics regardless of their taxonomic or functional identity. The relative simplicity of the size-based approach can hence potentially ensure that the parameterisation is not overcomplicated and that the relevant empirical data are already available or can be easily attained. The first step in size-based investigations is to assess whether the models are capable of explaining the patterns observed in the empirical data. This means that additional complexities such as functional groups (e.g. deposit- and

suspension feeders) are excluded. A successful size-dependent model may help to improve the understanding of processes that control the functioning and dynamics of benthic communities.

A size-based modelling approach was adopted by Peters (1978) and Griesbach et al. (1982) for hypothetical animal communities. Peters (1978) constructed a size-dependent model that predicted the biomass distribution of a community in terms of four processes: ingestion, respiration, defecation and mortality. Organisms within the community were assigned to one of five size classes that all fed from the same detritus food pool. Peters stated that a pelagic lake community separated into continuous size classes may represent a "real-life" analogue of this hypothetical assemblage. Griesbach et al. (1982) displayed that one use of this model could be in bioaccumulation studies where the distribution of a chemical pesticide (DDT) was modelled within the framework described by Peters (1978). Although the approach was again hypothetical, the model results showed a qualitative similarity with previously published empirical data. Although both studies demonstrated the potential and flexibility of a simple size-based modelling approach, they also outlined the need to improve the empirical bases of the model in order to make quantitative predictions.

The model described here attempts to make those quantitative predictions by applying the approach presented by Peters (1978) to a marine benthic community in the deep Faroe-Shetland Channel. High-quality replicate size distribution data have been collected and analysed for the metazoan benthic infauna (45-500 μm) and these results have served as a basis for the current model that seeks to reproduce the observed biomass distribution. Modifications have been made to the Peters model by

increasing the number of size classes and by adapting the equations and parameter values so that they are based on published literature values relevant to benthic processes. The specific aims of this project were three-fold: (1) to construct a body size-based model that describes the benthic community biomass distribution, (2) to assess if the size-based approach alone can reproduce the patterns observed in the field data and if so (3) to identify the processes that control the distribution of biomass in the model.

## 8.2 Model description

### 8.2.1 Basic description

The model describes a closed system in which meio- and macro-fauna feed from the same food source (detritus; figure 8.1). There are 16 size classes in the model encompassing the reliable part of the empirical biomass spectra (i = 5:20) as well as a detritus compartment. The organic matter is assumed to be of uniform composition regardless of whether it is biologically bound within the size classes or forms part of the detritus pool. Biomass is determined by four processes: ingestion (I), respiration (R), defecation (D) and mortality (Z). At each time step losses through respiration, defecation and mortality are returned to the detritus compartment representing the closure term. In reality some of these processes would represent true losses from the system (e.g. respiration in the form of $CO_2$) but as this model describes a closed system, these losses have been retained to simulate the flux of incoming organic material. Net growth is determined by the difference between ingestion (I) and the loss terms (R, D & Z) within each size class at each time step. The biomass flux for each size class ($B_i$) is described by:

$$\frac{dB_i}{dt} = (1 - R - D)(B_i I(\frac{Det}{k_{ing} + Det}) - (B_i Z(\frac{B_i}{k_Z + B_i})) \quad (8.1)$$

where a Michaelis-Menten type function limits both ingestion and mortality. Det and $B_i$ represent the biomass in the detritus compartment and in the body size class *i* whilst $k_{ing}$ and $k_Z$ are the ingestion and mortality half saturation constants,

respectively. Time is represented by t. The transfer of material through the detritus compartment is described by:

$$\frac{dDet}{dt} = \sum R[B_i I(\frac{Det}{k_{ing} + Det})] + \sum D[B_i I(\frac{Det}{k_{ing} + Det})] + \sum B_i Z(\frac{B_i}{k_Z + B_i}) - \sum [B_i I(\frac{Det}{k_{ing} + Det})] \quad (8.2)$$

8.2.3 Parameterisation: body size relationships

The parameter values for ingestion and mortality have been derived from published, body size-based relations. Cammen (1980) summarised previously published data relating organic matter ingestion rates (adjusted for sediment organic content) and individual body size of benthic deposit feeders and detrivores. These data were converted so that ingestion and body size were expressed as a specific rate ($d^{-1}$) and grams wet weight (assuming 0.25 dry-to-wet weight ratio), respectively. The resulting data were used to derive a linear regression model ($n = 19$; $r^2 = 0.69$; $p < 0.001$; figure 8.2) that was converted to a power function format:

$$I = 0.091M^{-0.26} \quad (8.3)$$

where M represents body mass (g wet weight) and I represents the ingestion rate ($d^{-1}$). Although these data exclude suspension feeding organisms, they are still likely to provide a reasonable reflection of the benthic community at the FSC site were most of the organisms (in the included size range) feed directly from the sediment.

Natural mortality rates for benthic organisms are difficult to parameterise, as little experimental data exists. However, at steady state, annual production should be balanced by the amount of material lost and thus mortality has been suggested to scale closely with annual production rates (Banse & Mosher, 1980). Brey (1999) established an approximation between production (expressed as somatic production/biomass ratio, P/B) and specific mortality rates (Z) as displayed by the linear regression model in equation 8.4 ($n = 103$; $r^2 = 0.92$; $p < 0.001$).

$$Z = 0.082 + 0.925(P/B) \quad (8.4)$$

The determination of size-based mortality rates then required an allometric equation relating P/B ratios to individual body size. Schwinghamer et al. (1986) established this relation for meio- and macro-faunal organisms from published literature values (eq. 8.5 – P refers to somatic production), where

$$P/B = 0.696M^{-0.208} \quad (8.5)$$

Equations 8.4 and 8.5 were then used in combination for the parameterisation process of mortality rates (table 8.1). Respiration and defecation are expressed as fractions of total organic matter ingested (equations 8.6 & 8.7). Little published data exists on providing estimates on what fraction of ingested material is accounted for by respiration. Cammen (1989) estimated that benthic organisms lose between 2 to 5% of the total ingested carbon through respiration and consequently this range was used as an initial estimate in the model with the highest respiration parameter value ($\alpha_i = 0.05$) assigned to the smallest size class ($B_i$). Brey (2001) estimated that 1-79 % of ingested

material is lost through defecation (21-99 % assimilation efficiency) in aquatic invertebrates and again this range was used in the parameterisation process for defecation with the highest parameter value ($\beta_i = 0.8$) assigned to the smallest size class ($B_i$).

$$R_i = \alpha_i \; ; \; R_{i+n} = \alpha_i - 0.002 \qquad (8.6)$$

$$D_i = \beta_i \; ; \; D_{i+n} = \beta_i - 0.05 \qquad (8.7)$$

In the absence of published data, the parameterisation process of the half saturation constants for ingestion ($k_{ing}$) and mortality ($k_z$) is difficult but the initial sensitivity analysis revealed that constant numeric values (in the range of 0.05-100) make negligible difference to the model outcome. The gradients in k values can be effectively taken to reflect the species turn-over rate or 'pace of life' with the smaller organisms following the 'live fast, die young' or r-selection mode. Consequently both half saturation constants were nominally set to range from 0.1 (g) at the smallest size class to 1.6 (g) at the largest.

The 16 size classes included in the model followed a logarithmic scale (base 2) and the mean body sizes of the size classes ranged from $8.9 \times 10^{-7}$ to $2.9 \times 10^{-2}$ grams wet weight (table 8.1). These values were used to derive the relevant numeric values for the ingestion and mortality rates (equations 8.3-8.5). Model components and flows are expressed in grams of mass wet weight and grams per day, respectively. The model is initialised by evenly distributing the measured total biomass from Faroe-Shetland Channel (7 g wwt $m^{-2}$) among the 16 size classes and the detritus pool with the time step set to 0.05 d.

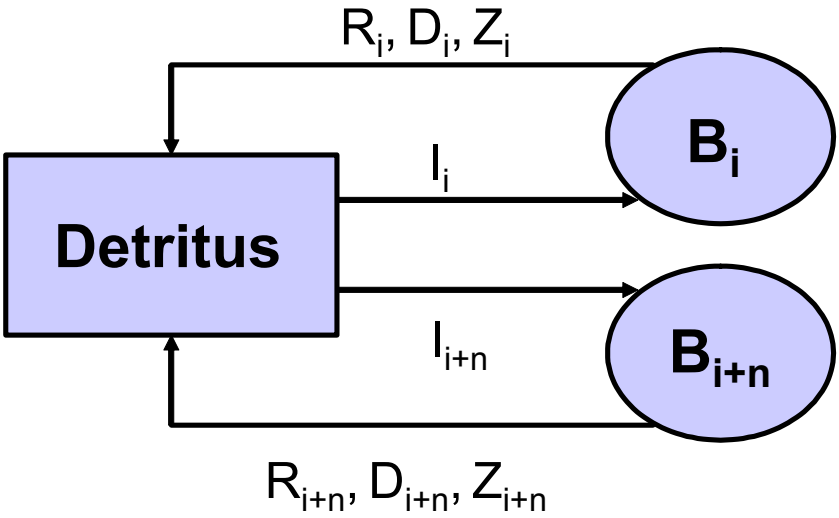


Figure 8.1. Schematic presentation of the model structure. Only two size classes (i, i + n) are shown. I = ingestion, R = respiration, D = defecation, Z = mortality.

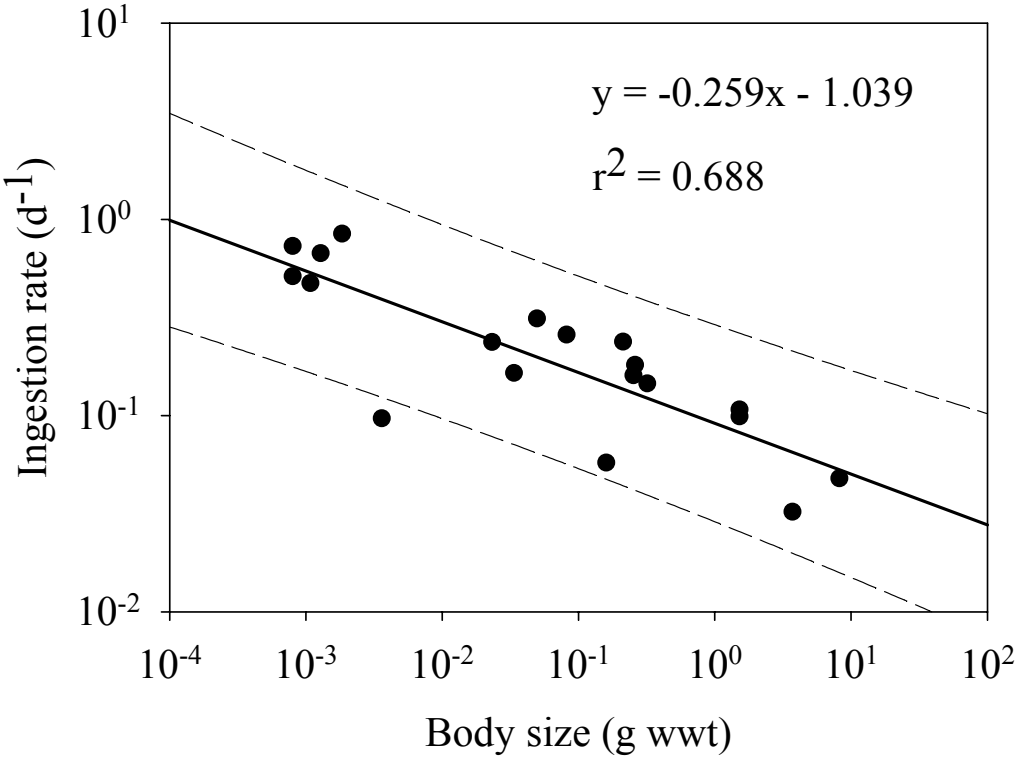


Figure 8.2. Linear regression model describing the relationship between ingestion rate of organic material and individual body size for benthic organisms. The broken lines represent 95 % prediction intervals. The regression model is statistically significant ($p<0.01$). The data are from Cammen (1980).

Table 8.1. The parameter values used in the model.

| | | **Standard parameter values** | | | | | |
|---|---|---|---|---|---|---|---|
| | | **I ($d^{-1}$)** | **R** | **D** | **Z ($d^{-1}$)** | **$k_{ing}$ (g)** | **$k_Z$ (g)** |
| | | 0.9 | 0.035 | 0.45 | 0.01 | 1 | 1 |
| | | **Gradients in parameter values** | | | | | |
| **X2** | **Mean wwt (mg)** | **I ($d^{-1}$)** | **R** | **D** | **Z ($d^{-1}$)** | **$k_{ing}$ (g)** | **$k_Z$ (g)** |
| 5 | 0.00089 | 3.40 | 0.050 | 0.800 | 0.032 | 0.1 | 0.1 |
| 6 | 0.0018 | 2.84 | 0.048 | 0.750 | 0.028 | 0.2 | 0.2 |
| 7 | 0.0036 | 2.37 | 0.046 | 0.700 | 0.024 | 0.3 | 0.3 |
| 8 | 0.0071 | 1.98 | 0.044 | 0.650 | 0.021 | 0.4 | 0.4 |
| 9 | 0.014 | 1.66 | 0.043 | 0.600 | 0.018 | 0.5 | 0.5 |
| 10 | 0.029 | 1.38 | 0.041 | 0.550 | 0.016 | 0.6 | 0.6 |
| 11 | 0.057 | 1.15 | 0.039 | 0.500 | 0.014 | 0.7 | 0.7 |
| 12 | 0.11 | 0.96 | 0.037 | 0.450 | 0.012 | 0.8 | 0.8 |
| 13 | 0.23 | 0.81 | 0.035 | 0.400 | 0.010 | 0.9 | 0.9 |
| 14 | 0.46 | 0.67 | 0.033 | 0.350 | 0.009 | 1 | 1 |
| 15 | 0.91 | 0.56 | 0.031 | 0.300 | 0.008 | 1.1 | 1.1 |
| 16 | 1.8 | 0.47 | 0.029 | 0.250 | 0.007 | 1.2 | 1.2 |
| 17 | 3.6 | 0.39 | 0.028 | 0.200 | 0.006 | 1.3 | 1.3 |
| 18 | 7.3 | 0.33 | 0.026 | 0.150 | 0.005 | 1.4 | 1.4 |
| 19 | 15.0 | 0.27 | 0.024 | 0.100 | 0.004 | 1.5 | 1.5 |
| 20 | 29.0 | 0.23 | 0.022 | 0.050 | 0.004 | 1.6 | 1.6 |

### 8.2.4 Standard model run

The initial model run acted as a standard against which all the subsequent runs were gauged. The standard model run was defined as a case where all parameters were set constant across the size classes (table 8.1; figure 8.3a). The parameter values for ingestion, respiration, defecation and mortality were determined as the approximate median values of the overall range as determined by equations 8.3-8.7. The parameter values for the half-saturation constants in the standard model run were set to 1.

### 8.2.5 Sensitivity analysis

The effect of size dependent parameter gradients on the resulting biomass distribution was examined in two ways. First, one process at a time was assigned a size-based gradient (figure 8.3b) and the model sensitivity was gauged against the standard run. The size-based gradients for ingestion and mortality were determined from the allometric equations 8.3-8.5 using the mean body size at each size class (table 8.1). The size-based gradients for respiration, defecation and the half saturation constants were set to vary according to the range of parameter values stated in table 8.1. These size-based gradients could be described by either linear or exponential functions but the initial sensitivity analysis indicated that both types of gradients produced similar results (not shown). Consequently, the simpler, linear functions were applied in this study.

The second sensitivity analysis involved applying the size-based gradients to all the processes simultaneously and then setting one parameter constant, across all size classes, at a time. These model runs are summarised in table 8.2.

The model was run to a steady state. A steady state was reached when the change in the biomass values of the state variables at the beginning of successive years was less than 1 percent. The amount of time taken to reach steady state varied depending on the parameter setup and ranged from 2 years for the standard run to 26 years for the model run 13. At equilibrium the biomass from each size class was plotted against the mean body size to produce the results in the same format as the empirical data.

The deviations of the model results were determined for each size class from the empirically determined data points (averaged for each size class) as well as from the linear regression model (figure 8.4). The actual (absolute) deviations at all size classes were summed for each run and this value provided a 'deviation index' of how well the model fitted the empirical data or the linear regression line.

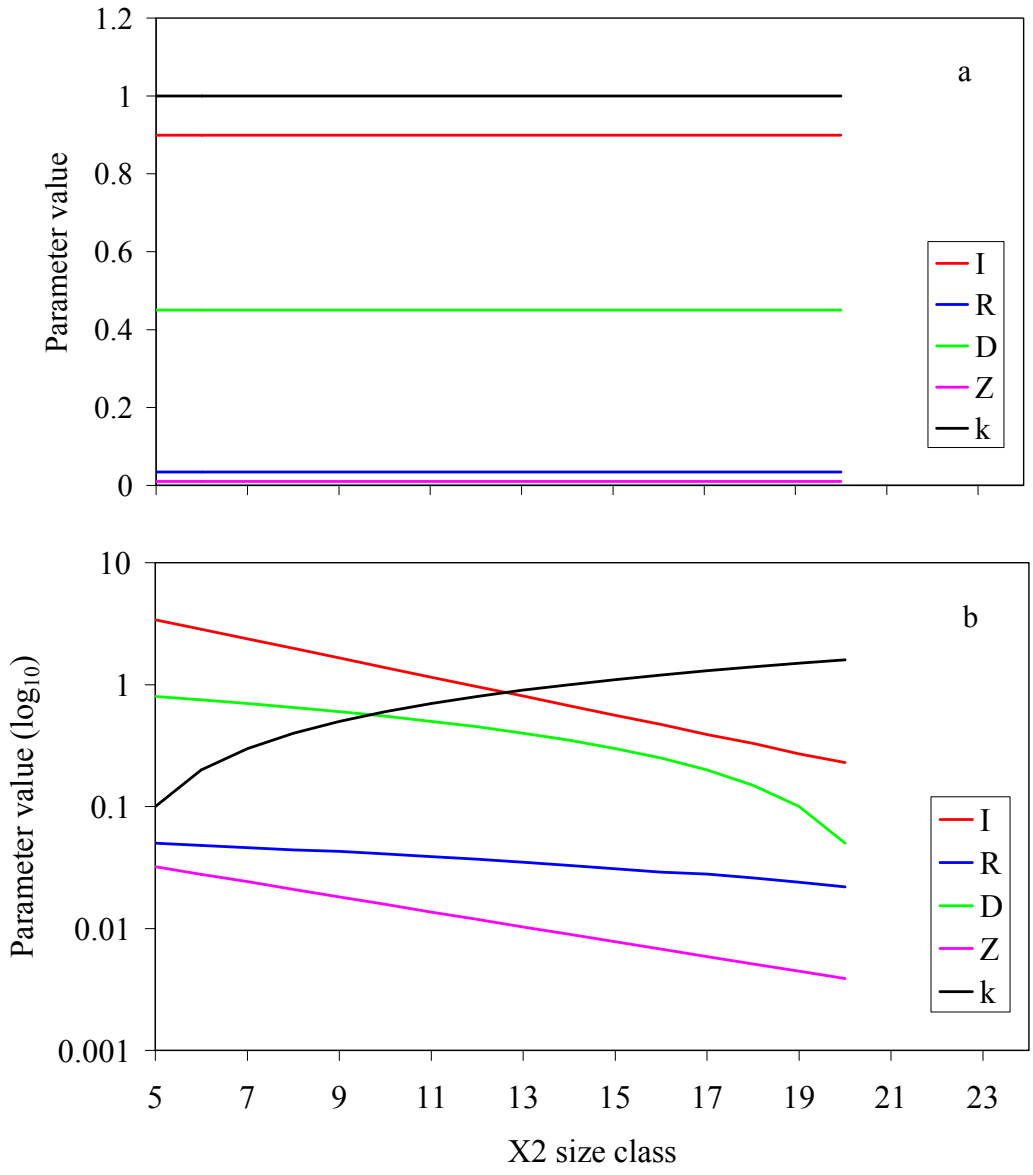


Figure 8.3. Graphical presentation of the parameter values used in the model: (a) constant values and (b) size based gradients. I = ingestion, R = respiration, D = defecation, Z = mortality and k = half-saturation constants for ingestion and mortality.

Table 8.2. Summary of model runs (c = standard parameter values; g = gradient in parameter values; $g_{mod}$ = modified gradient).

| Model run | | I | $K_{ing}$ | D | Z | $K_z$ | R |
|---|---|---|---|---|---|---|---|
| 1 | standard | c | c | c | c | c | c |
| 2 | I | g | c | c | c | c | c |
| 3 | $k_{ing}$ | c | g | c | c | c | g |
| 4 | D | c | c | g | c | c | c |
| 5 | Z | c | c | c | g | c | c |
| 6 | $k_z$ | c | c | c | c | g | c |
| 7 | R | c | c | c | c | c | g |
| 8 | $R_{mod}$ | c | c | c | c | c | $g_{mod}$ |
| 9 | all | g | g | g | g | g | g |
| 10 | all – I | c | g | g | g | g | g |
| 11 | all – $k_{ing}$ | g | c | g | g | g | g |
| 12 | all – D | g | g | c | g | g | g |
| 13 | all – Z | g | g | g | c | g | g |
| 14 | all – $k_z$ | g | g | g | g | c | g |
| 15 | all – R | g | g | g | g | g | c |
| 16 | all with $R_{mod}$ | g | g | g | g | g | $g_{mod}$ |

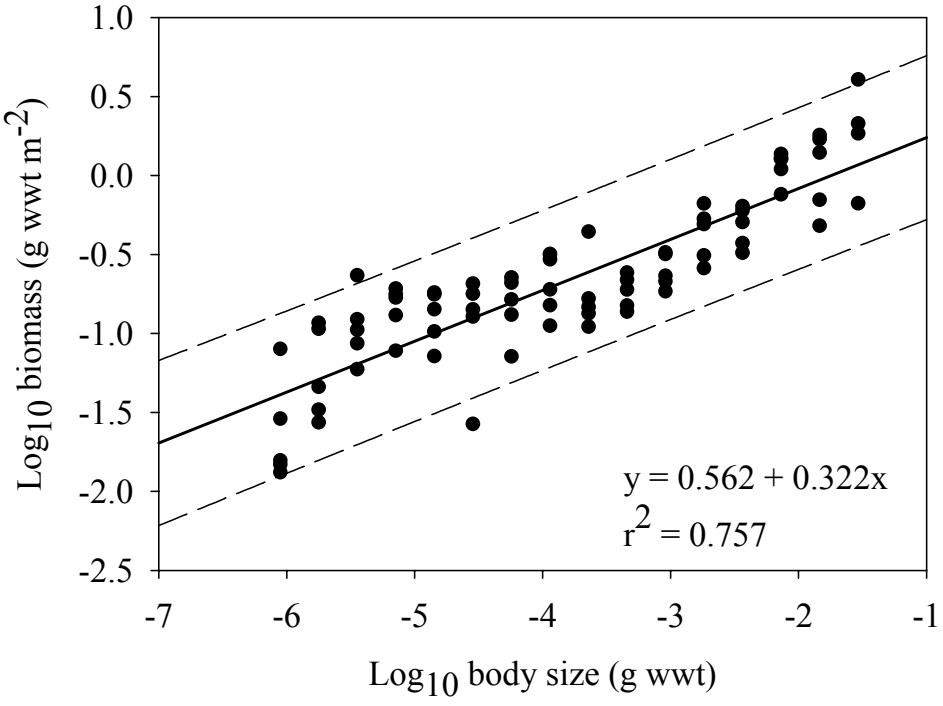


Figure 8.4. Biomass size spectrum at the FSC site. The individual data points refer to the replicate empirical data points. Ordinary least squares regression line is also plotted (with 95 % prediction intervals).

**8.3 Model results**

The standard run of the model (model run 1; no size-dependency) produces a uniform biomass distribution (figure 8.5a). Applying body size gradients to only ingestion and then only to the half saturation constants for ingestion (runs 2 & 3; figures 8.5b & c) results in the smallest organisms dominating the biomass distribution. This is an opposing trend to that observed in the field data and is also reflected in the relatively high deviation index values (table 8.3).

Applying gradients to all the other parameters (D, Z, $k_Z$ & R) one at a time results in model biomass increasing with larger size classes (model runs 4-7; figures 8.5d, e, f & g). Size-based gradient in defecation, mortality and half saturation constant for mortality ($k_Z$) produce biomass distribution patterns that resemble both the observed data and the linear regression model (model runs 4, 5 & 6; figures 8.5d, e & f). These visual observations are supported by the relatively low deviation index values (table 8.3). A size-based gradient in respiration alone (model run 7; figure 8.5g) results in a nearly identical biomass distribution of the standard run (figure 8.5a). Increasing the numeric range of respiration parameter values in the model to 4-14 % (note: R and D are expressed as fractions of total ingestion and their sum cannot exceed 1, hence the range of increased R values is limited) makes negligible difference (model run 8; figure 8.5h).

When size-based gradients are applied simultaneously to all the processes (model run 9; figure 8.6a), biomass is overestimated at the smaller size classes and underestimated at the larger end. When ingestion or $k_{ing}$ is held constant (with

gradients in all other processes) the model distribution resembles the empirical biomass distribution (model run 10-11; figures 8.6b & c).

When defecation, mortality, $k_Z$ or respiration is held constant (one at a time with gradients in all other parameters; figures 8.6d, e, f & g), the model biomass distribution does not resemble the data. This non-resemblance to the empirical data is highlighted by the relatively high deviation index values at these model runs (table 8.3). The notable exception is model run 16 that applies the modified range of respiration values in conjunction with gradients in all other parameters (figure 8.6h). This run results in a close resemblance to empirical data and the regression model (table 8.3).

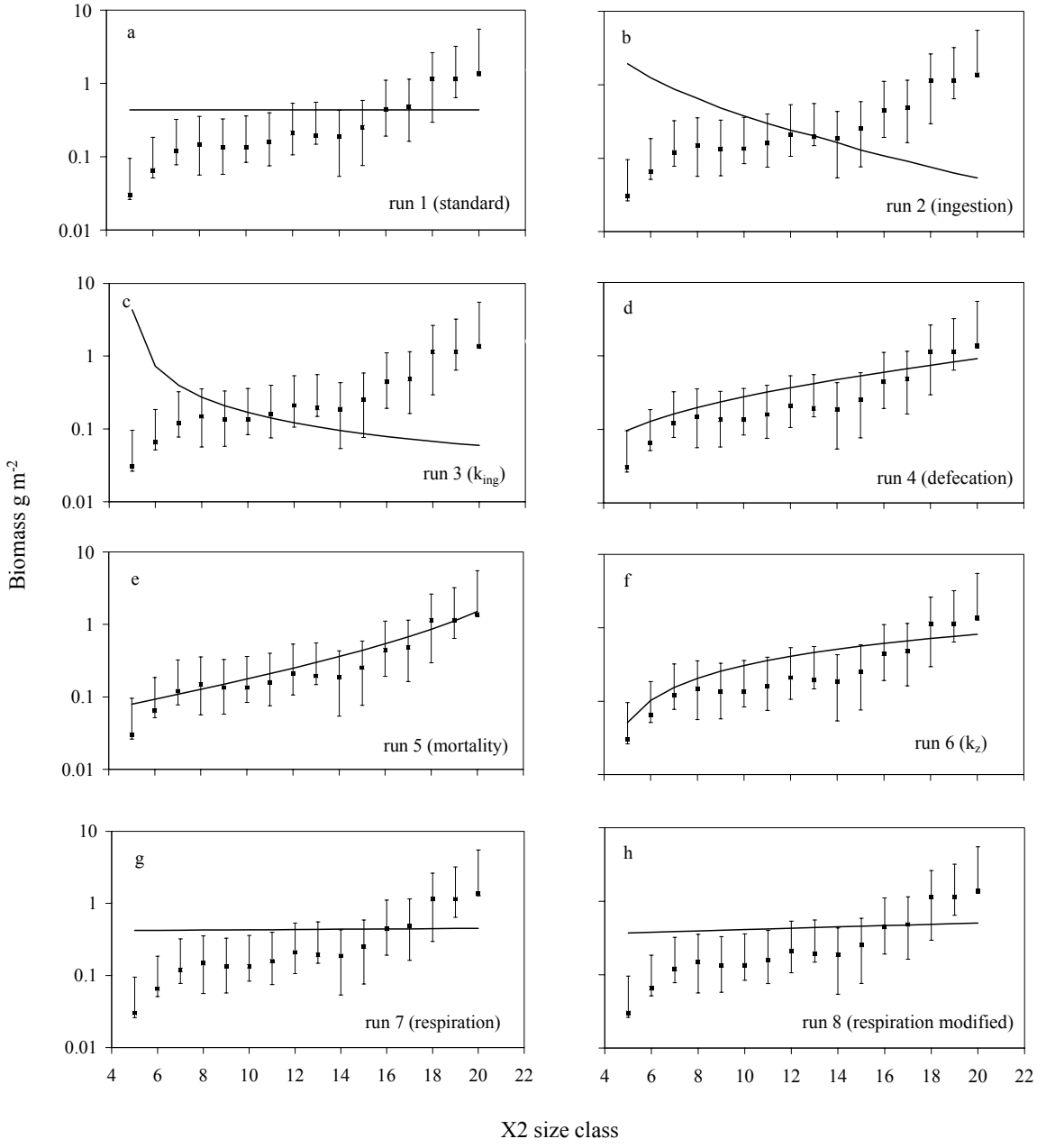


Figure 8.5. Comparison of the model (continuous line) and empirical data (black squares with 95 % confidence intervals) for the Faroe-Shetland Channel site. Model run 1 shows the results when all the parameter values were held constant. The subsequent graphs display results as gradients were applied to one parameter set at the time: (run 2) ingestion, (run 3) king, (run 4) defecation, (run 5) mortality, (run 6) kz, and (run 7) respiration and (run 8) modified respiration.

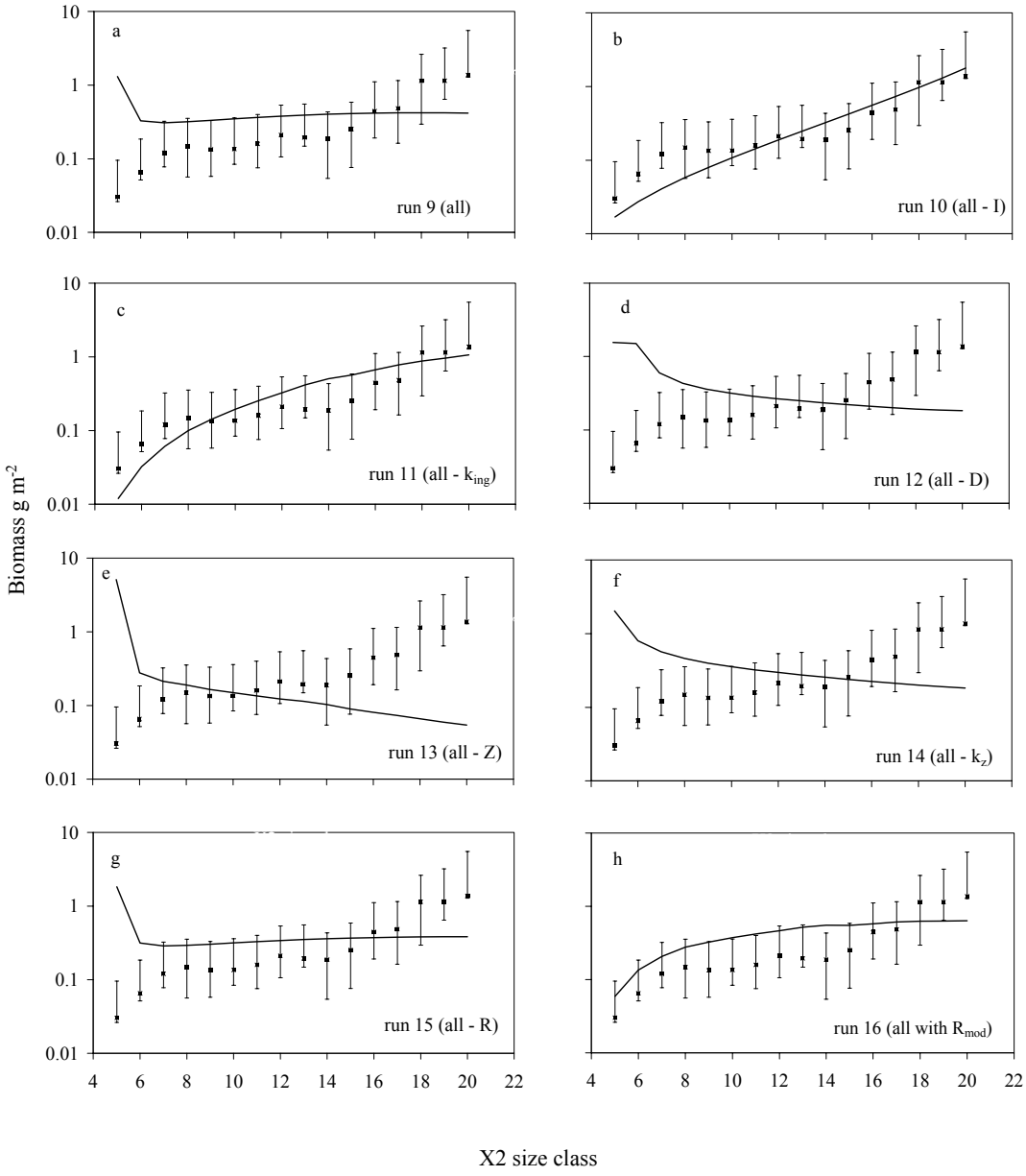


Figure 8.6. Comparison of the model (continuous line) and empirical data (black squares with 95 % confidence intervals) for the Faroe-Shetland Channel site. The graphs display the results body size-based gradients were applied to all processes (run 9) and then to all processes apart from: (run 10) ingestion, (run 11) $k_{ing}$, (run 12) defecation, (run 13) mortality, (run 14) $k_z$ and (run 15) respiration. Run 16 shows results when a size-based gradient was applied to all processes but increased parameter values were used for respiration (see text for details).

Table 8.3. The deviation indices of the predicted biomass values from both the empirical data and the linear regression model. The model runs have been ranked in an ascending order.

| **Empirical data** | | | **Linear regression** | | |
|---|---|---|---|---|---|
| **model run** | | **index** | **Model run** | | **index** |
| 5 | (Z) | 1.5 | 5 | (Z) | 1.3 |
| 10 | (all-I) | 1.8 | 10 | (all-I) | 1.6 |
| 11 | (all-$k_{ing}$) | 2.8 | 11 | (all-$k_{ing}$) | 1.7 |
| 4 | (D) | 3.1 | 4 | (D) | 2.0 |
| 6 | ($k_z$) | 3.5 | 6 | ($k_z$) | 2.4 |
| 16 | (all with $R_{mod}$) | 4.6 | 16 | (all with $R_{mod}$) | 3.6 |
| 8 | ($R_{mod}$) | 5.1 | 8 | ($R_{mod}$) | 4.3 |
| 7 | (R)) | 5.5 | 7 | (R)) | 4.7 |
| 1 | (standard) | 5.6 | 1 | (standard) | 4.8 |
| 9 | (all) | 5.8 | 9 | (all) | 5.0 |
| 15 | (all-R) | 6.1 | 15 | (all-R) | 5.4 |
| 14 | (all-$k_z$) | 8.0 | 14 | (all-$k_z$) | 7.6 |
| 12 | (all-D) | 8.1 | 12 | (all-D) | 7.7 |
| 2 | (I) | 9.6 | 2 | (I) | 9.4 |
| 3 | ($k_{ing}$) | 10.3 | 3 | ($k_{ing}$) | 10.0 |
| 13 | (all-Z) | 10.4 | 13 | (all-Z) | 10.2 |

## 8.4 Discussion

### 8.4.1 Empirical data

Reliable empirical data are required to assess the accuracy of model predictions. The sampling protocol in the current study has been specifically designed to cover the entire size range of benthic meio- and macro-faunal organisms with replicate sampling providing increased confidence in the observed trends. Although it is difficult to determine the exact shape of the observed size distribution, the sampling design and the recognition and exclusion of unreliable data (due to inherent sample bias) has ensured that the included size classes provide a high-quality estimation of the true size distribution of benthic metazoan organisms. The trend of biomass increasing with body size also generally conforms to the metabolic theory of ecology that provides a quantitative framework for predicting a number of biological processes (e.g. metabolic rate, abundance or biomass) in terms of individual body size and temperature (Brown et al., 2004). This theory predicts biomass to increase as a function of individual body size ($B = M^{1/4}$) and although the scaling exponents (the predicted and actual slope of the regression lines) differ slightly (possibly due to food limited FSC environment – see chapter 5), they are reasonably similar.

### 8.4.2 Size-based modelling approach

The model is shown to be capable of producing a variety of biomass distribution patterns depending on the parameterisation set-up. These results suggests that a simple, size-based approach is appropriate in modelling the benthic biomass

distribution without including functional groups or other factors that further help to characterise benthic communities. The omission of functional differentiation does not deny their existence but instead implies that they do not impose a strong enough influence to be included in the model structure. As the size-based modelling approach is capable of replicating the empirical data it can also help to outline some of the processes that control the size distributions of benthic communities.

### 8.4.3 Ingestion

The model results suggest that ingestion does not follow a size-dependent pattern. Previous hypotheses have predicted that benthic ingestion rates may instead be dependent on the organic content of the sediments where the rate will increase only up to a maximum level beyond which the utilisation of food is not limited by the availability but by the time it takes to process it (e.g. Lopez & Levington, 1987). Different feeding modes are also likely to influence the rate of ingestion (Taghon & Green, 1992). This implies that the ingestion process of benthic organisms is likely to be more complicated than a straightforward size dependency would suggest.

### 8.4.4 Defecation

A size-based gradient in defecation values alone produces a biomass distribution pattern that closely follows the observed data (figure 5d). Although this results from the fact that smaller organisms are placed at a disadvantage (losing more of the ingested material), there are some theoretical considerations why defecation values should be scaled to body size. For instance, when ingestion rates are set equal across

the size classes, the gradient in defecation values can be interpreted to reflect size dependent assimilation efficiency. Organisms with larger body size generally have greater gut volumes and hence longer gut passage times than smaller animals (Gage & Tyler, 1991). The increased gut passage time in turn could allow a more complete digestion of the same food material and result in increased assimilation efficiency (Jumars et al., 1990).

### 8.4.5 Respiration

Theoretical and empirical evidence suggests that respiration is likely to follow a size dependent relation (Peters, 1983; Brown et al., 2004). For instance, Mahaut et al. (1995) compiled data relating individual body size to respiration rate for deep-sea organisms. Considering only the deep-sea benthos, a statistically significant linear regression model can be derived from these data to relate the two variables ($r^2 = 0.84$; $p < 0.01$). In the current study respiration (like defecation) was expressed as a fraction of total ingestion and the influence of a size-based based gradient in the respiration values was found to be negligible to the overall biomass distribution. This can possibly be explained by the fact that respiration was expressed as a relatively small proportion (2-5 %) of total ingestion. Increasing the parameter values for respiration decrease the amount of biomass retained at the smallest size classes as these organisms now use more energy through respiration. These observations suggest that the original range of respiration values (2-5 %) probably underestimates the actual proportion and that even the increased values independently have a minimal influence on the observed biomass distribution (runs 7 & 8; figure 5g & h). However, when size based gradients are applied to all the processes simultaneously the use of increased

respiration parameter values results in a distinctively different size distribution that more closely resembles the empirical data (run 16; figure 6h) suggesting a synergistic effect.

### 8.4.6 Mortality

The deviation index values revealed that a size-based gradient in the mortality rates produced the closest fit to both the empirical data and the linear regression model (table 8.3). Parameter sensitivity analysis also reveals that the alteration of the mortality rate values is particularly important in controlling the elevation of the model biomass distribution along the y-axis. Application of increased mortality rate values (> 0.3; not shown) result in increased biomass accumulation in the detritus pool implying that whilst having a gradient in Z values is important in determining the shape of the model spectrum, the numeric values of mortality rates generally determine how much biomass is retained within the size classes. These results further suggest that mortality processes are important in shaping the benthic biomass distribution. Previous modelling studies investigating the impacts of bottom trawling on benthos have also shown that increased mortality caused by trawling can have significant impact on the size structure (Duplisea et al., 2002). These results highlight the need for further experimental work in determining and quantifying mortality rates for benthic organisms.

### 8.4.5 Half saturation constants

Of the two half saturation constants included in the model, mortality ($k_Z$) in particular seems to have a relatively strong influence on the resulting size distribution. It is difficult to assign a specific ecological meaning to either of the half saturation constants in benthic context. However, a size-based gradient in $k_Z$ values is supported by the model results. Considering the influence of the mortality rates on the resulting biomass distribution outlined previously, this observation re-emphasizes and warrants further empirical investigations of the mortality rates of benthic organisms.

## 8.5 Conclusions

Observed biomass size spectrum at the Faroe-Shetland Channel site shows that biomass increases with body size. This increase is further quantified by a significant linear regression. A size-based modelling approach is capable of replicating these data and as such can help to understand the processes that control empirical size distributions. The model results suggest that ingestion is not size-dependent and that the respiration rates do not seem to impose a strong influence on the predicted biomass distribution. Size-based defecation rates (with larger organisms displaying slower rates) produce model predictions with relatively close resemblance to the field data possibly reflecting size-dependent assimilation efficiency. Similarly mortality parameters are important in controlling the shape of the predicted size distribution with the numeric values of mortality rates generally determining the amount of biomass retained in the size classes.

As mortality parameter values are indirectly estimated from allometric production equations, further empirical studies are required to investigate the mortality rates of benthic organisms. The next steps in the development of this benthic model will also include moving from a closed system representation to an open model allowing a closer examination of how processes such as pulsed input of food or seasonality affect the benthic communities. This will require further data on both the incoming flux of organic matter to the seabed and its fate within the benthic community over an annual cycle.

# 9. CONCLUSIONS

The main objective of this thesis was to investigate benthic body size structure and to use such data to gain further insights into the functioning and dynamics of benthic communities. The aims outlined in chapter 1 have generally been met and the constructed size spectra have successfully served as a foundation for a number of further applications. This concluding chapter summarises the main finding, attempts to place them into a wider context and proposes some relevant future research directions.

## 9.1 Do biomass size spectra provide concrete evidence that meio- and macro-fauna form two distinct units of benthic organisms?

***Aim 1:***

***Construction of reliable biomass and abundance size spectra for a number of environmentally contrasting benthic communities. This enables a close scrutiny of the shape of the spectra under different environmental conditions as well as examining the existence of a true functional distinction between meio- and macro-fauna.***

The results from this project indicate that biomass size spectra are not reliable at distinguishing meio- and macro-fauna as two functionally distinct groups of organisms. In contrast to the trends reported by Schwinghamer (1981, 1983, 1985), the shapes of the biomass size spectra established in the current study sites do not conform to a bimodal distribution pattern. None of the three study sites display

statistically significant changes in biomass at the size classes covering the meio- and macro-faunal size range. The shapes of the spectra generally followed a pattern where the total biomass continuously increased with individual body size. The reasons for the observed disparity between the results from this study and those described by Schwinghamer may be related to sampling and data analysis protocols.

In terms of sample collection, equipment that potentially creates a bow wave that disturbs the sediment surface during sample collection (e.g. box corer) have been reported to lose up to 50% of the organisms in terms of abundance (Bett et al., submitted). At the processing stage the organisms are typically extracted from the sediment matrix by using an appropriate combination of sieve mesh size and sample surface area that largely determine the reliability of the resulting abundance and biomass estimates. If the sample collection and processing protocol do not reliably cover the entire size range included in the analysis, then it is likely that the resulting data will be either misleading or inconclusive. For example, when the results from the current study are compared to the data published by Schwinghamer (1981) it was evident that the latter data were characterised by increased variability at the intermediate body sizes possibly indicating inadequate sampling in this part of the spectrum.

Biomass size spectra do appear to vary both as a function of space and time as discussed in chapter 5. For example, in temperate latitudes macrofaunal development at fully marine locations is characterised by a planktonic phase that may give rise to seasonal bimodal benthic biomass distribution pattern (e.g. Udalov & Burkovsky, 2004). However, in environments such as fresh- and brackish-water habitats,

macrofaunal development is often direct and consequently bimodality in the biomass size spectra is not evident (e.g. Drgas, 1998; Duplisea & Drgas, 1999; Udalov & Burkovsky, 2004). The results from this project support these notions and indicate that biomass size spectra do not reliably distinguish meio- and macro-fauna as two functionally distinct units on a universal scale.

## 9.2 Do body size spectra reflect changes in the environmental conditions?

***Aim 2:***

***Investigation of the suggested body size miniaturisation of the deep-sea benthos.***

The sampling sites in the current project represented three environmentally contrasting locations and these variations were also reflected in the characteristics of the respective body size spectra. Although the general shape of the three spectra appeared visually similar (increasing biomass with individual body size), statistical analysis (ANOSIM) revealed significant differences between the study sites. At the Arabian Sea site this could mainly be attributed to the slight bimodality in the biomass size spectra where the two local biomass maxima corresponded to nematodes and polychaetes, respectively. The reduced oxygen levels at this site have resulted in the benthic community being overwhelming dominated by these two groups of organisms that have adapted for an existence in hypoxic environment. The biomass size spectra clearly reflected this change in the community structure.

Further differences were evident when the size spectra were investigated in greater detail. For instance, accumulative size distrubutions displayed a shift towards smaller

body sizes at the deeper FSC station (1600 m) in comparison to the shallower Fladen Ground site (150 m). The reasons for the observed deep-sea size miniaturisation are unclear but one possible explanation conforms to the hypothesis suggested by Thiel (1975), which stated that '*associations governed by constantly limited food availability are composed of smaller individuals on average*'. A similar trend of body size miniaturisation was observed at the Arabian Sea site and this could possibly be attributed to the additional effect of maximum body size being limited by the available oxygen as suggested by Chapelle and Peck (1999). These variations in the body size spectra imply that size distribution patterns do vary in response to environmental conditions and as such the body size spectra can provide a complimentary method to the taxonomic approach for detecting community level changes across environmental gradients.

## 9.3 What does a size-based approach of community analysis reveal about the functioning and dynamics of these systems?

***Aims 3 & 4:***

***Estimation of community production and energy flow by utilising the empirical size distribution data and the previously established allometric relations.***

***Development of a simple size-dependent benthic ecosystem model to assess the suitability of a size-based modelling approach in providing reasonable approximations of the field data. This also helps to identify the biological processes that are important in maintaining and controlling the observed community size structure.***

The fact that several biological processes are closely related to individual body size allowed this study to make indirect estimations of total benthic production at the community level as well as to develop a size-based simulation model that helped to highlight some of the controlling processes and to generate new testable hypotheses. Although this project did not involve a detailed taxonomic analysis of the sampled communities, most specimens were identified to higher taxonomic levels (i.e. class or family). This analysis revealed that the communities at the three study sites differed in terms of the constituent organisms.

The size-based approach may provide additional insights into the system dynamics. Indirect estimations of total benthic community production were made by utilising previously published allometric relations. The direct measurement of total production at community level is complicated especially for deep-sea environments. These data were therefore able to provide production estimates on scales that would be difficult to establish by any other means.

These results showed that, in general, the estimated carbon demand at the three locations was supported by the estimated flux of incoming organic material. The total infaunal production varied from 42 g wwt $m^{-2}$ $y^{-1}$ at the Fladen Ground location to approximately 14 g wwt $m^{-2}$ $y^{-1}$ at the FSC and the Arabian Sea (OM) sites. The downward flux of organic matter at the FG and OM sites exceeded the estimated carbon demand of the included infauna and further analyses suggested that microorganisms and megafauna account for some of the incoming organic carbon. This was in contrast to the energy budget estimated for the FSC location where the

incoming flux approximately equalled the energy demands of meio-, meso- and macro-fauna. Allowing for the carbon demands of micro- and mega-fauna (that also ultimately depend on this food source), these findings imply a degree of carbon recycling through the various trophic levels. This process may be more pronounced at the FSC site than at the other two locations and may influence the rates of nutrient recycling from benthos back to the water column.

A part of the incoming organic carbon will not or cannot be utilised as a food source and this fraction is consequently buried. The data suggest that although at the FSC site the carbon burial rate is probably low, at the FG and particularly at the OM site, where the incoming flux of organic material exceeds the estimated energy demand of the benthos, the rate may be significantly higher. This would imply increased carbon burial at the OM site hence conforming to earlier notions that the sediment environments below oxygen minimum zones may act as sinks for carbon arriving from the overlying water column and atmosphere (Cowie, 2005).

The simulation model constructed as part of this project showed that a size-based approach was appropriate in modelling the empirical size distribution patterns without the need to include any additional complexity (e.g. functional groups that typically characterise these systems). Furthermore, the model sensitivity analysis implied that size-based gradients in ingestion rates were not supported by model results or that respiration rates alone had a negligible influence on the observed size distribution patterns. Conversely, size-based defecation and mortality rates were supported by the model results. Size-dependent defecation rates can be related to assimilation efficiency with longer gut lengths and residence times of larger organisms allowing a

more complete digestion of the same food material. Similarly, the size-dependent mortality rates conform with existing observations of larger organisms having longer life spans.

## 9.4 The next steps in size-based community analysis

### 9.4.1 Temporal component in body size spectra

Although a few studies exist that have investigated the changes in body size spectra over an annual cycle (Schwinghamer, 1983; Udalov & Burkovsky, 2004; Stead et al., 2005), these data alone are unable to conclusively outline how biomass distribution patterns vary in time. Such data are essential in forming the empirical basis for further simulation modelling that attempts to investigate the effect of seasonal deposition of organic material to the seabed and the subsequent influence on the biomass size spectra.

### 9.4.2 Model development

The next steps in the development of the benthic model will include moving from a closed system representation to an open model allowing a closer examination of how processes such as pulsed input of food (seasonality) affect the benthic communities. The model results from this study also highlighted the need for experimental work to be carried out to determine the mortality rates of benthic organisms to improve the parameterisation process. Similarly, further empirical work could involve utilising tracer studies in attempting to find out what part of the benthos takes up the newly

arrived organic material and how it is transferred across the trophic levels before being recycled back into the water column or buried.

### 9.4.3 Utilisation and development of theoretical relations

The construction and integration of full body size spectra over an annual cycle can be time consuming and it would be advantageous if the shape of the spectrum could be derived by sampling only a part of the community. For example, the metabolic theory of ecology (Brown, 2004) states that biomass should increase as a function of individual body size with the scaling exponent of 1/4 characterising this relationship. This theoretical relation is generally expected to apply to communities that share a common energy source. The linear regression models derived in this study provided evidence that this theoretical relation may apply to benthic communities if additional factors such as food limitation are included in the process. Further investigations would therefore be useful in determining if the metabolic theory of ecology could provide a framework for the derivation of full size spectra from empirical data that only covers part of the size range (e.g. macrofauna).

# 10. REFERENCES

Alagarsamy, R., 2003. Organic matter composition in sediments of the Oman Margin. *Chemistry and Ecology*, **19**, 419-429.

Andrassy, I., 1956. Die rauminhalts- und gewichtsbestimmung der fadenwurmer (nematoden). *Acta Zoologica*, **2**, 1-15.

Ankar, S. 1977. The soft bottom ecosystem of the Northern Baltic Proper with special reference to the macrofauna. *Contributions. Asko Lab*, **19**, 1-62.

Arntz, W.E., Gutt, J. & Klages, M., 1997. Antarctic marine biodiversity: an overview. In *Antarctic communities, species, structure and survival* (ed. B. Battaglia et al.), pp. 3-14. Cambridge University Press, Cambridge.

Austen, M.C., Buchanan, J.B., Hunt, H.G., Josefson, A.B. & Kendall, M.A., 1991. Comparison of long-term trends in benthic and pelagic communities of the North Sea. *Journal of the Marine Biological Association of the United Kingdom,Plymouth*, **71**, 179-190.

Banse, K., 1979. On weight dependency of net growth efficiency and specific respiration rates among field populations of invertebrates. *Oecologia*, **38**, 111-126.

Banse, K. & Mosher, S., 1980. Adult body mass and annual production/biomass relationships of field populations. *Ecological Monographs*, **50**, 355-379.

Barber, R. T., Marra, J., Bidigare, R.R., Codispoti, L., Halpern, D., Johnson, Z., Latasa, M., Goericke, R. & Smith, S., 2001. Primary productivity and its regulation in the Arabian Sea during 1995. *Deep-Sea Research part II*, **48**, 1127-1172.

Basford, D. & Eleftheriou, A., 1988. The benthic environment of the North Sea (56 degree to 61 degree N). *Journal of the Marine Biological Association of the United Kingdom, Plymouth*, **68**, 125-141.

Berger, W.H., Fischer. K., Lai, C. & Wu, G., 1988. Ocean carbon flux: global maps of primary production and export production. In *Biogeochemical Cycling and Fluxes Between the Deep Euphotic Zone and Other Oceanic Realms* (ed. C.R. Agegian), pp. 131-176. National Undersea Research Program, Research Report 88-1.

Bernard, J.M. & Bowser, S.S., 1992. Bacterial biofilms as a trophic resource for certain benthic foraminifera. *Marine Ecology Progress Series*, **83**, 263-272.

Bett, B.J., 2000. Environmental Surveys of the Seafloor of the UK Atlantic Margin, Atlantic Frontier Environmental Network [CD-ROM]. Available from Geotek Limited, Daventry, Northants NN11 5EA, UK. ISBN 09538399-0-7

Bett, B.J., 2001. UK Atlantic Margin Environmental Survey: introduction and overview of bathyal benthic ecology. *Continental Shelf Research*, **21**, 917-956.

Bett, B.J. & Gage, J.D., 2000. Section 6.2, Practical approaches to monitoring the deep-sea environment of the UK Atlantic Margin. In Environmental Surveys of the Seafloor of the UK Atlantic Margin, Atlantic Frontier Environmental Network [CD-ROM]. Available from Geotek Limited, Daventry, Northants NN11 5EA, UK. ISBN 09538399-0-7

Bett, B.J., Hughes, J.A., Horton, T., Bamber, R., Robbins, R., Wilson, I., Kaariainen, J. & Levell, D. (submitted). Sampler bias in the study of deep-sea macrobenthos. *Limnololgy & Oceanography: Methods.*

Billett, D.S.M., Bett, B.J., Jacobs, C.L., Rouse, I.P. & Wigham, B.D., (submitted). Mass deposition of jellyfish in the deep Arabian Sea. *Limnology & Oceanography.*

Blackford, J.C., 1997. An analysis of benthic biological dynamics in a North Sea ecosystem model. *Journal of Sea Research*, **38**, 213-230.

Bourassa, N. & Morin, A., 1995. Relationships between size structure of invertebrate assemblages and trophy and substrate composition in streams. *Journal of North American Benthological Society*, **14**, 393-403.

Brey, T., 1999. Growth performance and mortality in aquatic macrobenthic invertebrates. *Advances in Marine Biology*, **35**, 153-223.

Brey, T., 2001. Population dynamics in benthic invertebrates. A virtual handbook. Version 01.2. http://www.awi-bremerhaven.de/Benthic/Ecosystem/FoodWeb/Handbook/main.html Alfred Wegener Institute for Polar and Marine Research, Germany.

Brey, T. & Gerdes, D., 1997. Benthic community productivity in the Magellan region and the Weddell Sea. In *Investigacion Biologica Marina en el Area de Magallanes en relacion con la Antardida* (ed. W. Arntz & C. Rios), p.15. Universidad de Magallanes, Punta Arenas, Chile.

Brey, T., Jarre-Teichmann, A. & Borlich, O., 1996. Artificial neural network versus multiple linear regression: Predicting P/B ratios from empirical data. *Marine Ecology Progress Series,* **140**, 251-256.

Brown, J.H. & Gillooly, J.F., 2003. Ecological food webs: high-quality data facilitate theoretical unification. *Proceedings of the National Academy of Sciences of the United.States of America*, **100**, 1467-1468.

Brown, J.H., Gillooly, J.F., Allen, A.P., Savage, V.M. and West, G.B., 2004. Toward a metabolic theory of ecology. *Ecology,* **85**, 1771-1789.

Cadée, G.C., 1986. Organic carbon in the water column and its sedimentation, Fladen Ground (North Sea), May 1983. *Netherlands Journal of Sea Research*, **20**, 347-358.

Cammen, L.M. (1980). Ingestion rate: an empirical model for aquatic deposit feeders and detrivores. *Oecolgia*, **44**, 303-310.

Cammen, L.M. (1989). The relationship between ingestion rate of deposit feeders and sediment nutritional value. In *Ecology of marine deposit feeders – Lecture notes on coastal and estuarine studies 31* (ed. G. Lopez et al.), pp. 201-222. Springer-Verlag, New York.

Carey, A.G. Jr, 1981. A comparison of benthic infaunal abundance on two abyssal plainsin the northeast Pacific Ocean. *Deep-Sea Research*, **28**, 467-479.

Cattaneo, A., 1993. Size spectra of benthic communities in Laurentian streams. *Canadian Journal of Fisheries and Aquatic Sciences*, **50**, 2659-2666.

Chapelle, G. and Peck, L.S., 1999. Polar gigantism dictated by oxygen availability. *Nature*, **399**, 114-115.

Chipman, D.W., Marra, J. & Takahashi, T., 1993. Primary production at 47 degrees N and 20 degrees W in the North Atlantic Ocean: A comparison between the carbon-14 incubation method and the mixed layer carbon budget. *Deep-Sea Research part II*, **40**, 151-169.

Clarke, A.H., 1960. A Giant ultraabyssal *Cocculina* (*C. superba*, *n.sp.*) from the Argentina Basin. *Natural history papers*, *National Museum of Canada*, **7**,1-4.

Clarke, K.R. & Green, R.H., 1988. Statistical design and analysis for a 'biological effects' study. *Marine Ecology Progress Series*, **46**, 213-226.

Clarke, K.R. & Warwick, R.M., 1994. *Changes in marine communities: an approach to statistical analysis and interpretation.* Plymouth Marine Laboratory, Plymouth, UK.

Cole, J.J., Honjo, S. and Erez, J., 1987. Benthic decomposition of organic matter at a deep-water site in the Panama Basin. *Nature*, **327**, 703-704.

Cook, A.A., Lambshead, P.J.D., Hawkins, L.E., Mitchell, N. & Levin, L.A., 2000. Nematode abundance at the oxygen minimum zone in the Arabian Sea. *Deep-Sea Research part II*, **47**, 75-85.

Cowie, G., 2005. The biogeochemistry of Arabian Sea surficial sediments: A review of recent studies. *Progress in Oceanography*, **65**, 260-289.

Crisp, D.J., 1984. Energy flow measurements. In *Methods for the study of marine benthos* (ed. N.A. Holme & A.D. McIntyre), pp. 197-279. Blackwell Scientific Publishing, Oxford. IPB handbook no. 16.

Damuth, J., 1981. Population density and body size in mammals. *Nature*, **290**, 699-700.

De Wilde, P.A.W.J., Berghuis, E.M. & Kok, A., 1986. Biomass and activity of benthic fauna on the Fladen Group (northern North Sea). *Netherlands Journal of Sea Research*, **20**, 313.

Dinmore, T.A. & Jennings, S., 2004. Predicting abundance-body mass relationships in benthic infaunal communities. *Marine Ecology Progress Series*, **276**, 289-292

Drgas, A., Radziejewska, T. & Warzocha, J., 1998. Biomass size spectra of near-shore shallow-water benthic communities in the Gulf of Gdansk (Southern Baltic Sea). *Marine Ecology*, **19**, 209-228.

Duplisea, D.E., 2000. Benthic organism biomass size-spectra in the Baltic Sea in relation to the sediment environment. *Limnology and Oceanography*, **45**, 558-568.

Duplisea, D.E. & Drgas, A., 1999. Sensitivity of a benthic, metazoan, biomass size spectrum to differences in sediment granulometry. *Marine Ecology Progress Series*, **177**, 73-81.

Duplisea, D.E., Jennings, S., Warr, K.J. & Dinmore, T.A., 2002. A size-based model of the impacts of bottom trawling on benthic community structure. *Canadian Journal of Fisheries and Aquatic Sciences*, **59**, *1785-1795.*

Ebenhöh, W., Kohlmeier, C. & Radford, P.J., 1995. The benthic biological submodel in the European Regional Seas Ecosystem Model. *Netherlands Journal of Sea Research*, **33** , 423-452.

Faubel, A., Hartwig, E. & Thiel, H., 1983. On the ecology of the benthos of sublittoral sediments, Fladen Ground, North Sea. 1. Meiofauna standing stock and estimation of production. *Meteor Forschungsergebnisse Reihe D:Biologie*, **36**, 35-48.

Ferguson, M.A., 1997. Environmental management in deep waters, the Atlantic Margin case study. In *Oil and gas development: science and environmental management* (ed. J.P. Ductroy), pp. 15-31. Marine Forum Report number 5.

Fransz, H.G. & Gieskes, W.W.C., 1984. The unbalance of phytoplankton and copepods and the North Sea. *Rappor et Proces-Verbaux Reunions. Conseil International pour l'Exploration de la Mer*, **183**, 35-48.

Gage, J.D., 1977. Structure of the abyssal macrobenthic community in the Rockall Trough. In *Biology of Benthic Organisms* (ed. B.F. Keegan et al.), pp. 247-260. Pergamon, Oxford.

Gage, J.D. & Tyler, P.A., 1991. *Deep Sea Biology: A natural history of organisms at the deep sea floor*, Cambridge University Press, Cambridge, UK.

Gage, J.D. & Bett, B.J. (2005). Deep-sea benthic sampling." In *Methods for the study of marine benthos* (ed. A. Eleftheriou & A. McIntyre), pp. 273-325. Blackwell Publishing.

Gage, J.D., Levin, L.A. & Wolff, G.A., 2000. Benthic processes in the deep Arabian Sea: Introduction and overview. *Deep-Sea Research Part II*, **47**, 1-8.

Games, P.A. & Howell, J.F., 1976. Pairwise multiple comparison procedures with unequal N's and/or variances, *Journal of Educational Statistics,* **1**, 113-125.

Gerlach, S.A., Hahn, A.E. & Schrage, M., 1985. Size spectra of benthic biomass and metabolism. *Marine ecology progress series*, **26**,161-173.

Giere, O. 1993. *Meiobenthology: The microscopic fauna in aquatic sediments*. Springer-Verlag, Berlin.

Gooday, A.J. & Lambshead, P.J.D., 1989. Influence of seasonally deposited phytodetritus on benthic foraminiferal populations in the bathyal northeastern Atlantic: the species response. *Marine Ecology Progress Series*, **58**, 53-67.

Gooday, A.J., Pfannkuche, O. & Lambshead, P.J.D., 1996. An apparent lack of response by metazoan meiofauna to phytodetritus deposition in the bathyal north-eastern Atlantic. *Journal of the Marine Biological Association of the United Kingdom, Plymouth*, **76**, 297-310.

Gooday, A.J., Bernhard, J.M., Levin, L.A. & Suhr, S., 2000. Foraminifera in the Arabian Sea oxygen minimum zone and other oxygen-deficient settings: taxonomic composition, diversity and relation to metazoan faunas. *Deep-Sea Research Part II*, **47**, 25-54.

Griesbach, S., Peters, R.H. & Youakim, S., 1982. An allometric model for pesticide bioaccumulation. *Canadian Journal of Fisheries and Aquatic Sciences*, **39**, 727-735.

Han, B. & Straskraba, M., 1998. Size dependence of biomass spectra and population density. I. The effects of size scales and size intervals. *Journal of Theoretical Biology*, **191**, 259-265.

Hansen, B. & Ockelmann, K.W., 1991. Feeding behaviour in larvae of the opisthobranch *Philine aperta*. I. Growth and functional response at the different developmental stages. *Marine Biology*, **111**, 255-261

Hansen, B. & Osterhus, S., 2000. North Atlantic – Nordic Seas exchanges. *Progress in Oceanography,* **45**, 109-208.

Hartwig, E., Faubel, A. & Thiel, H., 1983. On the ecology of the benthos of sublittoral sediments, Fladen Ground, North Sea. 2. Quantitative studies on macrobenthic assemblages. *Meteor Forschungsergebnisse.Reihe D:Biologie*, **36**, 49-64.

Herguera, J.C., 1992. Deep-sea benthic foraminifera and biogenic opal: glacial to postglacial productivity changes in the western equatorial Pacific. *Marine Micropaleontology*, **19**, 79-98.

Humphreys, W.F., 1979. Production and respiration in animal populations. *Journal of Animal Ecology*, **48**, 427-453.

Hynes-Hamilton, H.B.N. & Coleman, M., 1968. A simple method for assessing the annual production of stream benthos. *Limnology and Oceanography*, **13**, 569-573.

Jennings, S., Alvsvaag, J., Cotter, A.J.R., Ehrich, S., Greenstreet, S.P.R., Jarre-Teichmann, A., Mergardt, N., Rijnsdorp, A.D. & Smedstad, O., 1999. Fishing effects in northeast Atlantic shelf seas: patterns in fishing effort, diversity and community structure. III. International trawling effort in the North Sea: an analysis of spatial and temporal trends. *Fisheries Research*, **40**, 125-134.

Jochem, F.J., Pollehne, F. & Zeitschel, B., 1993. Productivity regime and phytoplankton size structure in the Arabian Sea. *Deep-Sea Research Part II*, **40**, 711-735.

Jones, D.O.B, Bett, B.J. & Tyler, P.A. (submitted). Megabenthic ecolgy of the deep Faroe-Shetland Channel: A photographic study. *Deep Sea Reasearch Part II.*

Jumars, P.A., Mayer, L.M., Deming, J.W., Baross, J.A. & Wheatcroft, R.A., 1990. Deep-sea deposit-feeding strategies suggested by environmental and feeding constraints. *Philosophical Transactions of the Royal Society of London, Series A*, **331**, 85-101.

Kendall, M.A., Warwick, R.M. & Somerfield, P.J., 1997. Species size distributions in Arctic benthic communities. *Polar Biology,* **17**, 389-392.

Kerr, S.R., 1974. Theory of size distribution in ecological communities. *Journal of Fisheries Research Board, Canada*, **31**, 1859-1862.

Koster, M., Charfreitag, O. & Meyer-Reil, L-A., 1991. Availability of nutrients to a deep-sea benthic microbial community: results from a ship-board experiment. *Kieler Meeresforschungen, Sonderheft*, **8**, 127-133.

Lambshead, P.J.D., Platt, H.M. & Shaw, K.M., 1983. The detection of differences among assemblages of marine benthic species based on an assessment of dominance and diversity. *Journal of Natural History*, **17**, 859-874.

Lamont, P.A. & Gage, J.D., 2000. Morphological responses of macrobenthic polychaetes to low oxygen on the Oman continental slope, NW Arabian Sea. *Deep-Sea Research Part II*, **47**, 9-24.

Lampitt, R.S., Bett, B.J., Kiriakoulaksis, K., Popova, E.E., Ragueneau, O., Vangriesheim, A. & Wolff, G.A., 2001. Material supply to the abyssal seafloor in the Northeast Atlantic. *Progress in Oceanography*, **50**, 27-63.

Leaper, R., Raffaelli, D., Emes, C. & Manly, B., 2001. Constraints on body-size distributions: an experimental test of the habitat architecture hypothesis. *Journal of Animal Ecology*, **70***, 248-259.*

Lee, A.J., 1980. North Sea: Physical Oceanography. In *The Northwest European Shelf Seas: The Sea Bed and The Sea in Motion II* (ed. F.T.Banner et al.), pp. 467-493. Physical and Chemical Oceanography, and Physical Resources. Elsevier, Amsterdam.

Lee, C., Murray, D.W., Barber, R.T., Buesseler, K.O., Dymond, J., Hedges, J.I., Honjo, S., Manganini, S.J., Marra, J., Peterson, M.L., Prell, W.L. & Wakeham, S.G., 1998. Particulate organic carbon fluxes: Results from the US JGOFS Arabian Sea Process Study. *Deep-Sea Research Part II*, **45**, 2489-2501.

Levin, L.A., 2003. Oxygen Minimum Zone Benthos: Adaptation and Community Response to Hypoxia. *Oceanography and Marine Biology: An Annual Review*, **41**, 1-45.

Levin, L.A., Gage, J.D., Martin, C. and Lamont, P.A., 2000. Macrobenthic community structure within and beneath the oxygen minimum zone, NW Arabian Sea. *Deep-Sea Research Part II*, **47**, 189-226.

Lochte, K., 1992. Bacterial standing stock and consumption of organic carbon in benthic boundary layer of the abyssal North Atlantic. In *Deep-sea food chains and global carbon cycle* (ed. G.T Rowe & V. Pariente), pp. 1-10. Kluwer Academic Press, London.

Lopez, G.R. & Levinton, J.S., 1987. Ecology of deposit-feeding animals in marine sediments. *The Quarterly Review of Biology*, **62** , 235-259.

Lutz, M., Dunbar, R. & Caldeira, K., 2002. Regional variability in the vertical flux of particulate organic carbon in the ocean interior. *Global Biogeochemical Cycles*, **16**, 91-110.

Mahaut, M., Sibuet, M. & Shirayama, Y., 1995. Weight-dependent respiration rates in deep-sea organisms. *Deep Sea Research Part I*, **42**, 1575-1582.

Manly, B. F. J. 1996. Are there clumps in body-size distributions? *Ecology* **77**: 81–86.

Marquet, P.A., Quinones, R.A., Abades, S., Labra, F., Tognelli, M., Arim, M. & Rivadeneira, M., 2005. Scaling and power-laws in ecological systems. *Journal of Experimental Biology*, **208**, 1749-1769.

Masson, D.G., 2001. Sedimentary processes shaping the eastern slope of the Faeroe-Shetland Channel. *Continental Shelf Reseach*, **21** , 825-857.

McClain, C.R. & Rex, M.A., 2001. The relationship between dissolved oxygen concentration and maximum size in deep-sea turrid gastropods: an application of quantile regression. *Marine Biology*, **139**, 681-685.

McIntyre, A.D., 1961. Quantative differences in the fauna of boreal mud associations. *Journal of the Marine Biological Association of the United Kingdom*, **41**,599-616.

Morin, A. & Nadon, D., 1991. Size distribution of epilithic lotic invertebrates and implications for community metabolism. *Journal of North American Benthological Society*, **10**, 300-308.

Owens, N.J.P., Burkill, P.H., Mantoura, R.F.C., Woodward, E.M.S., Bellan, I.E., Aiken, J., Howland, R.J.M. & Llewellyn, C.A., 1993. Size-fractionated primary production and nitrogen assimilation in the northwestern Indian Ocean. *Deep-Sea Research Part II*, **40**, 697-709.

Parry, D.M., Kendall, M.A., Rowden, A.A., & Widdicombe, S., 1999. Species body size distribution patterns of marine benthic macrofauna assemblages from contrasting sediment types. *Journal of the Marine Biological Association of the United Kingdom*, **79**, 793-801.

Parsons, T.R., Takahashi, M. & Hargrave, B., 1984. *Biological Oceanographic Processes.* 3rd edition, Springer-Verlag, New York.

Peters, R.H., 1978. Empirical Physiological Models of Ecosystem Processes. *Verhandlungen Internationale Vereinigung fur Theoretische ubd Angewandte Limnologie*, **20**, 110-118.

Peters, R.H., 1983. *The ecological implications of body size.* Cambridge University Press, Cambridge, UK.

Peters, R.H. & Wassenberg, K., 1983. The effect of body size on animal abundance. *Oecologia*, **60**, 89-96.

Pfannkuche, O., 1985. The deep-sea meiofauna of Porcupine Seabight and abyssal plain (NE Atlantic): Population structure, distribution and standing stock. *Oceanologica Acta*, **8**, 343-353.

Platt, T., 1985. Structure of the marine ecosystem: its allometric basis. *Ecosystem Theory for Biological Oceanography*, **213**, 55 – 64.

Platt, T. & Denman, K., 1978. The structure of pelagic marine ecosystems. *Rappor et Proces-Verbaux Reunions. Conseil International pour l'Exploration de la Mer*, **173**, 60-65.

Platt, H.M. & Warwick, R.M., 1983. *Free-living marine nematodes. Part I, British Enoplids. Synopsis of the British Fauna.* Cambridge, Cambridge University Press.

Poff, N.L., Palmer, M.A., Angermeier, P.L., Vadas, R.L. Jr, Hakenkamp, C.C., Bely, A., Arensburger, P. & Martin, A.P., 1993. Size structure of metazoan community in a Piedmont stream. *Oecologia,* **95**, 202-209.

Polloni, P., Haedrich, R., Rowe, G. & Clifford, C.H., 1979. The size-depth relationship in deep ocean animals. *Internationale Revue der gesamten Hydrobiologie.Berlin*, **64**, 39-46.

Quiroga, E., Quinones, R., Palma, M., Sellanes, J., Gallardo, V.A., Gerdes, D. & Rowe, G., 2005. Biomass size-spectra of macrobenthic communities in the oxygen minimum zone off Chile. *Estuarine Coastal and Shelf Science*, **62**, 217-231.

Raffaelli, D., Hall, S., Emes, C. & Manly, B., 2000. Constraints on body size distributions: an experimental approach using a small-scale system. *Oecologia*, **122**, 389-398.

Ramsay, P.M., Rundle, S.D., Attrill, M.J., Uttley, M.G., Williams, P.R., Elsmere, P.S. & Abada, A., 1997. A rapid method for estimating biomass size spectra of benthic metazoan communities. *Canadian Journal of Fisheries and Aquatic Sciences*, **54**, 1716-1724.

Rasmussen, J.B., 1993. Patterns in the size structure of littoral zone macroinvertebrate communities. *Canadian Journal of Fisheries and Aquatic Sciences*, **50**, 2192-2204.

Rex, M.A. & Etter, R.J., 1998. Bathymetric patterns of body size: implications for deep-sea biodiversity. *Deep-Sea Research Part II*, **45**, 103-127.

Ricker, W.E., 1973. Linear regressions in fishery research. *Journal of Fisheries Research Board, Canada*, **30**, 409-434.

Riegman, R. & Kraay, G.W., 2001. Phytoplankton community structure derived from HPLC analysis of pigments in the Faroe-Shetland Channel during summer 1999: the distribution of taxonomic groups in relation to physical/chemical conditions in the photic zone. *Journal of Plankton Research*, **23**, 191-205.

Robson, B.J., Barmuta, L.A. & Fairweather, P.G., 2005. Methodological and conceptual issues in the search for a relationship between animal body-size distributions and benthic habitat architecture. *Marine and Freshwater Research*, **56**, 1-11.

Rowe, G.T., 1971. Benthic biomass and surface productivity. In *Fertility of the Sea Vol. 2* (ed. J.D. Costlow), pp. 441-454. Gordon & Breach, New York

Rowe, G.T., 1983. Biomass and production of deep-sea macrobenthos. In *The sea Vol. 8. Deep-sea biology* (ed. G.T. Rowe), pp. 97-121. John Wiley & Sons, New York.

Rowe, G.T. & Staresinic, N., 1979. Sources of organic matter to the deep-sea benthos; The deep sea; ecology and exploitation; first symposium. *Ambio Special Report*, **6**, 19-23.

Saiz-Salinas, J.I. & Ramos, A., 1999. Biomass size-spectra of macrobenthic assemblages along water depth in Antarctica. *Marine Ecology Progress Series*, **178**, 221-227.

Schwinghamer, P., 1981. Characteristic Size Distributions of Integral Benthic Communities. *Canadian Journal of Fisheries and Aquatic Sciences*, **38**, 1255-1263.

Schwinghamer, P., 1983. Generating ecological hypotheses from biomass spectra using causal analysis: A benthic example. *Marine Ecology Progress Series*, **13**, 151-166.

Schwinghamer, P., 1985. Observations on size-structure and pelagic coupling of some shelf and abyssal benthic communities. In *Proceedings of the nineteenth European Marine Biology Symposium* (ed. P.E. Gibbs), pp. 371-380. Cambridge University Press, Cambridge.

Schwinghamer, P., 1988. Influence of pollution along a natural gradient and in a mesocosm experiment on biomass-size spectra of benthic communities. *Marine Ecology Progress Series*, **46**, 199-206.

Schwinghammer, P., Hargrave, B., Peer, D. & Hawkins, C.M., 1986. Partitioning of production and respiration among size groups of organisms in an intertidal benthic community. *Marine Ecology Progress Series*, **31**, 131-142.

Scmidt-Nielsen, K., 1984. *Scaling - Why is animal size so important?* Cambridge, Cambridge University Press.

Sheldon, R.W., Paraksh, A. & Sutcliffe, W.H., 1972. The size distribution of particles in the ocean. *Limnology and Oceanography*, **17**, 327-340.

Shirayama, Y., 1983. Size structure of deep-sea meio-and macrobenthos in the western Pacific. *Internationale Revue der gesamten Hydrobiologie.Berlin*, **68**, 799-810.

Smith, KL J.R. & Hinga, K.R., 1983. Sediment community respiration in the deep sea. In *Deep-Sea Biology* (ed. Rowe GT), pp. 331-370. Wiley, New York.

Soetaert, K. & Heip, C., 1989. The size structure of nematode assemblages along a Mediterranean deep-sea transect. *Deep-Sea Research*, **36**, 93-102.

Sokal, R.R. & Rohlf, F.J., 1995. *Biometry. The principles and practice of statistics in biological research*. 3rd edition. New York, W.H. Freeman and Company.

Sokolova, M.N., 2000. *Feeding and Trophic Structure of the Deep-Sea Macrobenthos*. Amerind Publishing Co., New Delhi

Soltwedel, T., Pfannkuche, O. & Thiel, H., 1996. The size structure of deep-sea meiobenthos in the north-eastern Atlantic: Nematode size spectra in relation to environmental variables. *Journal of the Marine Biological Association of the United Kingdom*, **76**, 327-344.

Sprung, M., 1993. Estimating macrobenthic secondary production from body weight and biomass: A field test in a non-boreal intertidal habitat. *Marine Ecology Progress Series*, **100**, 103-109.

Stead, T.K., Schmid-Araya, J.M., Schmid, P.E. & Hildrew, A.G., 2005. The distribution of body size in a stream community: one system, many patterns. *Journal of Animal Ecology,* **74**, 475-487.

Steele, J.H., 1956. Plant production on the Fladen Ground. *Journal of the Marine Biological Association of the United Kingdom*, **35**, 1-33.

Steele, J.H., 1974. *The structure of marine ecosystems.* Blackwell Scientific Publishing, Oxford, UK.

Strayer, D., 1986. The size structure of a lacustrine zoobenthic community. *Oecologia*, **69**, 513-516.

Suess, E., 1980. Particulate organic carbon flux in the oceans; surface productivity and oxygen utilization. *Nature*, **288**, 260-263.

Taghon, G.L. & Green, R.B., 1992. Utilization of deposited and suspended particulate matter by benthic "interface" feeders. *Limnology and Oceanography*, **37**, 1370-1391.

Thiel, H., 1975. The size structure of the deep-sea benthos. *Internationale Revue der gesamten Hydrobiologie, Berlin,* **60**, 575-606.

Thiel, H., 1979. Structural aspects of the deep-sea benthos. *Ambio Spec Report*, **6**, 25-31.

Thurston, M.H., 1979. Scavenging abyssal amphipods from the north-east Atlantic *Oceanography and Marine Biology*, **51**, 55-68.

Tietjen, J.H., 1989. Ecology of deep-sea nematodes from the Puerto Rico Trench area and Hatteras Abyssal Plain. *Deep-Sea Research*, **36**, 1579-1594.

Travis, J.L. & Bowser, S.S., 1991. The motility of foraminifera. In *Biology of Foraminifera* (eds. J.J. Lee & O.R. Andersson), pp. 91-155. Academic Press, London.

Tumbiolo, M.L. & Downing, J.A., 1994. An empirical model for the prediction of secondary production in marine benthic invertebrate populations. *Marine Ecology Progress Series*, **114**, 165-174.

Turley, C.M., Lochte, K. & Patterson, D.J., 1988. A barophilic flagellate isolated from 4500 m in the mid-North Atlantic. *Deep-Sea Research*, **35**, 1079-1092.

Turrell, W.R., 1992. New hypothesis concerning the circulation of the northern North Sea and its relation to North Sea fish stock recruitment. *ICES Journal of Marine Science*, **49**, 107-123.

Turrell, W.R., Slesser, G., Adams, R.D., Payne, R. & Gillibrand, P.A., 1999. Decadal variability in the composition of Faroe Shetland Channel bottom water. *Deep-Sea Research Part I*, **46**, 1-25.

Udalov, A.A. & Burkovsky, I.V., 2002. The role of mesobenthos in the size structure of intertidal ecosystem. *Oceanology*, **42**, 527-536.

Vanaverbeke, J., Steyaert, M., Vanreusel, A. & Vincx, M., 2003. Nematode biomass spectra as descriptors of functional changes due to human and natural impact. *Marine Ecology Progress Series*, **249**, 157-170.

Vidondo, B., Prairie, Y.T., Blanco, J.M. & Duarte, C.M., 1997. Some aspects of the analysis of size spectra in aquatic ecology. *Limnology and Oceanography*, **42**, 184-192.

Warwick, R.M., 1984. Species size distributions in marine benthic communities. *Oecologia*, **61**, 32-41.

Warwick, R.M., 1986. A new method for detecting pollution effects on marine macrobenthic communities. *Marine Biology*, **92**, 557-562.

Warwick, R.M., 1989. The role of meiofauna in the marine ecosystem: Evolutionary considerations. *Zoological Journal of the Linnean Society*, **96**, 229-224.

Warwick, R.M. & Price, R. 1979. Ecological and metabolic studies on free-living nematodes from an estuarine mud-flat. *Estuarine and Coastal Marine Science*, **9**, 257-271.

Warwick, R.M. & Clarke, K.R., 1991. A comparison of some methods for analysing changes in benthic community structure. *Journal of the Marine Biological Association of the United Kingdom*, **71**, 225-244.

Waters, T.F., 1977. Secondary production in inland waters. *Advances in Ecological Research*, **10**, 91-164.

Wilson, E., 2000. *Philine aperta.* Lobe shell. Marine life information network: Biology and sensitivity key information sub-programme (on-line). Plymouth: Marine Biological Association of the United Kingdom. http://www.marlin.ac.uk/species/philiniaperta.htms.

Wolff, T., 1962. The systematics and biology of bathyal and abyssal Isopoda, *Asellota*. *Galathea Report*, **6**, 1-358.

Zehnder, A., 1988. *Biology of anaerobic organisms.* New York: John Wiley.

# 11. APPENDIX

**Biomass and abundance data from the three study sites**

Biomass values (g wwt $m^{-2}$) at the FG site.

| X2 size class | 55526#1 | 55526#2 | 55527#2 | 55528#1 | 55528#2 |
|---|---|---|---|---|---|
| 0 | $3.3x10^{-5}$ | $2.0x10^{-6}$ | $1.9x10^{-6}$ | $3.3x10^{-4}$ | 0 |
| 1 | 0 | 0 | 1.3x10-$^{3}$ | 0 | 0 |
| 2 | $1.9x10^{-3}$ | $3.7x10^{-3}$ | $8.0x10^{-3}$ | $3.9x10^{-3}$ | $7.6x10^{-3}$ |
| 3 | $1.2x10^{-2}$ | $2.2x10^{-2}$ | $2.6x10^{-2}$ | 1.3x10-$^{2}$ | $5.0x10^{-2}$ |
| 4 | $2.7x10^{-2}$ | $5.8x10^{-2}$ | $6.3x10^{-2}$ | 5.2x10-$^{2}$ | $8.0x10^{-2}$ |
| 5 | $5.7x10^{-2}$ | $7.2x10^{-2}$ | $1.3x10^{-1}$ | $7.3x10^{-2}$ | $1.4x10^{-1}$ |
| 6 | $2.2x10^{-1}$ | $2.5x10^{-1}$ | $3.0x10^{-1}$ | $1.2x10^{-1}$ | $1.6x10^{-1}$ |
| 7 | $2.3x10^{-1}$ | $3.0x10^{-1}$ | $5.7x10^{-1}$ | $4.3x10^{-1}$ | $4.3x10^{-1}$ |
| 8 | $2.5x10^{-1}$ | $3.9x10^{-1}$ | $3.2x10^{-1}$ | $2.1x10^{-1}$ | $2.8x10^{-1}$ |
| 9 | $2.9x10^{-1}$ | $2.8x10^{-1}$ | $1.1\ x10^{0}$ | $4.8x10^{-1}$ | $1.1\ x10^{0}$ |
| 10 | $8.6x10^{-1}$ | $6.3x10^{-1}$ | $3.0\ x10^{0}$ | $1.1\ x10^{0}$ | $2.2\ x10^{0}$ |
| 11 | $5.1x10^{-1}$ | $7.3x10^{-1}$ | $2.7\ x10^{0}$ | $7.5x10^{-1}$ | $1.3\ x10^{0}$ |
| 12 | $2.4x10^{-1}$ | $1.7x10^{-1}$ | $1.2\ x10^{0}$ | $7.0x10^{-1}$ | $8.9x10^{-1}$ |
| 13 | $2.8x10^{-1}$ | $3.0x10^{-1}$ | $8.0x10^{-1}$ | $5.8x10^{-1}$ | $8.1x10^{-1}$ |
| 14 | $4.0x10^{-1}$ | $3.1x10^{-1}$ | $6.8x10^{-1}$ | $8.2x10^{-1}$ | $6.7x10^{-1}$ |
| 15 | $6.2x10^{-1}$ | $2.3x10^{-1}$ | $2.3x10^{-1}$ | $8.2x10^{-1}$ | $1.0\ x10^{0}$ |
| 16 | $8.7x10^{-1}$ | $3.4x10^{-1}$ | $1.1\ x10^{0}$ | $1.0\ x10^{0}$ | $6.8x10^{-1}$ |
| 17 | $8.2x10^{-1}$ | $2.9x10^{-1}$ | $1.9\ x10^{0}$ | $1.8\ x10^{0}$ | $1.3\ x10^{0}$ |
| 18 | $1.6x10^{0}$ | $7.2x10^{-1}$ | $4.1\ x10^{0}$ | $1.5\ x10^{0}$ | $3.3x10^{-1}$ |
| 19 | $7.9x10^{-1}$ | $8.5x10^{-1}$ | 7.1x10-1 | $1.0\ x10^{0}$ | $1.8\ x10^{0}$ |
| 20 | 0 | $2.1\ x10^{0}$ | $3.5\ x10^{0}$ | $2.0\ x10^{0}$ | 0 |
| 21 | $1.7\ x10^{0}$ | $1.3\ x10^{0}$ | 0 | $1.0\ x10^{0}$ | 0 |
| 22 | 0 | 0 | 0 | $3.1\ x10^{0}$ | $2.3\ x10^{0}$ |
| 23 | 0 | 0 | 0 | $1.3x10^{1}$ | 0 |
| 24 | 0 | 0 | 0 | 0 | 0 |
| 25 | 0 | 0 | 0 | 0 | $1.810^{1}$ |
| 26 | 0 | 0 | 0 | 0 | 0 |
| 27 | 0 | 0 | 0 | 0 | 0 |
| 28 | 0 | 0 | 0 | 0 | 0 |
| 29 | $1.2x10^{3}$ | 0 | 0 | 0 | 0 |

Biomass values (g wwt $m^{-2}$) at the FSC site.

| X2 size class | 55447#6 | 55447#8 | 55447#9 | 55447#10 | 55447#11 |
|---|---|---|---|---|---|
| 0 | $1.2x10^{-4}$ | $2.6x10^{-4}$ | $1.6x10^{-3}$ | $2.5x10^{-3}$ | $5.5x10^{-4}$ |
| 1 | $9.4x10^{-4}$ | $1.0x10^{-3}$ | $1.2x10^{-2}$ | $9.6x10^{-3}$ | $2.0x10^{-3}$ |
| 2 | $5.4x10^{-3}$ | $4.2x10^{-3}$ | $1.3x10^{-2}$ | $1.9x10^{-2}$ | $7.6x10^{-3}$ |
| 3 | $1.1x10^{-2}$ | $1.1x10^{-2}$ | $1.1x10^{-2}$ | $1.9x10^{-2}$ | $8.9x10^{-3}$ |
| 4 | $9.6x10^{-3}$ | $1.7x10^{-2}$ | $5.3x10^{-2}$ | $1.3x10^{-2}$ | $2.2x10^{-2}$ |
| 5 | $1.5x10^{-2}$ | $2.9x10^{-2}$ | $8.0x10^{-2}$ | $1.6x10^{-2}$ | $1.3x10^{-2}$ |
| 6 | $2.7x10^{-2}$ | $4.6x10^{-2}$ | $1.2x10^{-1}$ | $1.1x10^{-1}$ | $3.3x10^{-2}$ |
| 7 | $1.1x10^{-1}$ | $1.2x10^{-1}$ | $5.9x10^{-2}$ | $2.3x10^{-1}$ | $8.7x10^{-2}$ |
| 8 | $1.7x10^{-1}$ | $1.3x10^{-1}$ | $7.8x10^{-2}$ | $1.9x10^{-1}$ | $1.8x10^{-1}$ |
| 9 | $1.8x10^{-1}$ | $1.8x10^{-1}$ | $7.2x10^{-2}$ | $1.4x10^{-1}$ | $1.0x10^{-1}$ |
| 10 | $1.4x10^{-1}$ | $1.3x10^{-1}$ | $2.1x10^{-1}$ | $1.8x10^{-1}$ | $2.7x10^{-2}$ |
| 11 | $2.3x10^{-1}$ | $7.2x10^{-2}$ | $1.6x10^{-1}$ | $2.1x10^{-1}$ | $1.3x10^{-1}$ |
| 12 | $3.2x10^{-1}$ | $2.9x10^{-1}$ | $1.9x10^{-1}$ | $1.5x10^{-1}$ | $1.1x10^{-1}$ |
| 13 | $1.7x10^{-1}$ | $1.5x10^{-1}$ | $4.4x10^{-1}$ | $1.3x10^{-1}$ | $1.1x10^{-1}$ |
| 14 | $2.4x10^{-1}$ | $2.2x10^{-1}$ | $1.4x10^{-1}$ | $1.9x10^{-1}$ | $1.5x10^{-1}$ |
| 15 | $3.3x10^{-1}$ | $3.2x10^{-1}$ | $2.3x10^{-1}$ | $1.8x10^{-1}$ | $2.1x10^{-1}$ |
| 16 | $3.1x10^{-1}$ | $4.9x10^{-1}$ | $2.6x10^{-1}$ | $6.7x10^{-1}$ | $5.3x10^{-1}$ |
| 17 | $5.1x10^{-1}$ | $3.7x10^{-1}$ | $3.2x10^{-1}$ | $6.0x10^{-1}$ | $6.4x10^{-1}$ |
| 18 | $1.3x10^{0}$ | $7.6x10^{-1}$ | $1.1x10^{0}$ | $1.4x10^{0}$ | $1.3x10^{0}$ |
| 19 | $1.8x10^{0}$ | $4.8x10^{-1}$ | $1.7x10^{0}$ | 7.0x10-$^{1}$ | $1.4x10^{0}$ |
| 20 | $2.1x10^{0}$ | $1.8x10^{0}$ | $4.0x10^{0}$ | 0 | $6.7x10^{-1}$ |
| 21 | $1.9x10^{0}$ | $7.2x10^{-1}$ | 0 | $6.8x10^{0}$ | $6.5x10^{-1}$ |
| 22 | $2.1x10^{0}$ | 0 | $3.4x10^{0}$ | $4.3x10^{0}$ | $1.3x10^{0}$ |
| 23 | 0 | 0 | 0 | 0 | 0 |
| 24 | 0 | 0 | 0 | 0 | 0 |
| 25 | 0 | 0 | 0 | 0 | 0 |
| 26 | 0 | 0 | 0 | 0 | 0 |
| 27 | 0 | 0 | 0 | 0 | 0 |
| 28 | 0 | 0 | 0 | 0 | 0 |
| 29 | 0 | 0 | 0 | 0 | 0 |

Biomass values (g wwt $m^{-2}$) at the OM site.

| X2 size class | 55764#1 | 55754#2 | 55754#3 | 55754#4 | 55754#5 |
|---|---|---|---|---|---|
| 0 | $1.5x10^{-5}$ | $5.4x10^{-4}$ | $2.8x10^{-3}$ | $5.1x10^{-4}$ | $6.5x10^{-4}$ |
| 1 | $1.9x10^{-3}$ | $3.2x10^{-3}$ | $1.9x10^{-2}$ | $5.2x10^{-3}$ | $1.0x10^{-2}$ |
| 2 | $1.1x10^{-2}$ | $3.1x10^{-2}$ | $7.0x10^{-2}$ | $2.7x10^{-2}$ | $3.7x10^{-2}$ |
| 3 | $2.8x10^{-2}$ | $3.8x10^{-2}$ | 5.2x10-$^{2}$ | $2.4x10^{-2}$ | $3.1x10^{-2}$ |
| 4 | $1.2x10^{-1}$ | $4.2x10^{-2}$ | $1.5x10^{-2}$ | $8.2x10^{-2}$ | $3.2x10^{-2}$ |
| 5 | $3.3x10^{-1}$ | $1.0x10^{-1}$ | $6.0x10^{-4}$ | $5.4x10^{-2}$ | $6.7x10^{-2}$ |
| 6 | $1.7x10^{-1}$ | $1.4x10^{-1}$ | $3.3x10^{-3}$ | $3.8x10^{-2}$ | $8.5x10^{-2}$ |
| 7 | $3.4x10^{-1}$ | $1.4x10^{-1}$ | $8.0x10^{-3}$ | $7.6x10^{-3}$ | 1.7x10-$^{1}$ |
| 8 | $6.7x10^{-1}$ | $1.5x10^{-1}$ | $1.8x10^{-2}$ | $2.0x10^{-2}$ | $2.5x10^{-2}$ |
| 9 | $9.5x10^{-1}$ | $5.9x10^{-1}$ | $5.9x10^{-2}$ | $2.9x10^{-1}$ | $4.9x10^{-1}$ |
| 10 | $2.5x10^{-1}$ | $1.8x10^{-1}$ | $3.5x10^{-2}$ | $7.2x10^{-2}$ | $3.4x10^{-1}$ |
| 11 | $5.7x10^{-2}$ | $6.7x10^{-2}$ | $3.2x10^{-2}$ | $2.9x10^{-2}$ | $1.6x10^{-1}$ |
| 12 | $7.7x10^{-2}$ | $5.1x10^{-2}$ | $3.0x10^{-2}$ | $4.7x10^{-2}$ | $1.1x10^{-1}$ |
| 13 | $3.5x10^{-1}$ | $2.9x10^{-1}$ | $6.6x10^{-2}$ | $3.6x10^{-2}$ | $2.5x10^{-1}$ |
| 14 | $6.4x10^{-1}$ | $1.1x10^{0}$ | $2.5x10^{-1}$ | $6.3x10^{-2}$ | $5.6x10^{-1}$ |
| 15 | $1.1x10^{0}$ | $2.0x10^{0}$ | $4.3x10^{-1}$ | $7.0x10^{-2}$ | $4.5x10^{-1}$ |
| 16 | $4.8x10^{-1}$ | $3.1x10^{-1}$ | $4.3x10^{-1}$ | $2.3x10^{-1}$ | 0 |
| 17 | $7.8x10^{-1}$ | $5.6x10^{-1}$ | $8.8x10^{-2}$ | $2.3x10^{-1}$ | $4.8x10^{-1}$ |
| 18 | 0 | $1.1x10^{0}$ | 0 | $2.4x10^{-1}$ | 0 |
| 19 | 0 | 0 | $1.6x10^{-1}$ | 0 | 0 |
| 20 | $5.1x10^{-1}$ | 0 | 0 | 0 | 0 |
| 21 | 0 | 0 | 0 | 0 | 0 |
| 22 | 0 | 0 | 0 | 0 | 0 |
| 23 | 0 | 0 | 0 | 0 | 0 |
| 24 | 0 | 0 | 0 | 0 | 0 |
| 25 | 0 | 0 | 0 | 0 | 0 |
| 26 | 0 | 0 | 0 | 0 | 0 |
| 27 | 0 | 0 | 0 | 0 | 0 |
| 28 | 0 | 0 | 0 | 0 | 0 |
| 29 | 0 | 0 | 0 | 0 | 0 |

Abundance values (ind. $m^{-2}$) at the FG site.

| X2 size class | 55526#1 | 55526#2 | 55527#2 | 55528#1 | 55528#2 |
|---|---|---|---|---|---|
| 0 | 1168 | 64 | 64 | 12000 | 0 |
| 1 | 0 | 0 | 24000 | 0 | 0 |
| 2 | 17000 | 33000 | 72000 | 35000 | 68000 |
| 3 | 56000 | 98000 | 118000 | 59000 | 226000 |
| 4 | 60000 | 130000 | 142000 | 117000 | 181000 |
| 5 | 64508 | 82000 | 142127 | 82000 | 158050 |
| 6 | 123788 | 141862 | 167310 | 67382 | 91375 |
| 7 | 63710 | 82549 | 160065 | 119879 | 119884 |
| 8 | 36662 | 56318 | 45826 | 29605 | 38253 |
| 9 | 21217 | 20254 | 76535 | 33172 | 77867 |
| 10 | 30156 | 21914 | 108614 | 39414 | 80287 |
| 11 | 9828 | 13760 | 52457 | 14879 | 24258 |
| 12 | 2142 | 1536 | 11260 | 6828 | 8246 |
| 13 | 1260 | 1408 | 4013 | 2701 | 3775 |
| 14 | 1008 | 736 | 1593 | 1962 | 1600 |
| 15 | 714 | 288 | 255 | 968 | 1275 |
| 16 | 546 | 192 | 765 | 637 | 425 |
| 17 | 210 | 96 | 573 | 484 | 375 |
| 18 | 210 | 96 | 573 | 229 | 50 |
| 19 | 42 | 64 | 64 | 76 | 125 |
| 20 | 0 | 64 | 191 | 76 | 0 |
| 21 | 42 | 32 | 0 | 25 | 0 |
| 22 | 0 | 0 | 0 | 25 | 25 |
| 23 | 0 | 0 | 0 | 51 | 0 |
| 24 | 0 | 0 | 0 | 0 | 0 |
| 25 | 0 | 0 | 0 | 0 | 25 |
| 26 | 0 | 0 | 0 | 0 | 0 |
| 27 | 0 | 0 | 0 | 0 | 0 |
| 28 | 0 | 0 | 0 | 0 | 0 |
| 29 | 84 | 0 | 0 | 0 | 0 |

Abundance values (ind. $m^{-2}$) at the FSC site.

| X2 size class | 55447#6 | 55447#8 | 55447#9 | 55447#10 | 55447#11 |
|---|---|---|---|---|---|
| 0 | 4000 | 18 | 58000 | 92000 | 20000 |
| 1 | 16000 | 17000 | 208000 | 172000 | 35000 |
| 2 | 48127 | 38000 | 113000 | 172000 | 69000 |
| 3 | 48000 | 50000 | 50000 | 88000 | 40484 |
| 4 | 21273 | 39789 | 118946 | 30000 | 50968 |
| 5 | 17268 | 33724 | 90109 | 17725 | 14611 |
| 6 | 15240 | 26998 | 67715 | 60775 | 18025 |
| 7 | 29490 | 37518 | 17566 | 67133 | 24843 |
| 8 | 24601 | 19021 | 11149 | 27129 | 25629 |
| 9 | 13048 | 13538 | 5238 | 10747 | 7362 |
| 10 | 5099 | 4471 | 7538 | 6300 | 939 |
| 11 | 3732 | 1319 | 3215 | 3934 | 2576 |
| 12 | 3044 | 3092 | 1760 | 1700 | 1003 |
| 13 | 755 | 673 | 1637 | 615 | 509 |
| 14 | 560 | 491 | 309 | 467 | 350 |
| 15 | 356 | 364 | 273 | 212 | 271 |
| 16 | 178 | 273 | 164 | 318 | 271 |
| 17 | 153 | 109 | 91 | 170 | 191 |
| 18 | 153 | 109 | 127 | 170 | 159 |
| 19 | 127 | 36 | 127 | 42 | 96 |
| 20 | 102 | 73 | 182 | 0 | 32 |
| 21 | 25 | 18 | 0 | 106 | 16 |
| 22 | 25 | 0 | 36 | 42 | 16 |
| 23 | 0 | 0 | 0 | 0 | 0 |
| 24 | 0 | 0 | 0 | 0 | 0 |
| 25 | 0 | 0 | 0 | 0 | 0 |
| 26 | 0 | 0 | 0 | 0 | 0 |
| 27 | 0 | 0 | 0 | 0 | 0 |
| 28 | 0 | 0 | 0 | 0 | 0 |
| 29 | 0 | 0 | 0 | 0 | 0 |

Abundance values (ind. $m^{-2}$) at the OM site.

| X2 size class | 55764#1 | 55754#2 | 55754#3 | 55754#4 | 55754#5 |
|---|---|---|---|---|---|
| 0 | 582 | 19000 | 99000 | 18000 | 23000 |
| 1 | 33328 | 57000 | 332000 | 92000 | 188000 |
| 2 | 95910 | 283000 | 630000 | 239000 | 328000 |
| 3 | 125164 | 170000 | 232000 | 110000 | 141000 |
| 4 | 279582 | 94000 | 33517 | 184000 | 72101 |
| 5 | 373366 | 117253 | 708 | 60038 | 75602 |
| 6 | 93525 | 78599 | 2499 | 21754 | 47796 |
| 7 | 94926 | 39703 | 2213 | 2110 | 47860 |
| 8 | 95006 | 21595 | 2515 | 2922 | 3343 |
| 9 | 66852 | 41956 | 4290 | 20388 | 33993 |
| 10 | 8738 | 6897 | 1289 | 2318 | 11750 |
| 11 | 1067 | 1210 | 621 | 509 | 3149 |
| 12 | 700 | 462 | 287 | 446 | 1019 |
| 13 | 1560 | 1258 | 302 | 175 | 1130 |
| 14 | 1417 | 2372 | 541 | 159 | 1226 |
| 15 | 1258 | 2229 | 541 | 80 | 494 |
| 16 | 271 | 175 | 271 | 127 | 0 |
| 17 | 239 | 159 | 32 | 80 | 143 |
| 18 | 0 | 143 | 0 | 32 | 0 |
| 19 | 0 | 0 | 16 | 0 | 0 |
| 20 | 16 | 0 | 0 | 0 | 0 |
| 21 | 0 | 0 | 0 | 0 | 0 |
| 22 | 0 | 0 | 0 | 0 | 0 |
| 23 | 0 | 0 | 0 | 0 | 0 |
| 24 | 0 | 0 | 0 | 0 | 0 |
| 25 | 0 | 0 | 0 | 0 | 0 |
| 26 | 0 | 0 | 0 | 0 | 0 |
| 27 | 0 | 0 | 0 | 0 | 0 |
| 28 | 0 | 0 | 0 | 0 | 0 |
| 29 | 0 | 0 | 0 | 0 | 0 |